UNIVERSITY OF PARMA

Department of Chemistry, Life Sciences and Environmental Sustainability

Ph.D. in Biotechnologies and Biosciences

XXX COURSE

Saccharomyces cerevisiae as a model for the study of mitochondrial diseases and for the identification of beneficial molecules

Coordinator:
Prof. **Simone Ottonello**

Mentor:
Prof. **Claudia Donnini**

Tutor:
Dr. **Cristina Dallabona**

Ph.D. Student: **Micol Gilberti**

2015/2017

Table of contents

1. Introduction

1.1 Mitochondrial diseases

Mitochondrial diseases (MD) are a group of clinically and genetically heterogeneous disorders induced by dysfunction of the mitochondrial electron transport chain complexes that all together are amongst the most common inherited human diseases, with a prevalence of 1:5000 (Diodato *et al*., 2014 a). The impaired oxidative phosphorylation (OXPHOS) results in an inability to generate adequate energy to meet the needs of different tissues, particularly organs with high-energy demands, including the central nervous system, cardiac and skeletal muscles, endocrine system, liver, and renal system. This energy deficiency in various organs results in a multiorgan dysfunction that lead to the variable manifestations observed in MD, including cognitive impairment, epilepsy, cardiac and skeletal myopathies, nephropathies, hepatopathies, and endocrinopathies (Chinnery *et al*., 2014; Munnich *et al*., 2012) (figure 1.1).

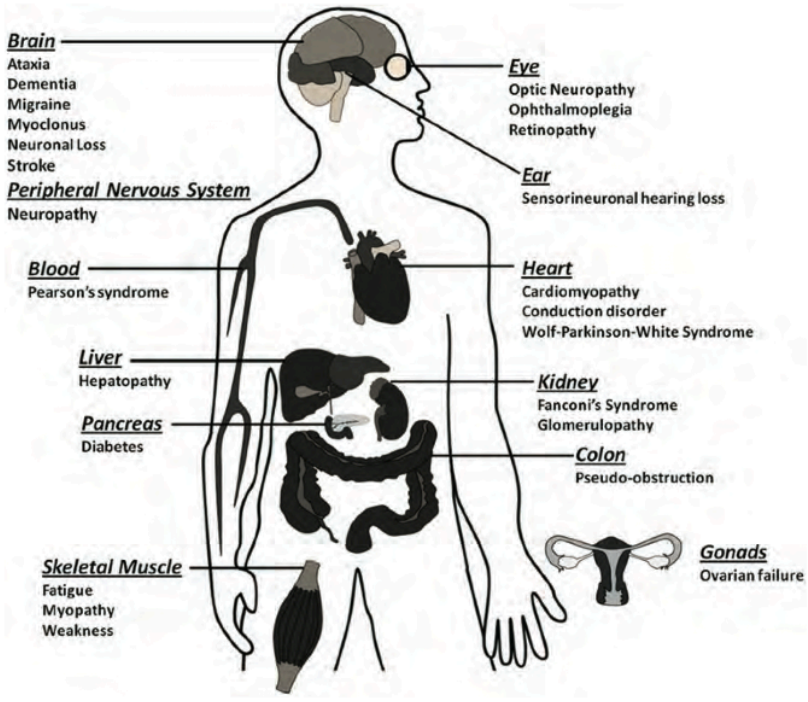

Figure 1.1. Clinical spectrum of mitochondrial diseases. Schematic diagram showing the organ and corresponding disease affected by mitochondrial dysfunction (from Chinnery and Hudson, 2013).

It has been estimated that 1500 proteins are needed for the structure and function of normal mitochondria. They contain their own DNA (mitochondrial DNA; mtDNA) that encodes a very small fraction of mitochondrial proteins, 13 essential subunits of the mitochondrial respiratory chain

complexes CI, CIII, CIV, and CV (Schon *et al.,* 2012), two ribosomal RNAs (rRNAs; 12S and 16S), and 22 transfer RNAs (tRNAs), whereas all the other components of the respiratory chain and all of the other proteins constituting the mitochondrial proteome, are encoded by the nuclear genome, synthesized in cytoplasm, and imported into mitochondria (El-Hattab and Scaglia, 2016; Ylikallio and Suomalainen, 2012). Therefore, mitochondrial bioenergetics are under the double genetic control of both nuclear and mitochondrial DNA. This genetic duality has relevant consequences for human pathology. In fact, MD are due to mutations in a) mitochondrial DNA or b) nuclear genes encoding mitochondrial proteins (Chinnery *et al*., 2014; Munnich *et al*., 2012).

Defects in mtDNA can be classified in two classes: point mutations and mtDNA rearrangements (deletions and insertions-duplications). Point mutations in mtDNA can affect genes coding for proteins, tRNAs or rRNAs, and can be heteroplasmic or homoplasmic. These mutations are maternally inherited and typically associated with very variable phenotypes. Rearrangements of mtDNA differ in size and position and typically interest several genes. In contrast to point mutations, these rearrangements are typically sporadic and heteroplasmic.

Mutations in nuclear DNA (nDNA) genes are inherited in an autosomal recessive, autosomal dominant, or X-linked manner. These mutations lead to diseases that can be classified into four distinct groups: (i) disorders resulting from mutations in nuclear-encoded components or assembly factors of the OXPHOS system; (ii) disorders resulting from mutations affecting mitochondrial translation; (iii) disorders due to defects in genes controlling mitochondrial network dynamics and (iv) disorders resulting from a reduction in mtDNA stability (Chinnery and Hudson, 2013).

Regarding the pathologies associated with mtDNA instability, they are due to mutations in nuclear genes coding for mitochondrial proteins necessary for mtDNA stability. In this case, mutations in nuclear genes are the primary cause of pathology that can ultimately damage the structural integrity of the mtDNA molecules or the mtDNA copy number (Zeviani *et al*., 1995; Gasser *et al.*, 2001). The stability/maintenance of mtDNA depends of a number of nuclear genes coding for proteins that function in mtDNA synthesis and in maintenance of a balanced mitochondrial nucleotide pool (El-Hattab and Scaglia, 2013; Spinazzola, 2011). Mutations in these genes induce mtDNA instability, in particular quantitative decrease of the mtDNA copy number, i.e. tissue-specific depletion of mtDNA, and qualitative alterations, i.e. multiple deletions of mtDNA, with the former typically occurs during infancy as severe diseases, whereas the latter usually induces milder clinical phenotype with onset during adulthood. The current understanding that both mtDNA depletion and multiple mtDNA deletions have the same pathomechanism and that defects in many of the mtDNA maintenance genes

can result in both mtDNA depletion and multiple mtDNA deletions, has suggested that these two disease groups can represent the spectrum for a single disease group (El-Hattab *et al*., 2017 a). However, these defects have been classically considered as two distinct groups of diseases.

1.2 Mitochondrial DNA depletion syndromes

Mitochondrial DNA depletion syndromes (MDS) are autosomal recessive disorders with a broad genetic and clinical spectrum caused by mutations in nuclear genes (Zeviani and Antozzi, 1997; El-Hattab and Scaglia, 2013). Despite the very different clinical manifestations of these severe diseases, all are characterized by profound reduction in mitochondrial DNA copy number in one or several tissues, leading to impaired energy production in affected tissues and organs (Suomalainen and Isohanni, 2010). Until now, pathogenic variants in at least 16 genes have been associated with low copy number of mtDNA within cells. These genes code for enzymes of mtDNA replication machinery (mtDNA polymerization: *POLG, TWNK, TFAM*; and nucleases removing primers and flap intermediates: *RNASEH* and *MGME1*), genes encoding proteins that function in maintaining a balanced mitochondrial nucleotide pool (mitochondrial salvage pathway: *TK2, DGUOK, SUCLG1, SUCLA2*, and *ABAT*; cytosolic nucleotide metabolism: *RRM2B, TYMP* and mitochondrial nucleotide import: *AGK*), and genes encoding proteins involved in mitochondrial dynamics (*OPA1)* (Copeland 2012, El-Hattab *et al*., 2017 a). The genes *FBXL4* and *MPV17* have a not clear function. Mutations in the *MPV17* gene were described as cause of hepatocerebral MDS (Spinazzola *et al.*, 2006) and Navajo neuro-hepathopathy (Karadimas *et al*., 2006). Although a role for *MPV17* has been proposed in the cellular response to metabolic stress and maintenance of nucleotide pool (Spinazzola *et al*., 2006; Dalla Rosa *et al.,* 2016), its function remains elusive. Mutations in any of these genes lead to severe reduction in mtDNA content that results in impaired synthesis of key subunits of mitochondrial electron transport chain complexes.

MDS are typically characterized by early-onset. Some children present myopathy, others liver failure in infancy, and some multisystem involvement. Consistent with the different phenotypes, mtDNA depletion may affect either a specific tissue (most commonly muscle or liver and brain) or multiple organs, including heart, brain, and kidney (Viscomi and Zeviani, 2017). This group of pathologies are usually classified as myopathic, encefalomyopathic and hepatocerebral.

1.3 Mitochondrial aminoacyl-tRNA synthetases and related mitochondrial diseases

Some mitochondrial disorders result from genetic defects that impair mitochondrial protein synthesis. Mutations in any component of the translation machinery can affect the mitochondrial respiratory chain complexes containing mtDNA-encoded subunits (cI, cIII, cIV, cV), with the preservation of complex II, the only complex that has no mtDNA-encoded proteins. Mutations in mitochondrial tRNAs, aminoacyl-tRNA synthetases (aaRSs), elongation factors and ribosomal proteins were identified (Rötig, 2011). These mutations result in a broad spectrum of mitochondrial phenotypes and disorders (Riley *et al*., 2013).

The aminoacyl-tRNA synthetases are a group of enzymes critical for protein synthesis that are required for the recognition and conjugation of specific amino acids to their cognate mitochondrial tRNAs in a two-step reaction (Ibba and Söll*,* 2000):

1) amino acid + ATP → aminoacyl-AMP + PPi
2) aminoacyl-AMP + tRNA → amino acid-tRNA + AMP

The first stage is activation of the amino acid molecule; the synthetase binds ATP and the corresponding amino acid to form an aminoacyl-adenylate (aminoacyl-AMP), releasing inorganic pyrophosphate (PP_i). Then, the adenylate-aaRS complex binds the appropriate tRNA and the amino acid is transferred from the aminoacyl-AMP to the 2'- or the 3'-OH of the last tRNA nucleotide at the 3'-end.

As previously describe, mammalian mitochondria have a translational apparatus that synthesizes 13 proteins encoded in the mitochondrial genome. While two rRNAs and a full set of tRNAs are encoded in the mtDNA, all other translational factors, including aaRSs, are encoded in the nuclear genome (Nagao *et al.,* 2009). Two sets of synthetases are encoded by separate nuclear genes in human cells, distinguished by cytoplasmic (referred to as *aaRS*) or mitochondrial (referred to as *aaRS2*) localization, with the exception of GARS and KARS, which are present in both cellular compartments and are encoded by the same loci as cytoplasmic enzymes, with the mitochondrial isoforms being generated by alternative translation initiation (GARS) (Chihara *et al.,* 2007) or alternative splicing (KARS) (Tolkunova *et al.,* 2000). Nineteen aaRSs, including the two with the double position, operate within the human mitochondrial matrix, whereas the gene for mitochondrial glutamyl-tRNA synthetase (EARS2) efficiently misaminoacylates the mitochondrial $tRNA^{Gln}$ to form glutamate charged-$tRNA^{Gln}$ (Nagao *et al*., 2009).

Typically aaRSs structure presents a catalytic domain and an anticodon-binding domain; AARS2 has also an editing domain to deacylate mischarged amino acids (in particular serine and glycine), preventing the insertion of uncorrect amino acids during protein synthesis (Beebe *et al*., 2008).

aaRSs can be classified into two distinct group based on the structure of the catalytic site and on the mechanism of aminoacylation reaction: class I enzymes typically contain the classical Rossmann fold that displays five parallel β-strands connected via α-helices and two highly conserved sequence motifs, are monomeric or dimeric, and aminoacylate at the 2'-OH of the ribose in the last nucleotide located at the 3' terminus of the tRNA; class II enzymes display an alternate folding, mainly constituted by a sheet of six antiparallel β-strands and three motifs of less-conserved sequences and aminoacylate at the 3'-OH of the appropriate tRNA (Bonnefond *et al*., 2005 a, Eriani *et al.*, 1990). In the course of evolution aaRSs have acquired additional domains and insertions in addition to preexisting domains, which expanded the range of functions performed by these enzymes, in particular acquiring different non canonical functions such as regulation of apoptosis and translation, synthesis of rRNA, or tRNA export to the cytosol (Smirnova *et al*., 2012).

aaRS2 mutations have emerged as an important cause of mitochondrial translation disorders, usually characterized by early-onset and autosomal recessive transmission, that first lead to tissue and cell-type specific phenotypes, including central nervous system involvement (*CARS2*, *DARS2*, *EARS2*, *FARS2*, *GARS*, *IARS2*, *MARS2*, *NARS2*, *PARS2*, *RARS2*, *TARS2*, and *VARS2*); myopathy, lactic acidosis, and sideroblastic anemia (MLASA) (*YARS2*); hypertrophic cardiomyopathy (*AARS2*); sensorineural hearing loss and ovarian dysgenesis (Perrault syndrome) (*LARS2* and *HARS2*); and hyperuricemia, pulmonary hypertension, renal failure, and alkalosis (*SARS2*) (Sommerville *et al*., 2017).

The basis of cell- or tissue-specific damage remains unclear, since all mt-aaRSs are ubiquitous enzymes operating in the same pathway (Rötig, 2011). However, as previously mentioned, several cytoplasmic aaRSs have been found to have additional functions besides their role in protein synthesis, so it is possible that other functions of mitochondrial aaRSs influence the distinct pathogenesis of aminoacyl-tRNA synthetase disorders (Antonellis and Green, 2008).

1.4 Yeast *Saccharomyces cerevisiae* as model system for the study of human mitochondrial diseases

The yeast *Saccharomyces cerevisiae* is one of the most intensively studied model organisms to investigate the molecular and genetic basis of human diseases. Despite its simplicity, yeast shares many cellular activities and metabolic pathways with humans and for this reason *S. cerevisiae* has been defined "honorary mammal" (Resnick and Cox, 2000). It was the first eukaryote organism to have its genome fully sequenced and published (Goffeau *et al*., 1996). Remarkably, about 46% of human known proteins have homologs in yeast: among these, proteins involved in DNA replication, recombination, transcription and translation, cellular trafficking and mitochondrial biogenesis were found (Venter *et al*., 2001). Moreover, about 40% of human genes, mutations of which lead to diseases, have an orthologue in yeast (Bassett *et al*., 1996). For this reason yeast has been widely used to study molecular mechanisms underlying human diseases. The study of mitochondrial functions and dysfunctions and related mitochondrial diseases is of a special interest in yeast, because in this organism mitochondrial genetics and recombination have been discovered (Bolotin *et al*., 1971). Specific reasons led to choose *S. cerevisiae* for mitochondrial studies. The most important characteristic of *S. cerevisiae* is that it can survive even in the absence of respiratory functions and in the presence of partial or total deletions of mtDNA, so in the absence of the respiratory chain complexes. In fact, yeast metabolism is regulated in accordance to carbon sources and oxygen availability. When grown in the presence of glucose, yeast produce ATP using glycolysis, while respiration is almost completely suppressed. When glucose is exhausted there is a rapid metabolic shift from fermentation toward respiration, with the induction of all the genes encoding for subunits responsible for oxidative phosphorylation. Although glucose is the preferred source, yeast is able to use oxidative carbon sources as glycerol, ethanol, acetate and lactate. These carbon sources require functioning mitochondria, and are commonly exploited in mitochondria-related research to investigate mitochondrial dysfunctions. Moreover, yeast is the only eukaryote able to survive in the absence of both mitochondrial function and mtDNA, provided that a fermentable carbon source is available. Thus, *S. cerevisiae* is a useful model for the study of MD as phenotypes related with the mitochondrial dysfunction can be easily observed. Mutations that affect mitochondrial functionality generally induce simple phenotypes such as reduction/inhibition of the oxidative growth or alteration of the respiratory activity. Furthermore it is possible to determine if pathologic mutations are associated with mtDNA instability or with an increased of point mutations. Yeast mutants with impaired OXPHOS function,

defined respiratory-deficient mutants (RD), are distinguishable respect to respiratory sufficient strain for their morphology and physiology. In presence of low concentration of glucose as fermentable carbon source and high concentration of ethanol as oxidative carbon source they give rise to small colonies, so called *petite* mutants. The small size of *petite* mutants depends on their inability to metabolize the ethanol present in culture and this consequently results in a slow replication rate (Ephrussi *et al*., 1949). *Petite* colonies arise from mutations in genes for OXPHOS components encoded both by nuclear or mitochondrial genome. Given the higher occurence of mutations in mtDNA, compared to nDNA, the frequency of *petite* mutants is associated with the instability of the mitochondrial genome. For mutations that affect the mtDNA it is possible to distinguish rho$^-$ mutants with deletions on mtDNA, and rho^0 mutants with a complete loss of mtDNA (Dujon 1981; Tzagoloff & Dieckmann 1990).

Different approaches have been used in the study of human diseases in yeast. When a homolog of the gene involved in the disease is present in the yeast genome, the mutation can be introduced in the yeast gene and its effects can be evaluated both at a physiological and molecular level. Conversely, when the disease-associated gene does not have the counterpart in yeast the transgene can be heterologously expressed in yeast and the resulting strain can be subjected to functional analysis. Furthermore the possibility to duplicate as haploid or diploid makes this organism a flexible tool for assessing the dominant or recessive nature of a mutation.

1.4.1 Human *MPV17*-related hepatocerebral MDS and model organisms

The human *MPV17* gene, located on chromosome 2p23-21, encodes a small protein of 176 aminoacids (Karasawa *et al*., 1993) characterized by four predicted transmembrane spans and located in the inner mitochondrial membrane (Spinazzola *et al*., 2006) (figure 1.2).

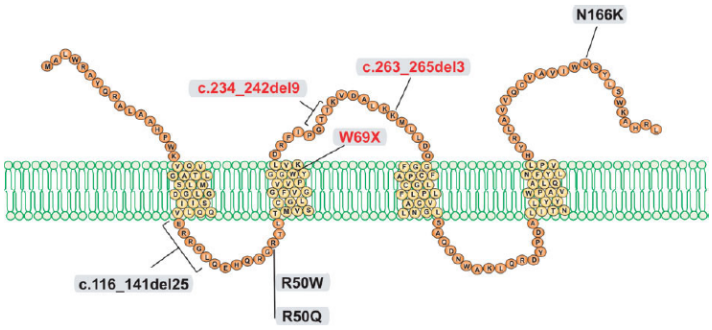

Figure 1.2. Schematic representation of the Mpv17 protein based on bioinformatic prediction models and relative localization of some the mutations identified (from Wong *et al*., 2007).

Mutations in *MPV17* were first described as causing hepatocerebral MDS (Spinazzola *et al.,* 2006) and Navajo neuro-hepathopathy (Karadimas *et al*., 2006). Since then, more than 30 different *MPV17* mutations were identified confirming these inherited autosomal recessive mutations as prominent cause of hepatocerebral MDS, accounting for about 50% of the cases. However, the functional link between Mpv17 and mtDNA maintenance is not yet completely understand.

The clinical presentations associated with *MPV17* mutations are rather broad, with hepatic and neurologic manifestations that appear to be the most characteristic findings. Typically, the disease-onset is between neonatality and childhood (El-Hattab *et al*., 2010), although several patients with adult-onset presentation of neuropathy and leukoencephalopathy with multiple mtDNA deletions in skeletal muscle have been described, indicating that *MPV17* mutations are associated with an evolving broader phenotype (Blakely *et al*., 2012; Garone *et al*., 2012).

All early-onset patients identified typically presented liver dysfunction, comprising cholestasis, jaundice and coagulopathy (El-Hattab *et al*., 2017 a). Most cases deteriorate to liver failure, which is the main cause of death for this pathology. In addition to hepatic damage, most young patients present neurologic manifestations, mainly involving developmental delay and hypotonia. Motor and sensory peripheral neuropathy and leukoencephalopathy were also described. Besides hepatic and neurologic indications, hepatocerebral MDS can result in metabolic manifestations, such as lactic acidosis and hypoglycemia, and it has frequently been observed that patients fail to thrive. Individuals with Navajo neurohepatopathy, prevalent in the Navajo community in the Southwestern United States, who were found to have homozygous p.Arg50Gln mutation in Mpv17 may manifest the pathology later in childhood (Karadimas *et al*., 2006). Three main subtypes of this pathology exist: infantile (onset <6 months) and childhood (<5 years) forms, characterized by hypoglycemic episodes and severe progressive liver dysfunction requiring liver transplantation, and a “classic” form characterized by moderate hepatopathy and progressive motor and sensoryaxonal neuropathy (Nogueira *et al.,* 2014).

At molecular level the mtDNA content is severely reduced in liver tissue, but can also be reduced in muscle tissue. Electron transport chain complexes activity assays in liver and muscle tissue typically show decreased activity of multiple complexes with complex I, III and IV that are the most affected (El-Hattab *et al.,* 2010).

A high degree of conservation has been observed between human *MPV17* and its mouse (*MPV17*), zebrafish (*TRA*) and yeast (*SYM1*) orthologs, respectively, although mutants in these genes show very different phenotypes.

MPV17 gene was first identified in a mouse strain, in which the *MPV17* gene was knocked out by random insertional inactivation with a recombinant retrovirus in the genome of mouse embryonic stem cells. The mutant mouse strain obtained showed renal disease characterized by focal segmental glomerulosclerosis and consequential nephrotic syndrome. *MPV17* mutant mice developed disease in early adulthood (2–3 months after birth) and most of them died of renal failure after 18 weeks of life (Weiher *et al*., 1990). In addition to renal phenotype, these mutant mice revealed also deterioration of the inner ear structures leading to hearing loss (Meyer zum Gottesberge and Felix, 2005). In mice, development of the mutant phenotype was prevented through transgenesis with human *MPV17*, indicating functional equivalence between the homologous (Schenkel *et al*., 1995).

The human homologous was identified by interspecific ibridization (Karasawa *et al*., 1993; Weiher, 1993). Sequence analysis revealed over 90% identity in a region coding in human for a protein of 176 amino acids. As previously mentioned the human *MPV17* gene, located on chromosome 2p23-21, encodes for an integral protein of the inner mitochondrial membrane, characterized by four predicted transmembrane spans. Its presence has been demonstrated in pancreas, kidney, muscle, liver, lung, placenta, brain and heart (Spinazzola *et al*., 2006). The import of the Mpv17 protein into the mitochondria is not mediated by a classical N-terminus sequence subsequently removed, contrary to what is usually seen for most protein of the inner mitochondrial membrane or mitochondria matrix protein (Spinazzola *et al*., 2006).

To understand the function of Mpv17 in mitochondrial biogenesis and the mechanism leading to tissue-specific mtDNA depletion, another *mpv17*$^{-/-}$ mouse model was created and studied. It was observed that in young mice, as in humans, the ablation of Mpv17 determines a profound reduction in mtDNA content in liver and, to a lesser extent, in skeletal muscle, but neither in brain nor in kidney (Viscomi *et al*., 2009). Measurement at different ages revealed that in wild type mouse the content of mtDNA in liver and muscle varied over time, contrariwise it remained constantly low throughout life in the same tissues of *mpv17*$^{-/-}$ mice. However, the absolute mtDNA content and its age-dependent variation were similar in the mutant and in the wild type mice brain. Although the role of Mpv17 remains elusive, these results demonstrate that the absence of this protein impairs a dynamic control on mtDNA copy number, in a tissue-specific and possibly developmentally regulated manner (Viscomi *et al*., 2009). The low mtDNA content in liver was associated with surprisingly mild morphological alterations of its cytoarchitecture, whereas, at the ultra structural level, mitochondria of *mpv17*$^{-/-}$ were profoundly altered, especially in 5-month and older mice. Mitochondria became ballooned, the *cristae* disappeared, an electron-dense amorphous material accumulated in the matrix; similar modification was observed

also in patients harbouring mutation in *MPV17* (Wong *et al*., 2007), in other hepatocerebral MDS (Mandel *et al*., 2001), and in yeast model (Dallabona *et al*., 2010).

The yeast *Saccharomyces cerevisiae* is a suitable model to evaluate the pathological effects of *MPV17* mutations related with MDS and to study molecular mechanisms underlying the pathology, thanks to the presence of the functional orthologous gene *SYM1*, coding for a protein of the inner mitochondrial membrane (Trott and Morano, 2004). The protein sequence of Sym1 shares high homology with Mpv17 (figure 1.3) and a strong conservation of transmembrane domains architecture with a proposed topology of four transmembrane spans in a N_{out}/C_{out} orientation (Trott and Morano 2004, Reinhold *et al.,* 2012).

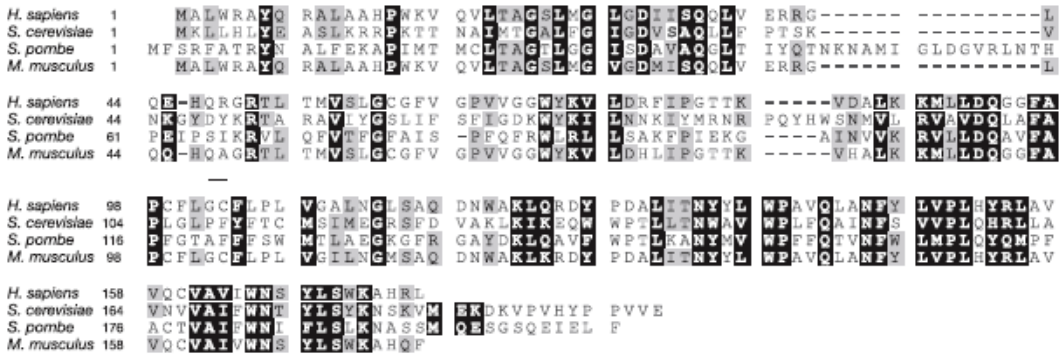

Figure 1.3. ClustalW2 sequence alignment of Sym1 orthologues in fungi and mammals. Black boxes indicate 100% similarity, and grey boxes indicate 75% similarity (from Reinhold *et al*., 2012).

The deletion of *SYM1* in *S. cerevisiae* being complemented by the expression of the human *MPV17* gene and the absence of *SYM1* functional paralogues has established Sym1 as a good model for the study of Mpv17 function (Trott and Morano 2004). In yeast, another protein shows sequence similarity to Mpv17, Yor292c. This protein was localized in the vacuole in a large-scale study (Huh *et al.*, 2003). Experiments performed in our laboratory did not reveal any role for this protein on mitochondrial function, as its open reading frame deletion did not affect oxidative growth nor mtDNA stability. Furthermore, the *sym1Δ* phenotype is not worsened by *YOR292c* deletion, suggesting that the function is not redundant (Dallabona, Ph.D. thesis).

Sym1 protein is required for OXPHOS metabolism in stress conditions (high temperature, high ethanol concentration), with a role in controlling the flux of Krebs' cycle intermediates, e.g. alpha-ketoglutarate and/or oxalacetate, across the mitochondrial membrane (Dallabona *et al.*, 2010). In addition, point mutations equivalent to those found in patients affected by MDS, cause mtDNA instability, leading to

increased accumulation of mitochondrial respiratory deficient "*petite*" mutants (Spinazzola *et al*., 2006). Moreover, studies performed in our laboratory, based on blue native gel electrophoresis, have demonstrated that Sym1 takes part within a high molecular weight complex >600 kDa, the composition of which is, however, unknown (Dallabona *et. al*, 2010). By reconstitution into lipid bilayers, Sym1 has been confirmed to aggregate in a high molecular weight complex to form a membrane pore in the inner mitochondrial membrane, whose dimension is sufficient to allow the transport of large molecules such as metabolites across the inner mitochondrial membrane (Reinhold *et al*., 2012). The role of Mpv17 as Δψm-modulating channel that apparently contributes to mitochondrial homeostasis under different conditions, such as membrane potential, redox state, pH, and protein phosphorylation, was more recently demonstrated also for the human protein (Antonenkov *et al.*, 2015). However the physiological role of the channel and the nature of the cargo remain elusive. Notably, in both cell cultures and mouse tissues, Mpv17 is part of a high molecular weight complex of unknown composition, which is essential for mtDNA maintenance in critical tissue, i.e. liver, of a *MPV17* knockout mouse model (Bottani *et al*., 2014), these findings confirm yeast as a good model for the study of the molecular mechanisms underlying the pathology.

More recently, it was demonstrated in a *mpv17*$^{-/-}$ mouse model, characterized by a significant reduction of mtDNA in liver cells, that liver mitochondria displayed reduced levels of dGTP (30% relative to the wild-type) and dTTP (35% of wild-type), whereas there was no decrease in mitochondrial dNTPs levels in kidney or brain, suggesting that mitochondrial nucleotide insufficiency is responsible for the depletion of mtDNA in the liver of the *mpv17*$^{-/-}$ mice (Dalla Rosa *et al.*, 2016). Furthermore, to evaluate the effect of the nucleotide insufficiency on DNA replication, the intermediates of mitochondrial DNA replication in *mpv17*$^{-/-}$ were analysed, identifying high abundance of the replication intermediates. This result indicates that many mtDNA molecules are in the process of being replicated in liver mitochondria lacking Mpv17. The increase in mitochondrial replication intermediates, associated with mtDNA loss and nucleotide insufficiency, suggested that the rate of mtDNA replication is much slower than normal in the liver of the *MPV17* ablated mouse. Together these data suggested that loss of function of Mpv17 causes nucleotide insufficiency in the mitochondria that slows rate of mtDNA replication and induce mtDNA depletion (Dalla Rosa *et al*., 2016). Also in quiescent Mpv17-deficient human fibroblasts it was observed a marked decreases in all three dNTPs (dTTP, dGTP and dCTP) that could be quantified (dATP levels were disregarded owing to the low values obtained for the control). Notably, nucleoside supplementation in the culture medium was able to prevente mtDNA depletion in the quiescent Mpv17-deficient fibroblast lines (Dalla Rosa *et al*., 2016).

In zebrafish, the loss of the orthologous gene (*TRA)* results in a severe decrease of pigment cells iridophores (Krauss *et al*., 2013). As these cells have a special requirement of guanine, it has been suggested that iridophores death in *tra* mutant might be the result of mitochondrial dysfunction, consistent with a defect in the import of either dGTP or its precursors.
Actually, despite these findings, the specific function of Mpv17 remains elusive.

1.4.2 Human *YARS2*-related MLASA and yeast as model organism

YARS2 encodes for the mitochondrial tyrosyl-tRNA synthetase (Yars2) that performs mitochondrial tyrosyl-tRNA aminoacylation by coupling tyrosine to its cognate mitochondrial tyrosyl-tRNA.
The structure of Yars2 consists in a conserved organization with an N-terminal catalytic domain followed by the C-terminal anticodon-binding region (figure 1.4) (Bonnefond *et al*., 2007 b). Among aminoacyl-tRNA synthetases, tyrosyl-tRNA synthetases present unique features. Although they belong to class I synthetases with the highly conserved sequences ‘‘HIGH’’ and ‘‘KMSKS’’ and a Rossmann-fold catalytic domain (Bedouelle 2005, Bonnefond *et al*. 2005), they act as homodimers and recognize tRNA from the major groove side of the amino acid acceptor stem, in a way reminiscent to what was found for class II synthetases (Bedouelle and Winter, 1986; Lee and RajBhandary, 1991; Yaremchuk *et al.*, 2002).

Figure 1.4. Organization of human mitochondrial tyrosyl-tRNA synthetase. The catalytic domain (orange), with the location of the HVGH and KLGKS signature sequences (blue), is disrupted by the CP1 (connective peptide 1) in black. The anticodon binding region includes the helical α-ACB (anticodon binding) domain (green) and the S4-like (S4 ribosomal protein-like) domain (yellow) for entire mt-TyrRS. The N-terminous mitochondrial targeting sequence (MTS) in the native enzyme is shown. Location of cysteine residues is indicated by SH-labeled lines (from Bonnefond *et al*., 2007 b).

Mutations of *YARS2* have been described predominantly in patients with autosomal recessive MLASA syndrome (myopathy, lactic acidosis, and sideroblastic anemia) with mitochondrial respiratory chain complex deficiencies (Riley *et al*., 2010; Riley *et al*., 2013; Sasarman *et al*., 2012; Shahni *et al*., 2013; nakajima *et al*., 2014; Ardissone *et al*., 2015). *YARS2*-related mitochondrial disease is phenotypically heterogeneous and has a variable prognosis ranging from infantile-onset- and often fatal-MLASA

syndrome to later adolescent-onset, slowly progressive myopathy. Progressive respiratory muscle weakness and cardiomyopathy are the major causes of death in these patients.

The MLASA syndrome was first described in patients with mutations in *PUS1* gene, (Bykhovskaya *et al*., 2004) coding for pseudouridylate synthase 1, a tRNA-modifying enzyme. Later it was identified in patients with *YARS2* mutations and with a clinically similar phenotype. Mutations in these genes lead to a decreased mitochondrial protein synthesis resulting in mitochondrial respiratory chain dysfunction (Riley *et al*., 2010, Riley *et al.,* 2013). Most recently, MLASA was described in 2 patients: one of these with a novel de novo heteroplasmic mutation in the mtDNA encoded *ATP6* gene, the first mtDNA point mutation associated with the MLASA phenotype (Burrage *et al*., 2014); the other patient harboured a heterozygous mutation in *LARS2* gene, mutations of which typically it was not associated with MLASA (Riley *et al*., 2016). Although rare, sideroblastic anemia is a prominent feature in Pearson syndrome caused by single, large-scale mtDNA deletions (Pearson *et al*., 1979, McShane *et al.,* 1991).

Until now a total of 17 patients has been identified carrying mutations in *YARS2* localized in both the catalytic domain and in the anticodon-binding region. Fifteen individuals (88%) exhibited an elevated blood lactate level accompanied by generalized myopathy; only 12 patients (71%) manifested with sideroblastic anemia. Hypertrophic cardiomyopathy (9 [53%]) and respiratory insufficiency (8 [47%]) were also prominent clinical features. Central nervous system involvement was rare. Muscle studies showed global cytochrome-c oxidase deficiency in all patients tested and severe, combined respiratory chain complex activity deficiencies (Sommerville *et al*., 2017). In table 1 a summary of the clinical features of all 17 patients is reported. In any case a definite correlation between genotype-phenotype is difficult to draw since the small number of patients reported in the literature (Ardissone *et al*., 2015).

No	Ethnicity	Myopathy/ Exercise intolerance	Respiratory insufficiency	Cardiomyopathy	SA/ Transfusion dependent	Lactic acidosis	Muscle biopsy		*YARS2* gene	
							Histochemistry	RC deficiency	cDNA change	Amino acid change
1.1 (M)	Scottish	Yes (MRC 4/5)	No	Yes, high output cardiac failure	Yes/No	Yes	Global COX deficiency	CI, CIII, CIV	Homozygous c.1175T>C	Homozygous p.Leu392Ser
1.2 (M)	Scottish	Yes	n.d.	Yes, high output cardiac failure	Yes/No	Yes	n.a.	n.a.	n.d.	n.d.
2 (F)	Scottish	Yes (MRC 4-/5) & facial weakness)	NIV at age 55	No	No	n.a.	Global COX deficiency	CI, CIV	Homozygous c.1175T>C	Homozygous p.Leu392Ser
3 (M)	Irish/Scottish	Yes (MRC 4/5)	Severe restrictive pattern	Yes	No	Yes	Global COX deficiency, RRF	CI, CIII, CIV	c.1106G>A/ c.1147_1164dup	p.Cys369Tyr/ p.Val383_Glu388dup
4.1[8] (M)	Jordanian	Yes (MRC 4/5)	Yes	Yes	Yes/ Yes	Yes	Global COX deficiency	CI, CIV	Homozygous c.137G>A	Homozygous p.Gly46Asp
4.2 (M)	Jordanian	Yes (MRC 3/5), scapular winging, facial & neck flexor weakness	NIV at age 33	No	Yes/No	n.a	RRF	n.d	n.d	n.d
5[9] (M)	Turkish	Yes (axial hypotonia)	n.d.	Yes	Yes	Yes	n.d.	n.d.	Homozygous c.1303A>G	Homozygous p.Ser435Gly
6[10] (M)	Lebanese	Yes (generalised weakness & ptosis)	NIV at age 12.5	Yes	Yes/Yes	Yes	n.d.	n.d.	Homozygous c.156C>G	Homozygous p.Phe52Leu
7[11] (M)	Lebanese	Yes (including ptosis & ophthalmoparesis)	n.d.	No	No	Yes	Reduced COX, increased SDH	CI, CIII and CIV	Homozygous c.137G>A	Homozygous p.Gly46Asp
8.1[12] (M)	Lebanese	Yes (wheelchair dependent)	Ventilatory support at age 17	Yes	Yes/Yes	Yes	Reduced COX, incipient RRF	CI, CIV	Homozygous c.156C>G	Homozygous p.Phe52Leu
8.2[12] (F)	Lebanese	Yes	n.d.	No	Yes/Yes	Yes	n.d.	CI, CIII and CIV	Homozygous c.156C>G	Homozygous p.Phe52Leu
9[12] (F)	Lebanese	Yes	n.d.	No	No	Yes	Lipids vacuoles	CI, CIV	Homozygous c.156C>G	Homozygous p.Phe52Leu
10[13] (F)	Lebanese	Yes	Mechanical ventilation	Yes	Yes/Yes	Yes	n.d.	CI, CIII and CIV	Homozygous c.156C>G	Homozygous p.Phe52Leu
11[13] (F)	Lebanese	Yes	FVC 70% predicted value	No	Yes/Yes	Yes	n.d.	n.d.	Homozygous c.156C>G	Homozygous p.Phe52Leu
12[13] (F)	French	Yes (nystagmus & strabismus)	n.d.	Yes, resolved	Yes/No	Yes	n.d.	n.d	c.572G>A/ c.1078C>T	p.Gly191Asp/ p.Arg360*
13.1[3] (M)	Italian	No	n.d.	No	Yes/No	Yes	Few hypo-atrophic fibers	CI, CIII and CIV	Homozygous c.933C>G	Homozygous p.Asp311Glu
13.2[3] (F)	Italian	No	n.d.	No	Yes/ probable	Yes	n.d.	n.d.	Homozygous c.933C>G	Homozygous p.Asp311Glu

*= deceased, CI= complex I, CIII= complex III, CIV= complex IV, COX= cytochrome *c* oxidase, F= female, M= male, n.d.= not done, NIV= non-invasive ventilation, RC= mitochondrial respiratory chain; RRF= ragged red fibres, SA= sideroblastic anaemia.

Table 1. Summary of the clinical features of 17 *YARS2* patients (from Sommerville *et al.*, 2017).

Recently, in our laboratory, *S. cerevisiae* model was created and studied in order to validate the pathological role of a new missense mutation in *YARS2* gene taking advantage of the presence in yeast of the orthologous gene *MSY1* (Ardissone *et al.,* 2015). The homologous mutation (c.933C>G p.Asp311Glu) was identified in two Italian siblings and was located in the anticodon-binding domain, involved in the interaction with the anticodon of the cognate mitochondrial tyrosyl-tRNA. The results obtained clearly indicated that the human *YARS2* mutation was deleterious in yeast and allowed to validate the pathological role of the mutation.

1.4.3 Human GatCAB complex and mitochondrial diseases and yeast as model organism

Traslational accuracy is required to properly decipher the genetic code to form proteins. The fidelity of protein synthesis largely depends on the formation of correct aminoacyl-tRNAs (aa-tRNAs) by the corresponding aminoacyl-tRNA synthetases (aaRSs).

aaRSs are highly specific enzymes, but in some case, non discriminating attachment can accur. Gln-tRNA formation is the least conserved mechanism of aminoacyl-tRNAs synthesis found in nature, and is generated by kingdom-specific pathways that guarantee correct glutamine incorporation during protein synthesis (Ibba and Söll 2004). In the eukaryotic cytoplasm and in some bacteria, a single cytosolic glutaminyl-tRNA synthetase (GlnRS) attaches glutamine directly to tRNA (figure 1.3). On the contrary, a different two-step pathway found in most bacteria and all archaea employs a pretranslational modification to generate Gln-tRNA^{Gln} (figure 1.5). First, a nondiscriminating glutamyl-tRNA synthetase (GluRS), which is able to synthesize both Glu-tRNA^{Glu} and Glu-tRNA^{Gln} generates a mischarged Glu-tRNA^{Gln} (Lapointe *et al*. 1986; Sekine *et al*. 2001). The resulting mischarged tRNA is then converted by glutamyl-tRNA^{Gln} amidotransferase (GluAdT), in presence of ATP and glutamine as an amide donor, into Gln-tRNA^{Gln} (Feng *et al*., 2004, Nagao *et al*., 2009).

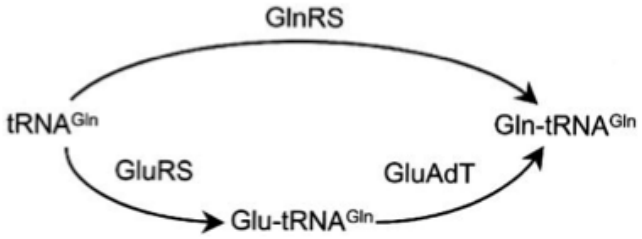

Figure 1.5. Pathways to Gln-tRNA^{Gln} formation. The direct aminoacylation pathway (top) and the transamidation pathway (bottom) are both abundant in nature. GluAdT refers to the tRNA-dependent amidotransferase of the transamidation pathway (from Rinehart *et al*., 2005).

Mitochondria and chloroplasts, in line with their bacterial ancestry, have the same mechanism of aa-tRNA synthesis with bacteria and archaea (Yang *et al*., 1985; Schön *et al*., 1988; Woese *et al.,* 2000). Proteins orthologous to bacterial amidotransferases are frequently found in the nuclear genomes of most eukaryotes. Bacterial and human mitochondrial amidotransferases are heterotrimeric enzymes, called GatCAB consisting of A, B, and C subunits. The first step of the transamidation reaction is the phosphorylation by the GatB subunit that uses ATP to phosphorylate the Glu moiety on the Glu-

$tRNA^{Gln}$, forming a γ-phosphoryl-Glu-$tRNA^{Gln}$ as an activated intermediate. Second, the GatA subunit catalyzes the amidation of the activated phosphorylated intermediate using the liberated ammonia from amide donor glutamine to form Gln-tRNA (Wilcox, 1969; Feng *et al.,* 2005; Nagao *et al*., 2009). GatC codes for a stable subunit of the complex required for linking and correct folding of the catalytic subunits GatA-GatB (Curnow *et al.,* 1997, Nakamura *et al.*, 2006). In human cells the three subunits A, B and C are coded by the *QSRL1, GATB* (also known as *PET112*) and *GATC* genes, respectively (Echevarria *et al.,* 2014 Nagao *et al.,* 2009).

As previously described, defects in genes encoding aminoacyl-tRNA synthetases cause a broad spectrum of mitochondrial disorders. Recently, mutations in the GatCAB subunit *QRSL1* has been identified in a large scale study in patients with a lethal infantile mitochondrial disorder. In particular, 3 patients with mutations in *QRSL1* gene were identified: a girl with tachypnea, hypertrophic cardiomyopathy, adrenal insufficiency, hearing loss, and combined respiratory chain complex deficiencies (I, II, III, and IV), harbored a homozygous mutation c.398G>T (p.G133V); her older brother, also ill, harbored the same homozygous mutation; a third patient harbored the compound heterozygous mutations c.350G>A (p.G117E) and c. 398G>T (p.G133V) (Kohda *et al.,* 2016).

More recently, other patients with defects in the GatCAB complex were identified. In particular, these patients presented mutations in the novel gene *GATB* in addition to mutations in the *QRSL1* gene. The impaired functionality of the complex resulted in a severe clinical phenotype with prominent cardiomyopathy and lethal infantile lactic acidosis, with variable deficiencies of the respiratory chain enzymes, which is typical for defects in mitochondrial tRNA aminoacylation (paper in submission).

In yeast, mitochondrial glutaminyl-$tRNA^{Gln}$ was shown to be formed by a transamidation pathway, similar to that operating in the human mitochondria (Frechin *et al*., 2009), involving an heterotrimeric transamidase named GatFAB. The GatA and GatB subunits are coded by *HER2* and *PET112* nuclear genes, respectively. The *HER2* and *PET112* gene products of *S. cerevisiae* share significant sequence similarity with the GatA and GatB products, respectively, to those of bacterial and eukaryotic GatCABs. These genes are essential for mitochondrial function; in fact, disruption of these genes destabilized the mitochondrial genome, causing cells to become rho^{-} (Mulero *et al*., 1994, Merz and Westermann *et al*., 2009). The subunit F of the complex coded by *GTF1* not share sequence similarity with the GatC subunit (Barros *et al*., 2011). Based on these observations, *S. cerevisiae* is a suitable model to evaluate the pathological role of mutations that affect the human GatA and GatB subunits.

1.5 Drug discovery for the treatment of mitochondrial disease: *S. cerevisiae* as a model

Actually, the treatment of mitochondrial diseases remains largely symptomatic and does not significantly alter the course of the diseaes (El-Hattab *et al*., 2017 b). In particular, management of MDS mainly consists in the symptomatic treatment for complications associated with these disorders. Treatment options include dietary modulation, cofactors and vitamins supplementation to support metabolism, liver transplantation, and stem cells transplantation (El-Hattab and Scaglia 2013). Liver transplantation has been performed for some individuals with hepatocerebral mtDNA depletion syndromes, which frequently progress to liver failure. However, liver transplantation in mitochondrial hepatopathy remains controversial, because of the multi-organ involvement and because neurological manifestations may occur or worsen after the transplantation (Thomson *et al.,* 1998). Another potential therapeutic approach was tested in a mouse model, in which the expression of Mpv17 was induced in *MPV17* mutant mice through gene replacement via an adeno-associated virus carrying human *MPV17*. As a consequence, mtDNA copy number was enhanced in liver restoring oxidative phosphorylation activity (Bottani *et al*., 2014). Recently, it was demonstrated that the supplementation with specific deoxiribonucleosides and/or inhibition of their catabolism are able to prevent the mtDNA depletion in different cell models, suggesting a potential strategy for the treatment of MDS (Camara *et al*., 2014, Dalla Rosa *et al.,* 2016).
Regarding the MLASA no specific curative therapies are available, early diagnosis and initiation of appropriate supportive therapy is likely to be important in the prevention of the long term complications of this disorder (Shanhi *et al*., 2013).

Drug discovery is a highly complex and multidisciplinary process whose goal is to identify compounds with therapeutic effects. The current paradigm for de novo drug discovery and development begins with identification of a potential target (usually a protein), and proceeds through validation of the target in animal and/or cell culture models, development and execution of a screening system to obtain small molecules that modulate the activity of the target, characterization and optimization of these small molecules, testing the efficacy, toxicity, and untoward effects of these molecules in animal and cell culture models, and finally a series of FDA-supervised clinical trials to evaluate safety, pharmacology, and efficacy in comparison to existing treatments for the same indications (Rowberg, 2001). Although the regulatory process has been streamlined by the FDA in recent years, the entire progression typically

lasts a decade, and costs at least $500 million for each drug reaching the market (Lipsky and Sharp 2001; Hughes 2002). It is therefore of interest from commercial, economic and medical viewpoints, an improvement and acceleration of the drug discovery and development process at virtually any step (figure 1.6).

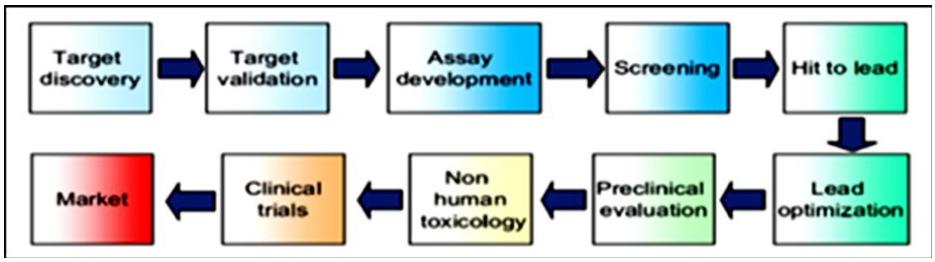

Figure 1.6. Diagram of the de novo drug discovery process (from Carnero, 2006).

For this reason current approaches to drug discovery require an assay that can test simultaneously hundreds of thousands of compounds, hence high throughput screenings (HTS) have become the major tools in this field. HTS allow the isolation of dozen to thousands of molecules to be further tested and ranked for development priority. In general HTS assay formats can be classified into two types; in vitro target-based biochemical assays and cell-based assays. In vitro target-based biochemical screening is an effective approach with a well-defined pathology and highly validated target. Its biggest advantage is that the exact target and mechanism of action are known. However, many of the most commonly used drugs function through unknown mechanisms and target-based approaches have a few drawbacks. First, the success of target-centric approaches hinges on correctly predicting the link between the chosen target and disease pathogenesis. Second, this biased approach may not actually target the best or most "druggable" protein to provide optimal rescue. Third, it is not always possible to accurately predict the activity of compounds in vivo. Finally, the small molecules obtained in vitro may have chemical drowbacks that preclude efficacy in vivo, including entry into cells, solubility, metabolism, distribution, excretion, and off-target effects. These potential pitfalls can hinder the validation of a compound in a cellular or animal model. In contrast, cell-based assays first, do not require a known target; screens may identify compounds targeting completely unexpected proteins or pathways. Second, in vivo screening more likely identifies drug-like molecules that (a) can get into cells, (b) are not readily metabolized, and (c) are not cytotoxic at effective concentrations.

The most significant barrier in cell-based screens is determining a compound mechanism of action and

protein target. However, the genetic tractability of model organisms offers new approaches for target discovery, although this is often difficult. Of course, a limiting factor for cell-based screening is that a compound potential is only as valid as the model from which it was derived (Tardiff and Lindquist, 2013). Cellular screens should ideally be performed with cells of human origin, which evidently provide the most physiologically relevant model system. However, human cells are expensive to culture and sometimes difficult to propagate in automated systems used for HTS. Yeast has emerged as powerful tool for drug discovery. It represents an inexpensive and simple alternative system to mammalian culture cells for the analysis of drug targets and for the screening of compounds. In fact, thanks to the high degree of conservation of basic molecular and cellular mechanisms between yeast and human cells the function of human proteins can often be reconstituted and aspects of some human physiological processes can be recapitulated. One major advantage of yeast over mammalian cells is provided by the versatile genetic malleability of this organism. This characteristic of yeast, as well as the long scientific experience in yeast genetics and molecular biology, has allowed the development of experimental tools and genetic selection systems that can be readily converted to HTS formats for drug discovery. These molecular and cellular tools include advanced plasmid systems, homologous recombination techniques and the easy application of conditional growth selection systems. Despite its numerous advantages, yeast assays are not without limitations for the purposes of drug discovery. In particular, the high concentration of compound often required to produce a biological response, likely due to the barrier presented by the cell wall, and the presence of numerous active efflux pumps and detoxification mechanisms (Smith *et al*., 2010). In addition, although many core processes are conserved between yeast and human, several "metazoan-specific" processes are not (Table 2).

Technology	*In vitro* HTS	Mammalian cellular HTS	Yeast cellular HTS
Pros	• A well-optimized assay has less data scatter than a cellular assay	• Target protein is presented in its native conformation in a physiological environment • Selection for membrane permeability and against cytotoxicity • Eukaryotic environment • Self-renewal system	• Genetic malleability and established wealth of genetic tools for analysis of biological functions • Target protein is presented in its native conformation in a physiological environment • Selection for membrane permeability and against cytotoxicity • Clean read-out in a heterologous, yet eukaryotic environment • Self-renewal system • Simple handling • Fast discrimination of real hits from false positives
Cons	• Target protein has to be purified and biochemically characterized • No self-renewal system • Suitable substrate must be identified and synthesized	• Function of the target protein is influenced by redundant cellular processes • Difficulty to discriminate real hits from false positives • Difficult and time-consuming genetic manipulations	• Reduced sensitivity to defined compound classes owing to efficient drug efflux pumps
Costs	• Expensive: protein purification, synthesis of substrate	• Expensive culture conditions	• Inexpensive culture conditions

Table 2. Comparison summary between in vitro HTS, mammalian cellular HTS and yeast cellular HTS (from Barberis *et al*., 2005).

Over the last decade, chemical screenings based on phenotype, named phenotype-based screenings, were used to find new potential therapeutic compounds (Mayer *et al*., 1999; Mundy *et al*., 1999; Haggarty *et al*., 2000). Recently, Couplan and collaborators developed a two-step yeast phenotype-based assay, called "Drug drop test", to identify active compounds with beneficial effects for human mitochondrial diseases affecting ATP synthase, in particular NARP (neuropathy, ataxia, and retinitis pigmentosa) syndrome. A suitable yeast model of such disorders is the deletion mutant for the nuclear gene *FMC1* that encodes a protein required at high temperatures (35-37°C) for the assembly of the F1 sector of ATP synthase. Indeed, when the *fmc1Δ* mutant is grown at high temperatures, its mitochondria contain fewer assembled ATP synthase complexes than a wild-type strain. The Drug drop test was composed of a primary screening in which about 12.000 compounds from various chemical libraries were tested for their ability to suppress the respiratory growth defect of the *fmc1Δ* mutant. Experimentally, *fmc1Δ* cells were spread on solid glycerol medium and exposed to filters spotted with the compounds. After incubation at 35°C, active compounds were then identified by a halo of enhanced growth around a filter (figure 1.7).

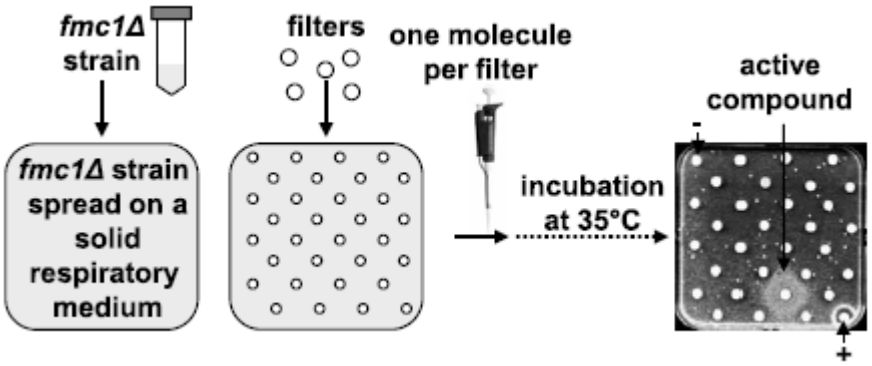

Figure 1.7. Schematic representation of the "Drug drop test" technique (from Couplan *et al*., 2011).

Active compounds, identified from primary screening, were tested in a secondary screening, on the five yeast *atp6*-NARP mutants which are the yeast models of the five most common mutations in *ATP6* related to NARP syndrome, using the same experimental procedure. The advantage of this method is that, in one simple experiment, numerous compounds were tested across a large range of concentrations, due to diffusion of the drugs in the growth medium. Through this approach, two compounds were identified as active. Further studies demonstrated that both these molecules were active also on human cells (Couplan *et al*., 2011).

A similar approach has recently used in yeast for the research of active molecules against mitochondrial disorders caused by mutations in the human *POLG* gene, which encodes for the catalytic subunit of the DNA polymerase γ, thanks to the presence of the orthologue gene *MIP1*. In this study, *mip1* mutated yeast strains carrying different thermo-sensitive mutations, which led to a high frequency of *petite* mutants at 37°C, were used. Using the "Drug drop test" method, six molecules, named MRS1-6, were identified as able to rescue the mutant phenotypes of the mip1 yeast strains. Interestingly one of these molecules, MRS3, was active also on *C. elegans* and human fibroblasts. This finding can lead the way, for MRS3, for a clinical trial in the search of treatments for human mitochondrial diseases related to *POLG* (Pitayu *et al.,* 2015). Altogether these results demonstrate that *S. cerevisiae* is a useful model for drug discovery approaches.

Aim of the research

The general purpose of this thesis was to create and study specific models of different mitochondrial diseases associated with mutations in the human genes *MPV17, YARS2, QRSL1* and *GATB* using *Saccharomyces cerevisiae* as a model system, taking advantage of the presence of the orthologous genes *SYM1, MSY1*, *HER2* and *PET112,* respectively. In particular:

MPV17

- First aim: to validate the potential pathological role of missense *MPV17* mutations identified in MDS patients and to investigate the molecular mechanisms by which the mutations lead to the pathology.
- Second aim: to search for an MDS treatment through a phenotypic screening of FDA-approved chemical libraries designed to identify molecules able to rescue the mitochondrial defective phenotypes induced by a pathogenic mutation in the *SYM1* gene. This drug discovery approach, through which several potential active compounds have been found, is the starting point to identify new pharmacological therapies aimed at recovering specific *MPV17* dysfunctions, thus improving the conditions of MDS patients.
- Third aim: to study the effect of increased dNTPs pool on mtDNA stability in *sym1* mutant strains through different strategies, a) overexpression of ribonucleotide reductase *RNR1* coding for the large subunit of ribonucleotide reductase which catalyses the rate-limiting step of dNTPs synthesis; b) deletion of its inhibitor *SML1* and c) supplementation of intermediates of dNTPs synthesis.

YARS2

Aim: to generate and study a *S. cerevisiae* model in order to evaluate the impact of six missense *YARS2* mutations, identified in MLASA patients, on mitochondrial phenotype, exploiting the presence of the orthologous gene *MSY1*. Furthermore, as part of the identification of beneficial molecules, I evaluated the capability of tyrosine supplementation, the specific substrate of tyrosyl-tRNA synthetase, to rescue the impaired respiratory rate on *msy1* mutant strains.

QRSL1 and *GATB*

Recently, new patients were identified with mutations in the *QRSL1* gene and in the novel *GATB* gene, coding for the subunit A and B of the GatCAB complex. Here I created specific yeast models and I evaluated the alleged pathological role of six missense mutations on mitochondrial functionality.

2. Results and discussion – Section I

2.1 Study of missense variants in conserved residues of Mpv17/Sym1

2.1.1 Study of the molecular mechanism of *MPV17* missense variants identified in hepatocerebral MDS patients

So far more than 30 mutations, spread through the entire *MPV17* sequence, were described. In particular nonsense, missense, deletion and insertion mutations have been identified in coding and splicing region of patients (table 3). The first aim of this section of the thesis was to study the pathological role of seven variants on mitochondrial functionality. The variants here studied are located in amino acids conserved between Mpv17 and Sym1, as shown by the protein alignment in figure 2.1 and in table 4.

The pathogenic role of the mutations R51Q, R51W, N172K, corresponding to the human mutations R50Q, R50W and N166K respectively, has already been demonstrated in yeast (Spinazzola *et al*., 2006). The validation of the potential pathological effect of the variants G24W, P104L, A168D and S176F corresponding to the human variants G24W, P98L, A162D and S170F respectively, was the first purpose of this thesis.

```
Mpv17   MALWRAYQRALAAHPWKVQVLTAGSLMGLGDIISQQLVER-RGLQEHQRGRTLTMVSLGC 59
Sym1    MKLLHLYEASLKRRPKTTNAIMTGALFGIGDVSAQLLFPTSKVNKGYDYKRTARAVIYGS 60
        * * : *: :*  :* ..:.: :*:*:*:**: :* *.   :  : ::  **   *  *.

Mpv17   GFVGPVVGGWYKVLD-----RFIPGTTKVDALKKMLLDQGGFAPCFLGCFLPLVGALNGL 114
Sym1    LIFSFIGDKWYKILNNKIYMRNRPQYHWSNMVLRVAVDQLAFAPLGLPFYFTCMSIMEGR 120
         :.. : . ***:*:     *  *     : : :: :** .***  *  ::. :. ::*

Mpv17   SAQDNWAKLQRDYPDALITNYYLWPAVQLANFYLVPLHYRLAVVQCVAVIWNSYLSWKAH 174
Sym1    SFDVAKLKIKEQWWPTLLTNWAVWPLFQAINFSVVPLQHRLLAVNVVAIFWNTYLSYKNS 180
        * :    *::.::  :*:**: :** .*  ** :***::** .*: **::**:***:*

Mpv17   RL--------------- 176
Sym1    KVMEKDKVPVHYPPVVE 197
        ::
```

Figure 2.1. CLUSTAL Omega alignment of the Mpv17 and Sym1 proteins. The missense variants conserved between the two proteins and analysed are shown in yellow.

Type of mutation	DNA Nucleotide Change	Protein Aminoacid Change	Protein Aminoacid Change in Yeast	Reference
Missense	c.62T>G	p.Leu21Arg	NC	Uusimaa et al 2014 - Al Hussaini et al 2014
	c.67G>C	p.Ala23Pro	NC	Uusimaa et al 2014
	c.70G>T	p.Gly24Trp	p.Gly24Trp	Spinazzola et al 2008
	c.107A>C	p.Gln36Pro	NC	Uusimaa et al 2014
	c.122G> A	p.Arg41Gln	NC	Choi et al 2015
	c.121C>T	p.Arg41Trp	NC	Uusimaa et al 2014 - Pyal et al 2017
	c.148C>T	p.Arg50Trp	p.Arg51Trp	Spinazzola et al 2006 - Wong et al 2007 - Vilarinho et al 2014
	c.149G>A	p.Arg50Gln	p.Arg51Gln	Spinazzola et al 2006 - Karadimas et al 2006 - El-Hattab et al 2010
	c.191C>G	p.Pro64Arg	NC	Uusimaa et al 2014 - Piekutowska-Abramczuk 2014
	c.197T>A	p.Val66Glu	NC	Kim et al 2016
	c.262A>G	p.Lys88Glu	NC	El-Hattab et al 2010
	c.263A>T	p.Lys88Met	NC	Garone et al 2012
	c.265A>T	p.Met89Leu	NC	Garone et al 2012
	c.278A>C	p.Gln93Pro	p.Gln99Pro	Uusimaa et al 2014 - Sarkhy et al 2014 - Al Hussaini et al 2014
	c.280G>T c.280G>C	p.Gly94Arg	NC	El-Hattab et al 2010 - Kim et al 2016
	c.293C>T	p.Pro98Leu	p.Pro104Leu	El-Hattab et al 2010 - Blakely 2012 et al - Uusima et al 2014 - Bijarnia-Mahay et al 2014 - Mendelson et al 2014 - Kim et al 2016
	c.485C>A	p.Ala162Asp	p.Ala168Asp	El-Hattab et al 2010
	c.498C>A	p.Asn166Lys	p.Asn172Lys	Spinazzola et al 2006 - Sarzi et al 2007
	c.509C>T	p.Ser170Phe	P.Ser176Phe	Kaji et al 2009
Nonsense	c.130C>T	p.Gln44Ter		Uusimaa et al 2014
	c.206G>A	p.Trp69Ter		Wong et al 2007
	c.359G>A	p.Trp120Ter		Spinazzola et al 2008
	c.408T>G	p.Tyr136Ter		Bijarnia-Mahay et al 2014
	c.428T>G	p.Leu143Ter		Garone et al 2012
In-frame deletion	c.234_242del9	p.Gly79_Thr81del		Wong et al 2007
	c.263_265del3	p.Lys88del		Wong et al 2007 - El-Hattab et al 2010
	c.271_273del3	p.Leu91del		El-Hattab et al 2010
Frame shift deletion	c.135delA	p.Glu45AspfsTer8		Uusimaa et al 2014
	c.116-141del26	p.Arg41ProfsTer24		Spinazzola et al 2006
Insertion	c.22_23insC	p.Gln8ProfsTer24		El-Hattab et al 2010
	c.451_452insC	p.Leu151ProfsTer39		Kaji et al 2009 - Kim et al 2016
Splicing site	c.IVS3+1G>T			Alsaman et al 2012
	c.70+5G>A			Navarro-Sastre et al 2008 - Navarro-Sastre et al 2010 - Navarro-Sastre et al 2012
	c.186+2T>C			El-Hattab et al 2010 - Nogueira et al., 2012
	c.279+1G>T			Uusimaa et al 2014 - Al Hussaini et al 2014
	c.461+1G>C			Uusimaa et al 2014
Large deletion	1.57 Kb deletion spanning exon 8			Spinazzola et al 2008 - El-Hattab et al 2010
	exons 3-8 deletion			Uusimaa et al 2014

Table 3. MPV17 pathogenic allelic variants and correspondent protein aminoacid change.

Mpv17	Sym1
G24W	G24W
R50Q	R51Q
R50W	R51W
P98L	P104L
A162D	A168D
N166K	N172K
S170F	S176F

Table 4. Equivalent variants in Mpv17 and Sym1.

To investigate the role of the seven missense variants, constructs carrying the orthologous *SYM1* sequence, wt or mutant versions, added of haemagglutinin epitope coding sequence (HA tag) were previously created. The tagged gene was under the control of the natural *SYM1* promoter and terminator. The strain BY4741 *sym1::kanMX4* was transformed through the Li-Ac method (Gietz and Woods, 2002) with the empty centromeric vector pFL38 (Bonneaud *et al.,* 1991) or with the vector carrying the *SYM1-HA* tagged wild type allele or the mutant tagged alleles.
The presence of the tag, required for immunodetection assays in the absence of an effective anti-Sym1 antibody, does not prevent the correct mitochondrial localization nor compromises Sym1 presence in the high molecular weight complex (Dallabona *et al*., 2010). Furthermore, the *SYM1-HA* construct was able to complement the *sym1*Δ OXPHOS defective phenotype and mtDNA instability, although the null mutant transformed with the untagged *SYM1* showed better performances regarding these two phenotypes (Dallabona, Ph.D. thesis).

2.1.2 Phenotypic analyses

To study the deleterious impact of the alleged pathological variants on OXPHOS phenotype, I first performed a spot assay on the oxidative carbon source ethanol at 37°C. As previously demonstrated for three of the mutations under consideration (Spinazzola *et al.*, 2006) the growth of the tested mutant strains was impaired in medium containing 2% ethanol as the sole carbon source at 37°C (figure 2.2). This temperature-sensitive OXPHOS phenotype was rescued by re-expressing the wild-type *SYM1* gene fused in frame with the hemagglutinin tag (*SYM1-HA*). The mutations R51W (hR50W), P104L

(hP98L), A168D (hA162D), N172K (hN166K), S176F (hS170F), resulted in a severe oxidative growth defect, comparable to that of the *sym1Δ* strain. The G24W (hG24W) and R51Q (hR50Q) mutations determined a less strong OXPHOS phenotype compared to that of the *sym1Δ* strain, however, the oxidative growth was severely compromised. In agreement with this observation, the human R50Q mutation equivalent to R51Q in yeast is associated with a milder phenotype. In fact, in contrast to most *MPV17* gene mutations that are associated with death in infancy or early childhood, the hR50Q mutation is associated with longer survival, suggesting that this is a hypomorphic mutation (El-Hattab *et al.*, 2010).

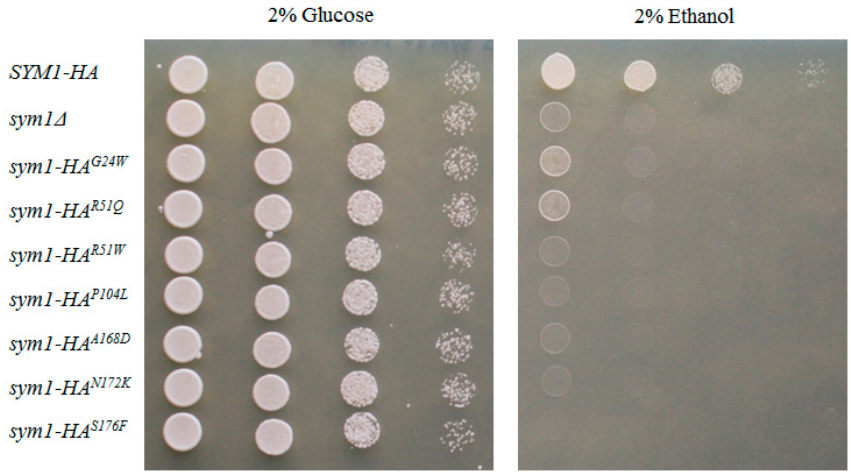

Figure 2.2. Oxidative growth phenotype at 37°C of BY4741*sym1*Δ strain transformed with pFL38*SYM1-HA*, pFL38 empty vector or with mutant alleles. Equal amounts of serial dilutions of cells from exponentially grown cultures were spotted ($5x10^4$, $5x10^3$, $5x10^2$, $5x10^1$ cells/spot) onto YP plates supplemented with the indicated carbon sources. Growth was scored after 3 days of incubation.

In *S. cerevisiae*, high mtDNA instability (depletion or deletions) is associated with increased segregation of respiratory-deficient "*petite*" mutants (Mounolou *et al.*, 1966). It was previously observed that the *sym1* mutant variants R51W, R51Q and N172K grown on ethanol- and glucose-containing medium at 37°C, displayed a significant increase of *petite* colonies frequency, caused by mtDNA instability (Spinazzola *et al*., 2006).

Here I determined the effect of the seven *SYM1*-tagged recombinant variants on mtDNA mutability, by measuring the frequency of mitochondrial respiratory deficient mutants (figure 2.3). This analysis was performed in stress conditions (high temperature, 37°C, and high concentration of ethanol), in presence of 2% glucose to allow to both respiratory sufficient and respiratory deficient cells to proliferate, as

described in Materials and Methods. The *sym1*Δ strain showed a significant increase of *petite* mutants (76%) compared to the *SYM1-HA* parental strain (33%). It is known that the strain expressing the *SYM1-HA* tagged gene shows an increased *petite* frequency respect to the strain expressing the untagged gene (Ph.D. thesis Dallabona). This result parallelized with the result observed relatively with the OXPHOS phenotype. Interestingly, all the strains expressing the mutant variants showed a significant increase of *petite* colonies compared to the wild type, according to the defects in mtDNA maintenance observed in hepatocerebral MDS patients.

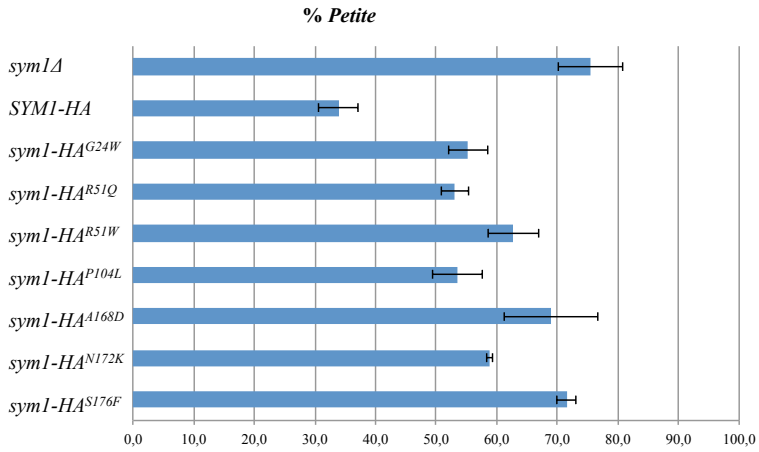

Figure 2.3. Respiratory-deficient mutant (*petite*) frequency after 15 generations of growth at 37°C. Blue bars represent the percentage of *petite*. More than 4000 colonies per strain were scored. All values are means of three independent experiments. The error bar represents the standard deviation.

Taken together, the phenotypic analyses demonstrated the deleterious effect of the missense mutations studied and confirmed a role of Sym1 in OXPHOS metabolism and in mtDNA stability.

2.1.3 Localization, stability and presence in a high molecular weight complex of the mutated Sym1 proteins

A reduction of steady-state protein levels of mutated *MPV17* in patient cells was previously observed (Spinazzola *et al*., 2006). This observation has raised questions regarding the stability or the mistargeting of the proteins within patient cells. So I used the yeast model to try to solve this issue.

To deepen the pathogenic effect of the mutations, I investigated whether they prevent the correct protein localization into the mitochondria, taking advantage of having strains expressing HA-tagged *SYM1* recombinant variants. Cytosolic and mitochondrial protein fractions were extracted, as described

in Materials and Methods, from cells grown in conditions in which the percentage of *petite* colonies was comparable between the *sym1Δ* mutant and the parental *SYM1* strain to prevent mtDNA damage that lead to physiological mitochondrial variations and consequently affect the experimental results.
The proteins were separated by gel electrophoresis and analyzed by Western blot, and the Sym1 protein was detected using an antibody against the HA tag. Antibodies against porine (Por1) and phosphoglycerate kinase (Pgk1) were used as markers for the mitochondrial and cytosolic fractions respectively. All of the Sym1 mutant proteins, beside the wild type one, correctly localized into the mitochondria, indicating that none of the mutations studied compromised the unknown mitochondrial target sequence (figure 2.4).

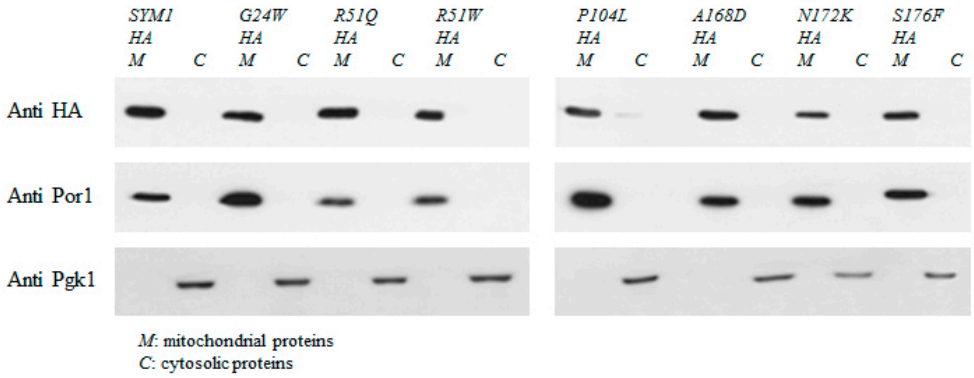

Figure 2.4. Western blot of denaturing SDS–PAGE of mitochondrial and cytosolic proteins from *sym1Δ* strains expressing the HA-tagged Sym1 recombinant variants. An antibody against HA-tag was used to detect the tagged Sym1 recombinant variants; antibodies against Por1 and Pgk1 were used as controls.

Two major import pathways direct nucleus-encoded proteins into the inner mitochondrial membrane. The majority of the proteins of the inner mitochondrial membrane and matrix contain an N-terminus sequence and are transported and integrated by the presequence translocase Tim23. Subsequently the N-terminus sequence is cleaved by the signal peptidase (Gakh *et al*., 2002, Koehler, 2004). Contrariwise, metabolite carriers and the channel proteins Tim22 and Tim23 are directed into mitochondria by internal signals and use the Tim22 translocase for membrane integration (Koehler, 2004; Wiedemann, 2004; Rehling, 2003). Although *In silico* analyses have suggested significant presequence probabilities for Mpv17 and Sym1, it has been demonstrated, both in human and yeast, that that the two proteins are not processed at the N-terminus during import into the mitochondria (Spinazzola *et al*., 2006; Reinhold *et al*., 2012). Furthermore the removal of N- or C-terminal segments of Sym1 did not block the import of the protein, excluding an essential role of these regions in the

transport process and indicating that an internal targeting sequence is involved in Sym1 transport (Reinhold *et al*., 2012).

To explore the other aspect, i.e. protein stability, I have evaluated whether the mutations affected it by measuring the steady-state level of the Sym1 mutated proteins respect to the wild type one. Cells were cultured and total proteins were extracted as described in Materials and Methods. The mitochondrial protein fraction was separated by gel electrophoresis and analysed by Western blotting analysis. I quantified the amount of the mutant proteins compared to that of the wild type strain and I found that the proteins carrying the G24W (hG24W) mutation showed a drastic amount reduction, the proteins carrying the R51W (hR50W), A168D (hA162D), N172K (hN166F) and S176F (hS170F) mutations showed a slight amount reduction, whereas no difference in steady-state level was observed for the proteins carrying the R51Q (hR50Q) and P104L (hP98L) mutations (figure 2.5). Based on these observations it is possible to hypothesize that the strong instability of the G24W (hG24W) protein is the molecular mechanism by which this mutation leads to the pathology.

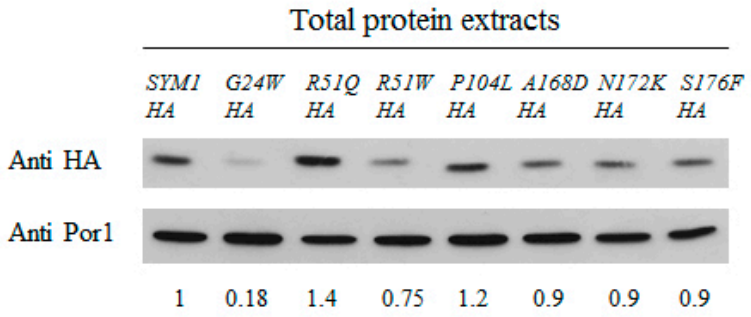

Figure 2.5. Western blot of denaturing SDS–PAGE of mitochondrial proteins from *sym1Δ* strains expressing the HA-tagged Sym1 recombinant variants. An antibody against HA-tag was used to detect the tagged Sym1 recombinant variants and the antibody against Por1 was used as loading control. The quantification was performed using the Quantity One software. Normalization was performed and the value 1.0 was attributed to the wild type.

To investigate if differences observed at protein level were due to any problem affecting transcription, the transcript levels were assessed by Real Time transcriptional analysis of *SYM1* wild type and mutant genes. Cell were grown in the same condition used for the protein stability analyses, as described in Materials and Methods. RNAs were extracted, cDNAs were synthesized and quantitative PCR was performed. As internal control we used *ACT1* that encodes a structural protein involved in cell

polarization. The RNA level of the gene of interest was normalized to *ACT1* levels (described in Materials and Methods).

As shown in figure 2.6, the mRNA levels of *sym1* mutant genes were increased compared to wild type, except for the mRNA of Sym1^{S176F} mutant gene which showed expression levels comparable to that observed for wild type gene. The increase of mRNA levels suggests that the unfunctional proteins induce a feedback increasing the gene transcription. However, this increment is not associated with a higher level of protein respect to the wild type, highlighting a certain instability in almost all the mutated proteins. In the strain carriyng the G24W mutation the protein quantity observed was very low confirming a high instability of this mutant protein.

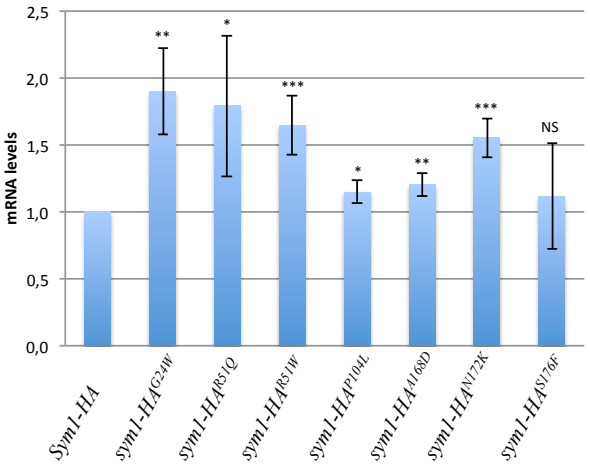

Figure 2.6. The mRNA levels of *SYM1* wild type and mutant genes were quantified by RT-qPCR. Values are reported as mRNA level normalized respect to WT. Expression was normalized to the mRNA levels of the internal control *ACT1*. NS: not significat, *p<0.5, **p<0.01, ***p<0.001.

As previously demonstrated in our laboratory, Sym1 takes part in a high molecular weight complex (Dallabona *et al*., 2010) whose function and composition is still unknown. Notably, in both cell cultures and mouse tissues, Mpv17 is part of a high molecular weight complex of unknown composition, essential for mtDNA maintenance in critical tissue, i.e. liver, of a *MPV17* knockout mouse model (Bottani *et al*., 2014). The presence of Sym1 in a high molecular weight complex (represented by dashed line in figure 2.7) offered another hint for investigations. So, to better understand the molecular mechanisms underpinning the pathology, I investigated whether the seven mutations prevented the Sym1 capability to take part in the fully assembled complex. I performed 2D-BNGE analysis on mitochondrial proteins extracted from strains expressing the HA-tagged Sym1

recombinant variants. The results showed that, according with the reduction in protein stability induced by the G24W mutation, the Sym1^{G24W} mutant protein detection needed a longer exposure time than that required by other proteins (figure 2.7). However, it is the only one able to partially take part in the fully assembled complex. All the other mutations, although to different extent, compromised at least partially the Sym1 interaction with the other complex components, giving rise to a not fully assembled complex, as shown by the signals of the mutated proteins that are shifted in the low molecular weight side of the gel. In addition, a consistent fraction of the Sym1 mutant proteins was found free (figure 2.7). Despite the function of the complex is still unknown, this result suggests that the pathogenic role of these mutations is related to the inability to take part in the fully assembled functional complex.

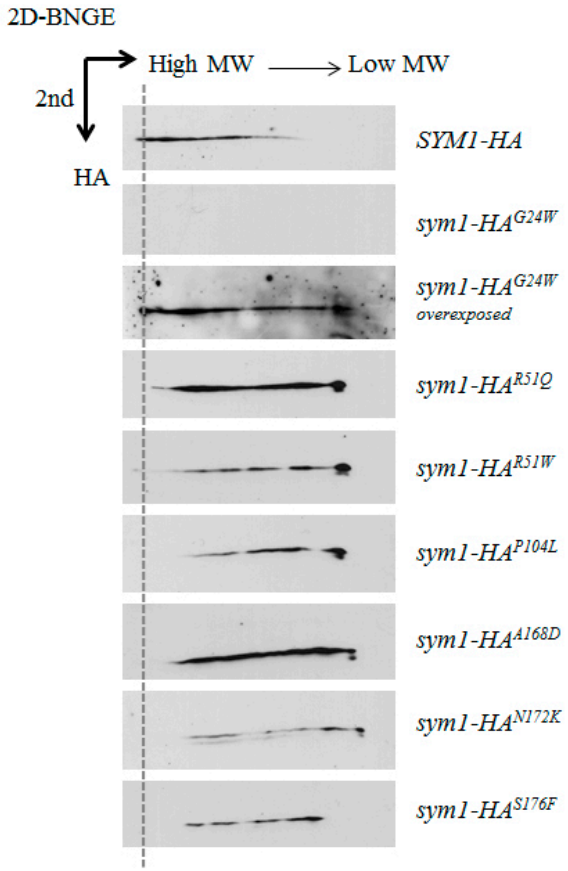

Figure 2.7. Western blot of second dimension blue-native gel electrophoresis of mitochondrial proteins from *sym1Δ* strains expressing the HA-tagged Sym1 recombinant variants. An antibody against HA-tag was used to detect the tagged Sym1 recombinant variants.

As previously demonstrated for the homologous peroxisomal membrane protein 2 (PXMP2) that form a relatively wide channel in the mammalian peroxisomal membrane (Rokka *et al.*, 2009), Sym1 was

found to form a channel with a pore size of about 1.6 nm capable of allowing the transport of large molecules, such as metabolites, across the inner mitochondrial membrane (Reinhold *et al*., 2012). A pore-forming activity in artificial membrane was determined also for human Mpv17 protein (Antonenkov *et al*., 2015). However the physiological role of the channel and the nature of the cargo remain elusive.

Taken together, the data showed that the analysed mutations do not compromise the import into the mitochondria and suggest, as cause of the pathology for the G24W (hG24W) mutation, a reduced amount of protein and, for the other mutations, a compromised formation of the high molecular weight complex, whose function remains to be determined. The purification of the whole complex and the identification of the Sym1 partner proteins may help to answer to this unsolved questions.

2.2 Research of potential therapeutic drugs for *MPV17*-related MDS

2.2.1 Drug drop test: procedure and theoretical results

Despite the advances in molecular and biochemical methodologies leading to a better understanding of the etiology and mechanisms of mitochondrial disorders, there are still no satisfactory therapies available for these diseases. Treatment for mitochondrial diseases remains largely symptomatic and does not significantly alter the course of the disease (El-Hattab *et al*., 2017 b).

High throughput screening has been defined as "the process of assaying a large number of potential effectors of biological activity against targets (a biological event)" (Armstrong J.W, 1999) and its goal is to accelerate drug discovery by screening large libraries often composed of thousands of compounds. In 2011 Couplan and collaborators set up a two-step yeast-based screening assay, called Drug drop test, to search for active compounds against NARP syndrome, a hereditary mitochondrial disease that affects ATP synthase activity (Couplan *et al*., 2011).

Here I applied this technique (described in Materials and Methods) for the identification of drugs for *MPV17*-related MDS treatment. This method of screening is usually performed in yeast using strains characterized by reversible damages. In particular, in the studied case, it was necessary that the strains maintained the mtDNA, since the complete loss of mtDNA could not be rescued in any way. The mutant cells were spread on 12x12 plates containing media supplemented with a non-fermentable carbon source and were exposed to filters spotted with the compounds to test. One filter was spotted with DMSO, the solvent in which the molecules were solubilized, as negative control (C-). Wild type

strain was spotted as positive control of growth (a number of cells equal as the mutant strain seeded in the same area). The plates were then incubated at not permissive temperature and the growth of mutant cells was monitored for some days. A schematic overview of the Drug drop test is reported in figure 2.8.

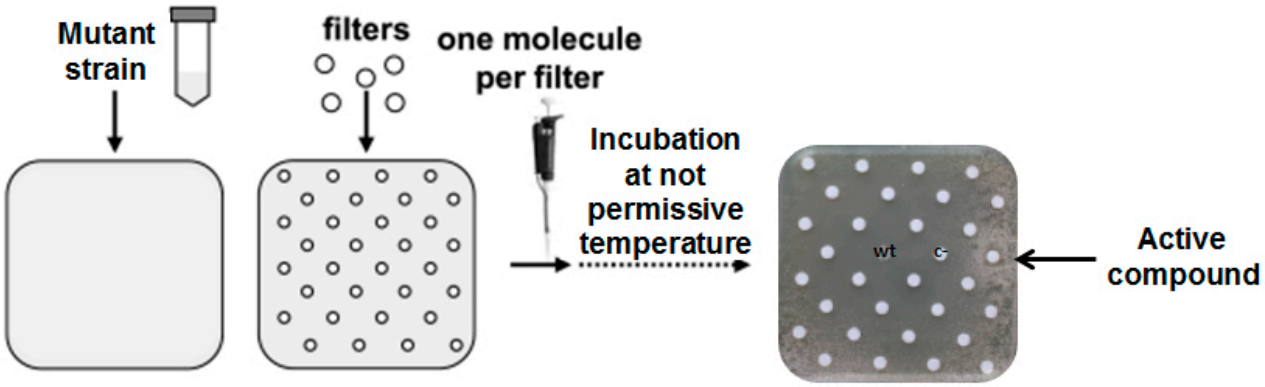

Figure. 2.8. Schematic representation of primary screening using Drug drop test method (modified from Couplan *et al*., 2011). After the growth in liquid media, cells are seeding on plates. Filters are placed on agar surface and spotted with drugs. Plates are incubated at not permissive temperature for 6-7 days. Finally, if active compounds are identified, they will be re-tested in secondary screening.

Depending on the presence/absence of a halo of growth and its position around the filters, the compounds were classified into three groups:

- compounds that led to formation of a halo of growth near the filter, (indicated in green in the example in figure 2.9). These molecules have a rescuing effect;
- compounds that led to formation of an external crown of growth, whereas no growth was observed near the filter (indicated in yellow in figure 2.9). These molecules are toxic at high concentrations (near the filter) and active at lower concentration (far from the filter);
- compounds without any effect (the majority of the screened molecules).

The screening was performed in two steps: the primary screening, to identify molecule potentially active (figure 2.9) and the secondary screening, to confirm the rescue effect of the molecules identified in the primary screening (figure 2.10). The secondary screening was performed using the same conditions used for the primary screening, except for the number of filters placed on each plate. In the secondary screening each plate contained only four equidistant filters to avoid any possible interference: one of them was spotted with DMSO, as negative control. The others were spotted with three different compounds to test. Wild type strain was spotted as positive control of growth. This two-step approach allows to minimize the number of false-positive molecules.

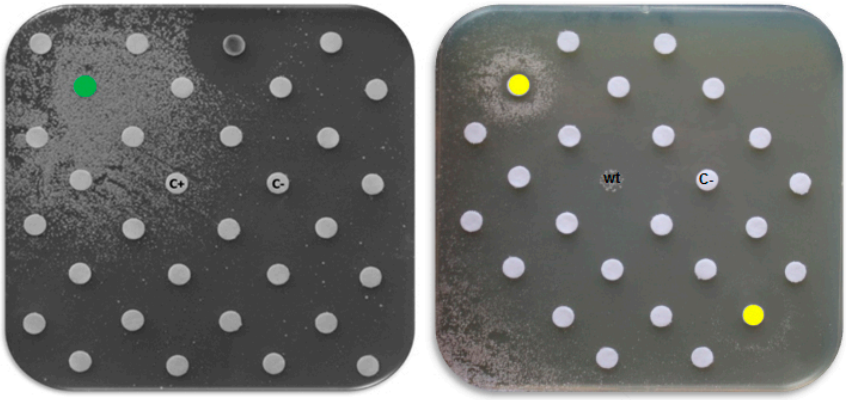

Figure 2.9. Primary screening. Examples of halo of enhanced growth indicated in green (active compound). Example of internal halo of no growth and external halo of enhanced growth indicated in yellow (active compounds at low concentration). C+: wild type (Wt). C-:DMSO.

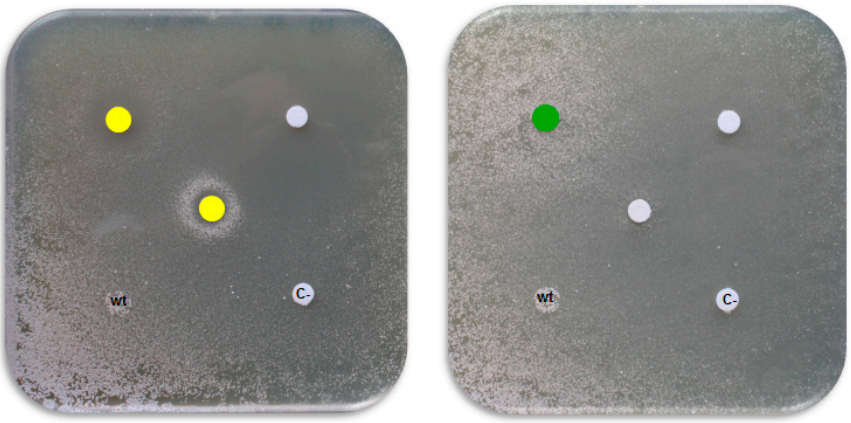

Figure 2.10. Secondary screening. Examples of halo of enhanced growth indicated in green (active compound). Example of internal halo of no growth and external halo of enhanced growth indicated in yellow (active compounds at low concentration). C+: wild type (Wt). C-:DMSO.

2.2.2 Selection of the mutant strain and optimal screening conditions

The choice of the mutant strain to be used in the analysis is very important. Mutant strains characterized by a leaky phenotype may not allow to identify beneficial molecules, the halo of growth might be confused with the background of growth. Moreover, the use of null mutant is generally not advisable as it allows to identify only beneficial molecules that act through a bypass of the protein function.

The *SYM1* thermo-sensitive mutant strains, here analysed, were characterized by an evident defective OXPHOS phenotype at 37°C and normal phenotype at optimal temperature of growth (28°C). As

previously described the mutant strains carrying the mutations G24W and R51Q showed a leaky phenotype, less suitable for the Drug drop test. The other mutants showed an identical severe OXPHOS phenotype and I chose to use the mutant BY4741*Δsym1*/pFL38*sym1*^{R51W} deprived of the HA-tag (figure 2.11), since, as previously mentioned, the strains transformed with the untagged alleles showed better performances than the strains transformed with the tagged alleles.

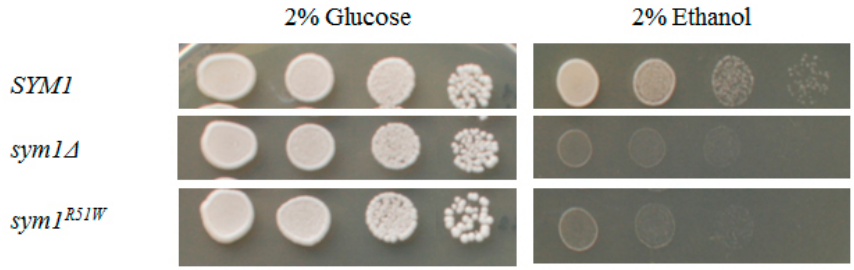

Figure 2.11. Oxidative growth phenotype at 37°C of BY4741Δ*sym1* transformed with pFL38*SYM1*, pFL38 empty vector and with mutant alleles *sym1*^{R51W}.

Firstly, I defined the optimal conditions for the screening. I focused on three different parameters: the concentration of the oxidative carbon source to be used (2%, 3%, 4% of ethanol concentration), the number of cells to be spread on plates (1-1,5-2-3-4-8x10^5 cell/plate) and temperature (36°C and 37°C). The screening was performed on YP medium, since in synthetic medium the molecules appeared to be less bio-available, maybe due to the interaction with the saline components of the medium. The optimal conditions chosen were: 4% ethanol, 1,5x10^{5}cell/plate and 37°C.

2.2.3 Screening of the Selleck FDA-approved drug library

I screened Selleck Chemical Library, a collection of 1018 drugs for high-throughput screenings. All compounds have been approved by Food and Drug Administration (FDA) and their bioactivity and safety were confirmed by clinical trials. This chemical library contains drugs used in several medicine branches including oncology, cardiology, immunology and neuropsychiatry. In the figure 2.12 the composition of the library with the specific human cellular target of the drugs is reported.

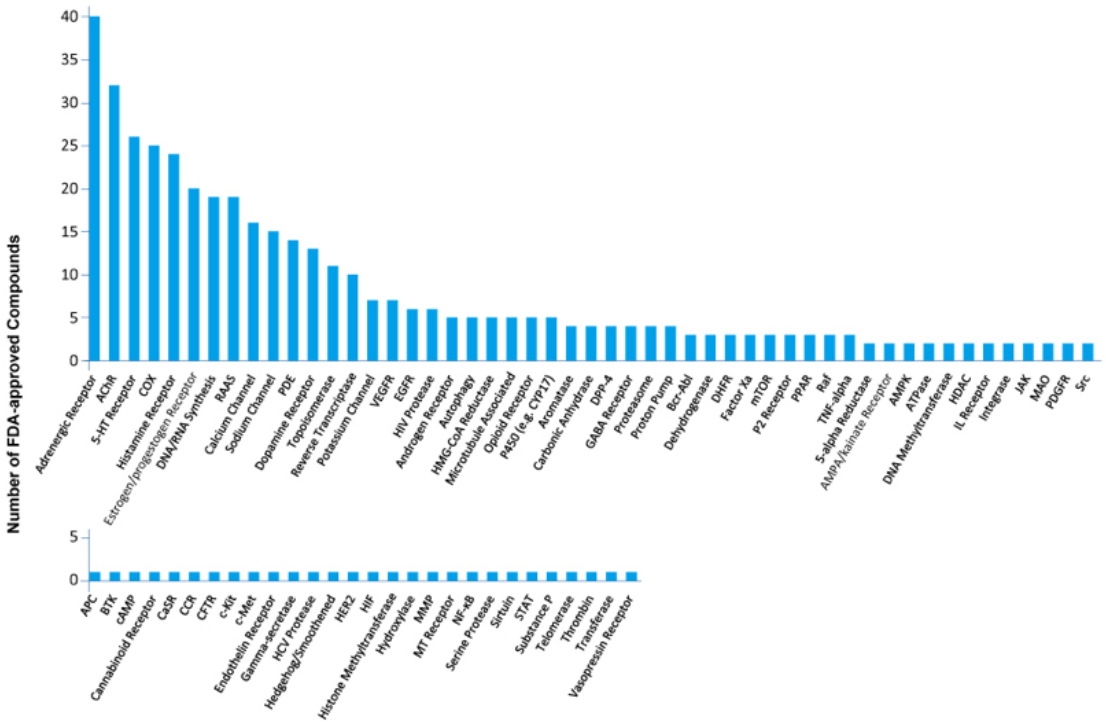

Figure 2.12. Composition of Selleck FDA-approved Drug library. The specific human cellular targets of the drugs are indicated. (http://www.selleckchem.com/screening/fda-approved-drug-library.html).

The advantage of the use of a FDA-approved drug library is that it allows a drug repurposing approach (also called drug repositioning), thus speeding up the drug discovery process by identifying new clinical use of drugs (Aubè 2012, Ashburn *et al*., 2004).

I then performed the primary screening on the 1018 molecules of the Selleck FDA-approved Drug library (http://www.selleckchem.com/). Every plate was seeded with $1{,}5x10^5$ cells of $sym1^{R51W}$ mutant. 31 equidistant sterile filters were placed, one of which was spotted with DMSO, while the remaining filters were spotted with 2.5 µl of every molecule of the chemical library (at a final concentration of 10 mM). The plates were incubated at 37°C and the growth of the mutant was monitored for 6 days.
From the primary screening 25 molecules were classified as alleged active compound and were re-tested in the secondary screening. The secondary screening confirmed 11 molecules as active compounds for their ability to rescue the growth defect (figure 2.13).

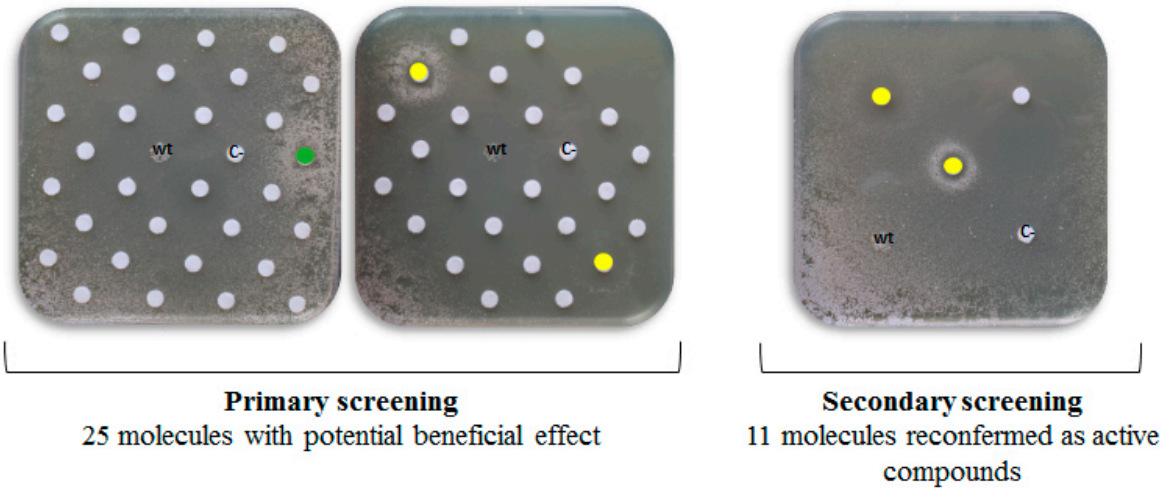

Figure 2.13. On the left, images of plates of the primary screening. On the right, an image of plate of the secondary screening. Active molecule is indicated in green. Molecules producing a halo of no growth near the filter and an external crown of growth are indicated in yellow (photo taken after 4 days of growth). C+: wild type (Wt). C-:DMSO.

2.2.4 Screening of six molecules of Prestwick Chemical Library®

Prestwick Chemical Library® is a collection of 1280 small molecules, mostly approved (FDA, EMA and other agencies), selected for high chemical and pharmacological diversity, as well as for known bioavailability and safety in humans (http://www.prestwickchemical.com).

I tested the effect of six compounds of the Prestwick chemical library, which had been previously identified in a similar screening performed in our laboratory as beneficial in another yeast model of MDS (data not shown). These molecules were able to rescue both the respiratory deficient (RD) phenotype and the high level of mtDNA instability in the *S. cerevisiae* mutant tested. Since *sym1* mutants share these two phenotypes, I wondered whether these compounds were able to exert their rescuing effects also on $sym1^{R51W}$ mutant. Interestingly, I found that Imazalil and Ebselen were able to rescue the growth defect of the mutant strain, as shown in figure 2.14.

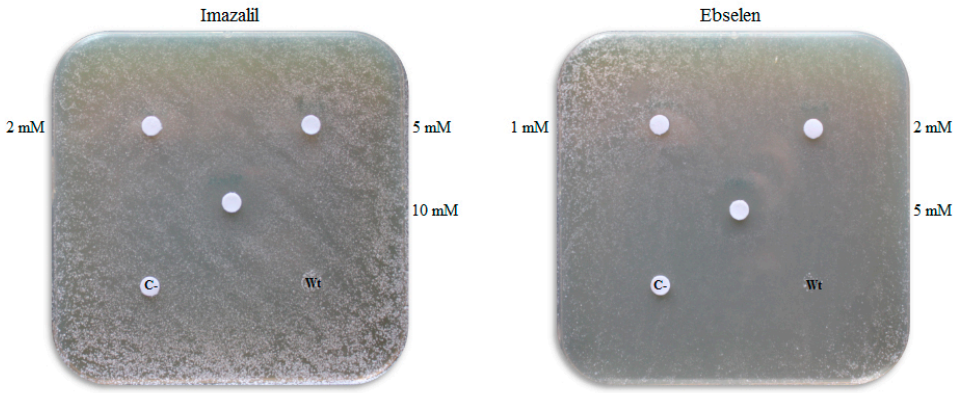

Figure 2.14. Example of plates of the secondary screening. In the left plate Imazalil was spotted on filters at different concentrations. The filters in the right plate were spotted with Ebselen at different concentrations. C+: wild type (Wt) and C-:DMSO. (Photo taken after 3 days of growth).

In table 5 the 13 beneficial molecules identified are reported. The molecules showed different degree of growth rescue. In particular, most of them had a beneficial effect at low concentrations tested, as indicated by the formation of a halo of no grown near the filter and a halo of growth far from the filter where the molecule was present at lower concentration. Three molecules (Haloperidol, fenticonazole nitrate and thonzonium bromide) had a beneficial effect at all concentrations tested, althought with different intensity depending on the drug (table 5).

Drug	Oxphos phenotype rescue	Growth rescue
Posaconazole	Inhibition+growth	+++
Haloperidole	Growth	+++
Fenticonazole nitrate	Growth	+
Itraconazole	Inhibition+growth	+++
Otilonium bromide	Inhibition+growth	+++
Sertaconazole nitrate	Inhibition+growth	+
Sertraline HCl	Inhibition+growth	+
Benzethonium chloride	Inhibition+growth	+++
Domiphen bromide	Inhibition+growth	++
Alexidine HCl	Inhibition+growth	+
Thonzonium bromide	Growth	++
Imazalil	Inhibition+growth	++
Ebselen	Inhibition+growth	+

Table 5: Rescue effect of the active compounds identified on phenotypes of *sym1*^{R51W} mutant strain. +++ Strong effect; ++ Medium effect; + Mild effect.

2.2.5 Study of the molecules effect on *petite* mutant frequency

As previously described, the *sym1*Δ strain and all strains expressing the mutant variants showed a significant increase of *petite* colonies, indicative of mtDNA instability. To deepen the effects of the active compounds, I evaluated their impact on mtDNA stability in the *sym1*^{R51W} mutant strain by measuring the *petite* frequency after treatment with different concentrations of molecules.

Notably, five molecules (Posaconazole, Fenticonazole nitrate, Itraconazole, Sertaconazole nitrate and Imazalil) belong to the class of azoles and they act through the same mechanism, so not all these molecules have undergone subsequent analyses. In particular, Itraconazole and Sertaconazole have not been tested.

Firstly, I evaluated the effect of the molecules on cellular growth of the wild type strain BY4741Δ*sym1*/pFL38*SYM1*, as described in Material and Methods, to identify the concentrations to be used for the analysis. The highest concentration tested for each molecule was 512 μM. Except for the Haloperidol, for all the molecules tested the minimum inhibitory concentrations (MIC) were identified.

To investigate the capability of the molecules to decrease the accumulation of *petite* mutants of the mutant strain carrying the *sym1*^{R51W} allele, I used sub-MIC concentrations. This analysis was performed in the same conditions previously described for the determination of mtDNA stability and adding the compounds to test in the medium at different concentrations. In figure 2.15 the results obtained are showed.

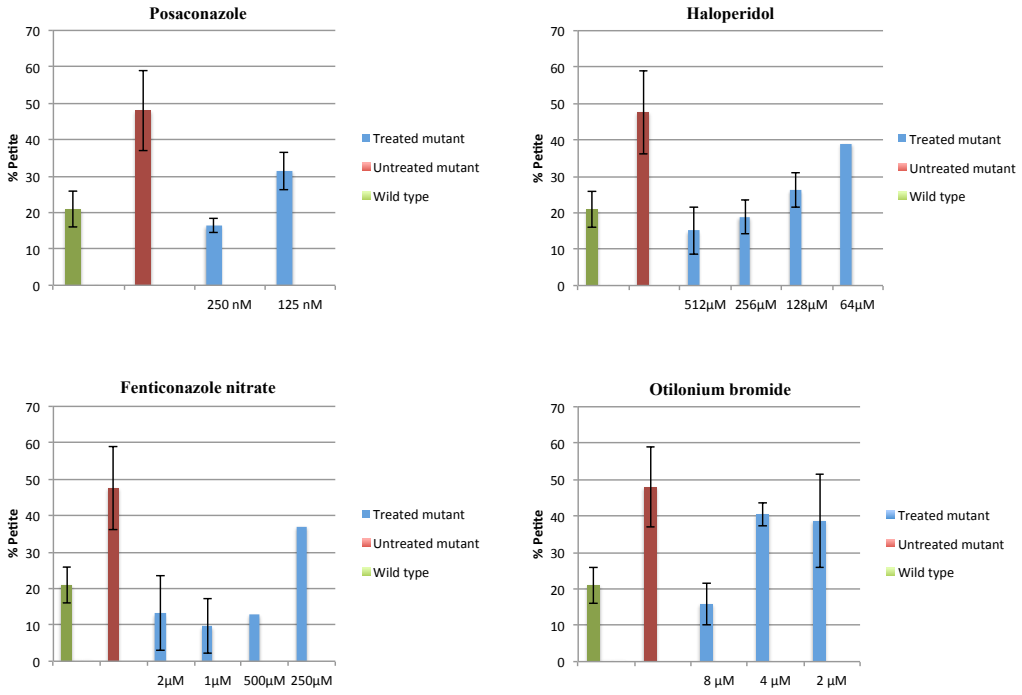

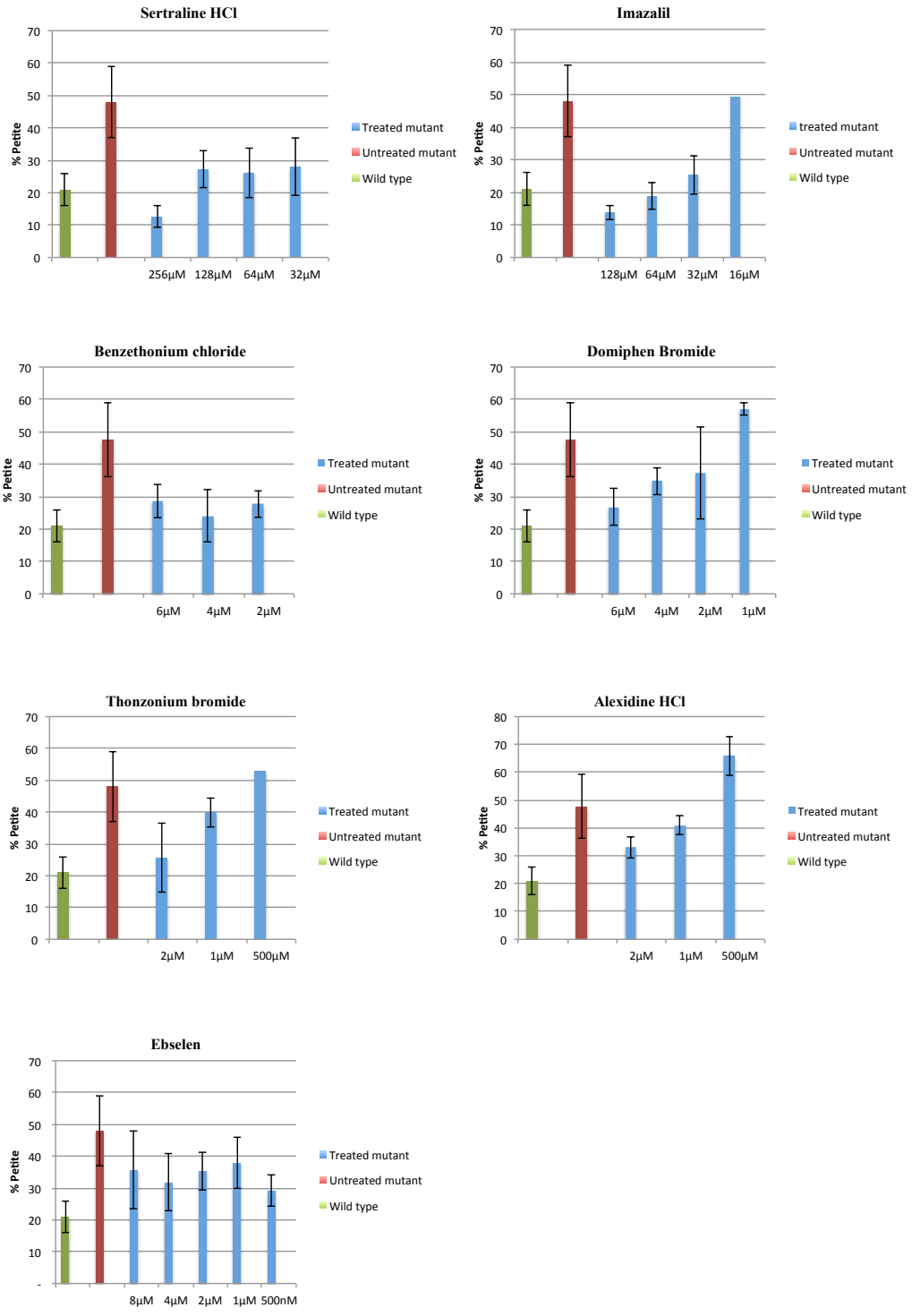

Figure 2.15. Respiratory-deficient mutants frequency after 15 generations of growth at 37°C. Blue bars represent the percentage of *petite* of the mutant strain *sym1*^{R51W} after treatment with different concentrations of molecules. Red bars represent the percentage of *petite* of the mutant strain *sym1*^{R51W} in absence of molecules. Green bars represent the percentage of *petite* of the wild type strain. More than 4000 colonies per strain were scored. All values are means of three independent experiments (except for the bars without error bar). The error bar represents the standard deviation.

Interestingly, all compounds were able to decrease the *petite* frequency in the *sym1*^{R51W} mutant strain, although with different intensity. In particular Posaconazole, Fenticonazole nitrate, Otilonium Bromide, Sertraline HCl, Imazalil and Haloperidol were the most active compounds. Benzethonium chloride, Thonzonium bromide and Domiphen bromide had a medium effect and Alexidine HCl and Ebselen had a minor effect. The table 6 shows an overview of the effects of the active compounds tested on phenotypes of *sym1*^{R51W} mutant (table 6).

Drug	**mtDNA instability rescue**
Posaconazole	+++
Haloperidole	+++
Fenticonazole nitrate	+++
Otilonium bromide	+++
Sertraline HCl	+++
Benzethonium chloride	++
Domiphen bromide	++
Alexidine HCl	+
Thonzonium bromide	++
MRS5	+++
MRS6	+

Table 6. Schematic overview of the effect of the active compounds on phenotypes of *sym1*^{R51W} mutant strain. +++ Strong effect; ++ Medium effect; + Mild effect.

2.2.6 Decrease in *petite* frequency: selective induction of mortality or increase in mtDNA stability?

The reduction of *petite* mutants observed in presence of the molecules may be due to two possible events: an increase of wild type molecules of mtDNA indicative of an effect of the molecules on mtDNA stability or a selective induction of mortality of the *petite* mutants. So, to evaluate these aspects I have set up a competition test between the strain BY4741 wild type (rho^+) and its derivative strain lacking mtDNA (rho^0). We put together rho^+ and rho^0 cells in a 1:1 ratio in presence or in absence of the molecule to test. If the ratio was maintained also in presence of the molecule tested we can conclude that the beneficial effect observed is not due to selective induction of mortality. The results obtained was reported in figure 2.16. As observed the percentages of *petite* mutants are similar both in presence and in absence of the molecules, except for the Fenticonazole nitrate which induced a reduction of the *petite* frequency in the treated strain respect to the untreated strain. These results suggest that for the majority of the molecules the reduction of *petite* frequency is attributable to a positive effect on mtDNA stability.

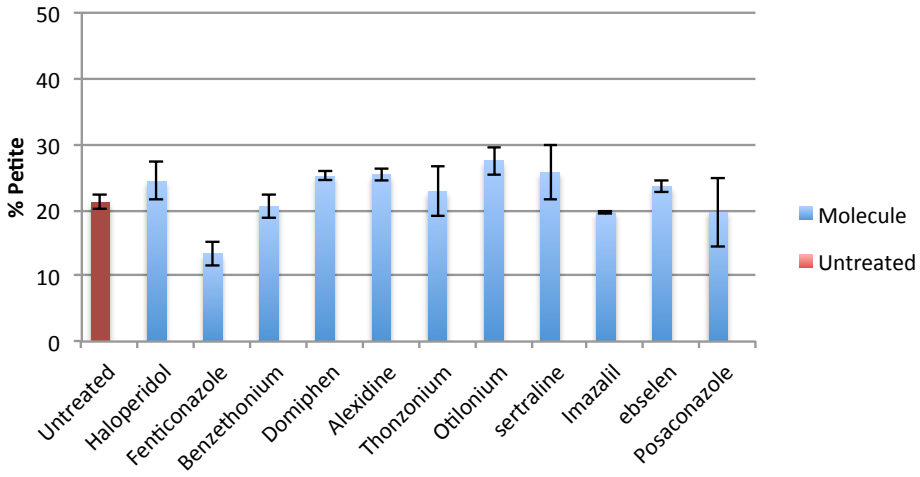

Figure 2.16. *Petite* frequency obtained by competition test between rho^+ e rho^0 yeast strains in presence (blue bars) or in absence (red bar) of the molecules.

2.2.7 Effects of drugs on OXPHOS phenotype of the null mutant *sym1Δ*

In order to better understand if the beneficial effect was due to an improvement of Sym1 functionality or a bypass of Sym1 function, I evaluated the molecules capability to rescue the defective OXPHOS phenotype also in *sym1Δ* strain, where the Sym1 protein was not expressed. I performed the same approach used in the secondary screening of Drug drop test, just changing slightly the experimental condition. In particular $2x10^5$ cells of the null mutant were spread onto YP containing 4% ethanol.
As shown in figure 2.17, all the molecules tested were able to rescue the oxidative growth defect of the null mutant suggesting that therapeutic effect acts through a mechanism that bypass Sym1 function.

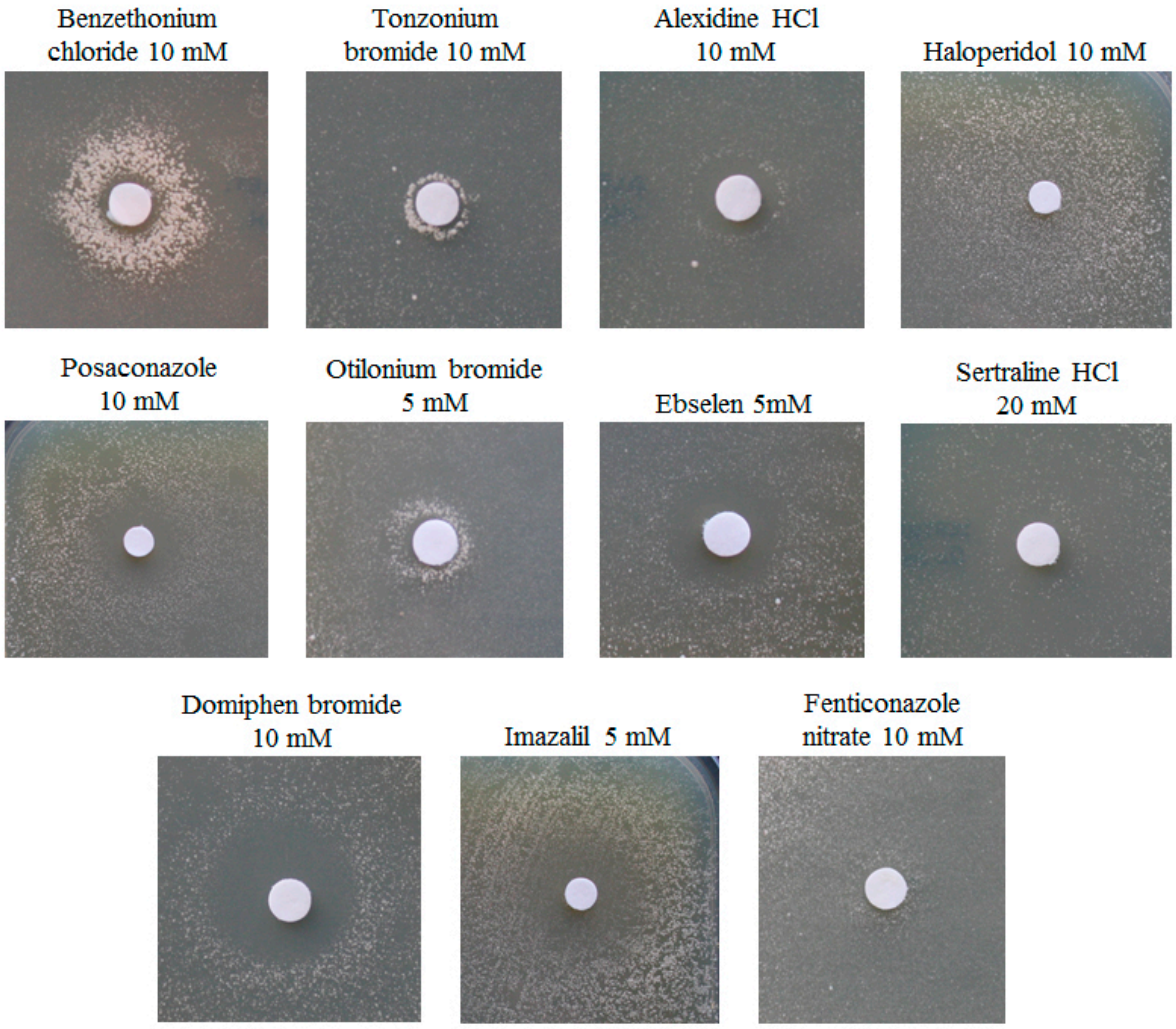

Figure 2.17. Rescue of the OXPHOS growth defect of the null mutant *sym1*Δ induced by active compounds.

In the table 7 all the 13 beneficial molecules identified are listed.

Drug	Target in yeast	Target in mammals
Posaconazole	Lanosterol 14 alpha-demethylase (ergosterol pathway)	Lanosterol 14 alpha-demethylase (cholesterol pathway)
Fenticonazole nitrate	Lanosterol 14 alpha-demethylase (ergosterol pathway)	Lanosterol 14 alpha-demethylase (cholesterol pathway)
Itraconazole	Lanosterol 14 alpha-demethylase (ergosterol pathway)	Lanosterol 14 alpha-demethylase (cholesterol pathway)
Sertaconazole nitrate	Lanosterol 14 alpha-demethylase (ergosterol pathway)	Lanosterol 14 alpha-demethylase (cholesterol pathway)
Imazalil	Lanosterol 14 alpha-demethylase (ergosterol pathway)	Lanosterol 14 alpha-demethylase (cholesterol pathway)
Haloperidol	Sterol C8-C7 isomerase (ergosterol pathway)	Dopamine receptors; sigma-1 receptor; 3-beta-hydroxysteroid Δ^8,Δ^7 isomerase (cholesterol pathway)
Sertraline HCl	Phospolipid membranes	Serotonin 5-HT transporter
Benzethonium chloride		HERG K-channel
Otilonium bromide		Muscarinic receptor, VD Ca-Channel, NK receptor
Domiphen bromide		HERG K-channel
Thonzonium Bromide	Vacuolar ATPase proton transporter	Vacuolar ATPase proton transporter
Alexidine HCl	Vacuolar ATPase proton transporter	Vacuolar ATPase proton transporter
Ebselen	Free radicals	Free radicals

Table 7. Active molecules identified by Drug drop test as able to rescue the OXPHOS phenotype of the mutant strain BY4741*Δsym1/*pFL38*sym1*^{R51W}. In grey are indicated the compounds that act in the same pathway in yeast.

The molecular target of the identified drugs in human cells is known. In yeast, however, the target is not always known (table 7). Moreover, since some specific targets identified in human cells do not exist in yeast, these molecules probably act by a secondary target in yeast cells.

Interestingly, six of 13 molecules identified have the same target in yeast (indicated in grey in table 7). The first five (Posaconazole, Fenticonazole nitrate, Itraconazole, Sertaconazole nitrate and Imazalil) belong to the class of azoles with antifungal effect. Azoles fungicides constitute around 40 broad-spectrum fungicides that contain at least one triazole or imidazole moiety in their structure and are used for agricultural, horticultural, and pharmaceutical applications. The primary antifungal action mechanism of these fungicides relies on inhibition of CYP51 (lanosterol 14 alpha-demethylase), encoded by *ERG11* gene, a key enzyme for sterol biosynthesis in fungi (Zarn *et al*., 2003). Inhibition of this enzyme leads to a depletion of ergosterol, the major sterol synthetized by yeast cell. In yeast cells, sterols not only contribute to the fluidity of lipid membranes, but also ensure many other vital processes, including vesicles formation and protein sorting, cytoskeleton organization, endocytosis and mating. Ergosterol has a determinant role in the regulation of membrane permeability and fluidity, and

for regulating the activity of membrane transporters (Daum *et al*., 1998). It is not present in equal amounts in all membranes and specific preference is shown for the incorporation of ergosterol rather than sterol intermediates. It is found in the highest concentrations in the plasma membrane and in the secretory vesicles. In contrast, the membrane ergosterol content in the microsomes, mitochondria and other intracellular membranes is significantly lower and the relative concentration of sterol intermediates is increased. Yeast differs from most eukaryotes in that the mitochondrial ergosterol is concentrated in the inner membrane rather than in the outer membrane (Zinser *et al*., 1993, Tuller and Daum, 1995). The azoles identified in the screening exerted their beneficial effect at low concentrations, whereas at high concentrations were toxic for the yeast, in accordance with the lethality of the deletion of the *ERG11* gene.

Haloperidol is used in human therapy as antipsychotic agent that primarily acts as an antagonist of D2 dopamine receptors. It is also known as a ligand of type 1-sigma receptors that interacts with the inositol 1,4,5-trisphosphate receptor to regulate Ca^{2+} transport from the ER lumen into mitochondria, non-opioid transmembrane proteins located at the ER, mitochondrial, and plasma membranes in various tissues (Hayashi and Su, 2007). In yeast it was found to inhibit both sterol Δ^8,Δ^7 isomerase, encoded by *ERG2* gene, and C-14 reductase, encoded by *ERG24* gene, resulting in decreased ergosterol levels (Lum *et al*., 2004, Moebius *et al*., 1996). These enzymes function in the ergosterol biosynthesis pathway, suggesting that also haloperidol interfere with sterol metabolism and trafficking.

I speculate that a moderate reduction of ergosterol in the cellular membranes increases the membrane permeability and this could favour the mitochondrial transmembrane flows that are altered in the *sym1* null mutant. This mechanism could act also in human cell where ergosterol is substituted by another sterol, cholesterol (Zarn *et al*., 2003), an essential component of all membranes, present also in mitochondrial membranes. Cholesterol critically influences membrane fluidity, permeability, curvature and membrane protein interaction (Elustondo *et al*., 2017). In particular, the sterol 14α-demethylase, encoded by *ERG11* in yeast, is not only expressed in fungi and yeast but is also found in many other species ranging from bacteria to mammals. The human orthologous gene is *CYP51A1*. On the protein level, the amino acid sequences are highly conserved along the phylogenetic tree (Debeljak *et al*. 2000; Kojima *et al*. 2000; Nitahara *et al*. 1999; Stromstedt *et al*. 1996). Also *ERG2* gene, inhibited by haloperidol, has an orthologous gene in human, *EBP* gene. In the figure 2.18 are reported the biosynthetic pathway of ergosterol and cholesterol, in fungi and human, respectively.

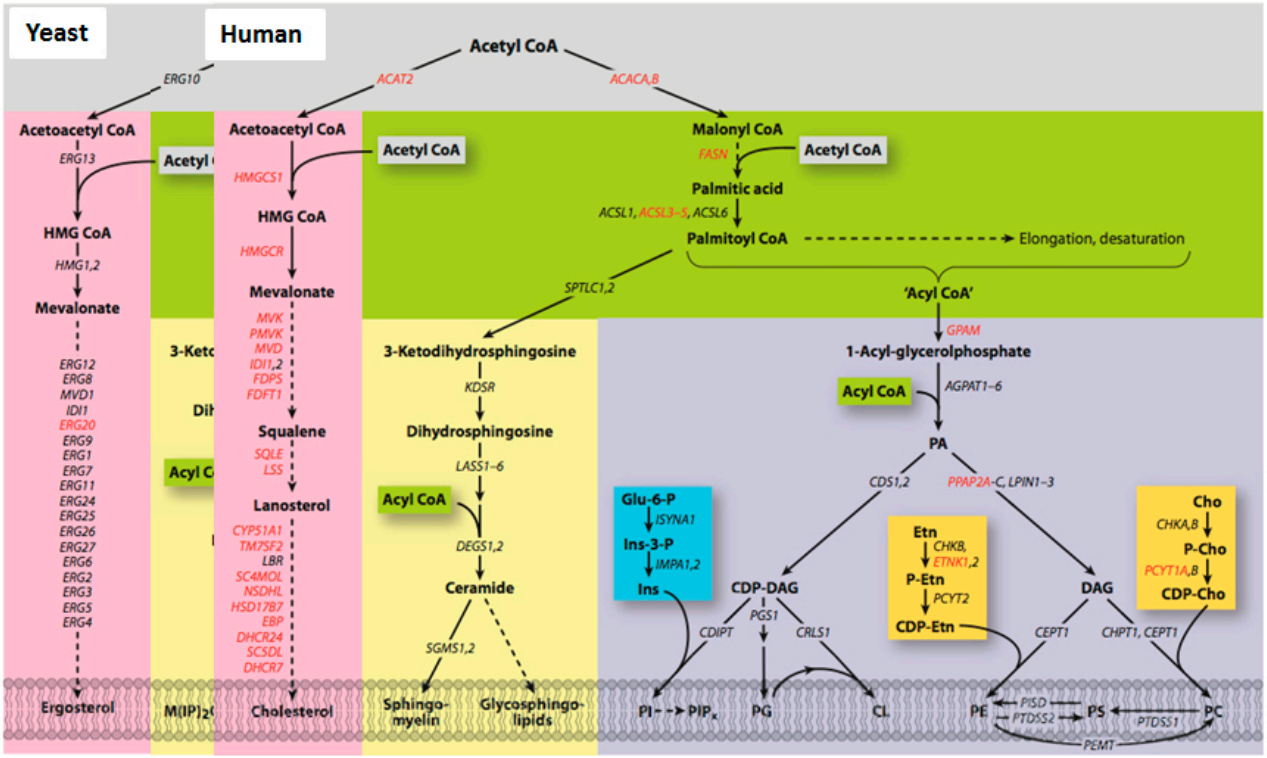

Figure 2.18. Gene coding for enzyme involved in the pathways for membrane lipid synthesis. In pink are represented the biosynthetic pathways for ergosterol and cholesterol in yeast and human, respectively (picture modified from Nohturfft and Zhang, 2009).

It is well known in human, that an increased content of cholesterol in cellular membranes induces an alteration in the transmembrane transports as consequence of altered membrane fluidity and permeability. In particular, variations in mitochondrial sterol content induce considerable changes in the function of mitochondrial membrane proteins and transporters such as the adenine nucleotide transporter (Haslam *et al*., 1977), the 2-oxoglutarate carrier, which also imports glutathione (Coll *et al*., 2003) and transporters for phosphate, pyruvate and citrate (Parlo *et al*., 1984; Paradies *et al.*, 1992; Paradies *et al.,* 1999). More recently, it has been observed that perturbation of cholesterol homeostasis due to Atad3 deficiency causes, in human, aberrant mtDNA organization and is associated with elevated free cholesterol and increased expression of genes involved in cholesterol metabolism (Desai *et al*., 2017). Atad3 is a mitochondrial membrane bound ATPase whose function has not yet been discovered.

Based on these observations it is possible to assume that also a moderate decrease in cholesterol content could ameliorate the transmembrane flows rescuing the mitochondrial defects.

Cholesterol-lowering drugs (statins) are currently used in clinical trials, in particular as anti-cancer chemotherapy. However, given at higher doses, statins cause serious side effects by inhibiting the formation of other biologically important molecules derived from mevalonate. Sterol 14-demetylase (Cyp51), which acts 10 steps down-stream, is potentially a more specific drug target because this portion of the pathway is fully committed to cholesterol production. However, screening of a variety of commercial and experimental inhibitors of microbial Cyp51 orthologs revealed that most of them (including all clinical antifungals) weakly inhibit human Cyp51 activity, even if they display an apparent high spectral binding affinity. Until now, one relatively potent compound, (*R*)-*N*-(1-(3,4′-difluorobiphenyl-4-yl)-2-(1*H*-imidazol-1-yl)ethyl)-4-(5-phenyl-1,3,4-oxadiazol-2-yl)benzamide (VFV), was identified (Hargrove *et al*., 2016).

The positive results induced by inhibitors of ergosterol pathway are particularly relevant as they could be a starting point to identify new pharmacological therapies to improve the condition of *MPV17*-related MDS patients. To better understand the molecular mechanism by which the molecules exert their beneficial effects, in the future it will be interesting to measure the mitochondrial transmembrane flows of different metabolites, such as nucleotides, nucleosides, Krebs' cycle intermediates and phosphate in presence and in absence of the identified molecules. Furthermore, the study of the molecules effects also in other model systems, in particular in Zebrafish, *Drosophila melanogaster* and in human cells, will be useful to validate their potential role in therapy.

Regarding the other molecules, Sertraline HCl is an antidepressant selectively inhibiting serotonin reuptake. This molecule is biologically active in model systems, including fungi, which do not express its putative protein target, the serotonin 5-HT transporter, thus demonstrating the existence of one or more secondary targets. In *S. cerevisiae* it has been showed that sertraline targets phospholipid membranes inducing phospolipidosis that is correlate with membrane ultrastructural changes (Rainey *et al.,* 2010).

Benzethonium chloride is a synthetic quaternary ammonium salt that is broadly used and widespread presence in the environment because of their antimicrobial and cationic surfactant properties. This drug inhibits the HERG channel activity, a member of a family of voltage-gated potassium (K+) channels that plays a critical role in the repolarization of the cardiac action potential. Interestingly this drug also induces membrane perturbation in yeast (Uesono *et al*., 2008).

Dhomiphen Bromide, like Benzethonium chloride, is a quaternary ammonium salt that inhibit the HERG K-channel (Long *et al*., 2013), so it is possible that they act by the same mechanism in yeast cells.

Thonzonium bromide and Alexidine selectively target in yeast the vacuolar-ATPase complex *in vitro* and *in vivo* by blocking proton transport. Consequently they alter cytosolic and vacuolar pH homeostasis and deplete the energy reserves of the cell, because uncoupled V-ATPase pumps will hydrolyze cytosolic ATP continuously (Chun-Yuan Chan *et al.,* 2012). Noticeably, V-ATPase mutants display a series of phenotype similar to those observed in mutants defective in *ERG2* gene that encodes the yeast sterol Δ^8, Δ^7 isomerase (Kane 2006, Pagani *et al*., 2007, Serrano *et al.*, 2004), suggesting that the alteration of V-ATPase induced, as secondary effect, an altered sterol composition of cellular membranes. Furthermore, defects leading to an accumulation of abnormal sterols were reported to affect V-ATPase and proposed as part of fungicidal effect of azole antifungal (Zhang and Rao, 2010, Zangh *et al*., 2010).

Otilonium bromide is a spasmolytic drug successfully used for the treatment of irritable bowel syndrome. Its efficacy has been attributed to the blockage of L- and T-type Ca^{2+} channels and muscarinic and tachykinin receptors in the smooth muscle (Rychter *et al*., 2014). Currently, no information is known about its target in yeast.

Ebselen is an organoselenium compound, mimics glutathione peroxidase activity. It has been indicated in several reports that the mithocondria is a potential target of this molecule (Boireau *et al*., 2000, Tiano *et al*., 2003, Moussaoui *et al*., 2000). It exerts a protective action on mitochondrial membrane against peroxidative reaction in the liver mitochondria isolated from glutathione-depleted rats (Narayanaswami and Sies, 1990). Another report showed a deleterious action of Ebselen on astrocyte physiology by altering mitochondrial membrane permeability and calcium homeostasis (Santofimia-Castano *et al*., 2013).

Further investigations are necessary to better understand the specific molecular target in yeast and to elucidate through which mechanisms the molecules exert their beneficial effect on studied mutant strains.

2.3 Effect of the increased dNTPs pool on mtDNA stability

As described in the Introduction, a deletion in the *MPV17*-homologues in Zebrafish determined a transparent mutant phenotype due to the lack of iridophores that contain large amounts of crystals of guanine, suggesting that the deficiency of this gene could induced a depletion in guanine (Krauss *et al*., 2013). More recently it has been observed, in mouse and patient-derived cells characterized by *MPV17* deficiency, a decrease in the mitochondrial dNTPs pool, accompanied by depletion of mtDNA and

highly abundant replication intermediates in liver mitochondria. Moreover, the adverse effects of *MPV17* deficiency on mtDNA could be prevented and rescued in cultured cell by deoxynucleoside supplementation, suggesting that *MPV17* deficiency caused deoxynucleotide insufficiency in mitochondria (Dalla Rosa *et al*., 2016).

Here I evaluated if the increase of dNTPs pool was able to ameliorate the phenotype of the mutant strain disrupted in *SYM1*. I used three different strategies to induce the intracellular increase of dNTPs: a) overexpression of ribonucleotide reductase *RNR1* coding for the large subunit of ribonucleotide reductase which catalyses the rate-limiting step of dNTPs synthesis; b) deletion of its inhibitor *SML1* (Chabes *et al*., 1999) and c) supplementation of intermediates of dNTPs synthesis, which can be transported through the cellular membrane.

In particular I evaluated the effect of the increased cytosolic dNTPs pool on mtDNA stability by measuring the *petite* frequency in the null mutant *sym1Δ*. So, I transformed BY4741 and BY4741*sym1Δ* strains with the multi copy recombinant construct YEplac195*RNR1* or as control with the empty vector YEplac195 as describe in Materials and Methods. Cells were grown in the same conditions previously described for the determination of mtDNA mutability. The analysis showed a reduction of *petite* colonies in the mutant strain overexpressing the Rnr1 enzyme respect to the *sym1Δ* strains (figure 2.19). However, a decrease of *petite* percentage is observed also in the wild type strain overexpressing Rnr1. This observation suggests that the dNTPs pool may be limiting in yeast cells.

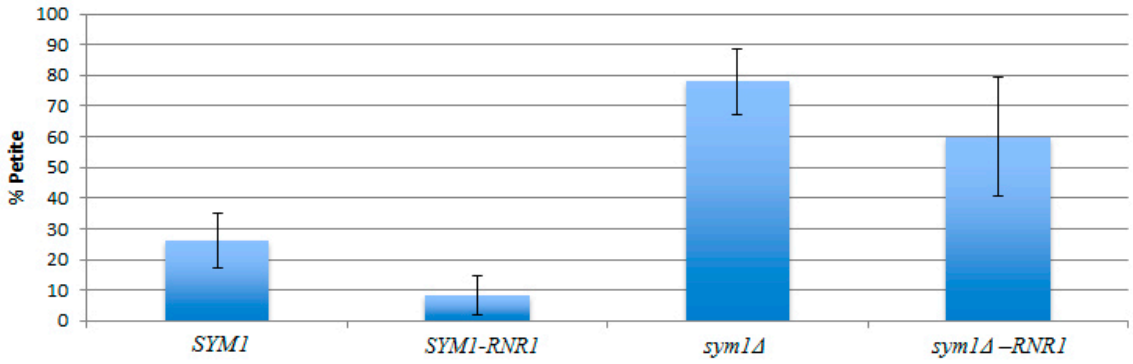

Figure 2.19. Analysis of mtDNA mutability performed on wild type (*SYM1*) strain and null mutant (*sym1Δ)* transformed with YepLac195 or YepLac195*RNR1*, after 15 generations of growth at 37°C. Blue bars represent the percentage of *petite*. More than 4000 colonies per strain were scored. All values are means of three independent experiments. The error bar represents the standard deviation.

I also evaluated the *petite* mutant frequency in the mutant *sym1Δ* lacking in *SML1*, the inhibitor of *RNR1 (sym1Δsml1Δ)*. To obtain the double mutant I performed the disruption of the *SYM1* gene at the chromosomal locus using a *sym1::Hig*^{R} cassette conferring higromycine resistance to the transformed yeast strain BY4741*sml1Δ* through high efficiency yeast transformation protocol (Giets and Woods, 2002).

In this case I observed a very strong reduction of *petite* mutants in the *sym1Δsml1Δ* strain respect to the *sym1Δ* strain, whereas in the *sml1Δ* strain the rescue was of lesser extent of that observed in the wild type strain (figure 2.20). In any case the data reconfirmed that the increased dNTPs pool is able to ameliorate the mtDNA stability. It remains unclear why the overexpression of *RNR1* and the deletion of *SML1* do not exactly parallelize. It is possible that the presence of a multicopy plasmid has a major negative impact in a defective yeast strain, as *sym1Δ*, respect to the wild type strain. It has also been showed that in yeast the elevation of intracellular dNTPs over a particular threshold level by overexpressing Rnr1 can induce genome instability (Tang *et al*., 2009).

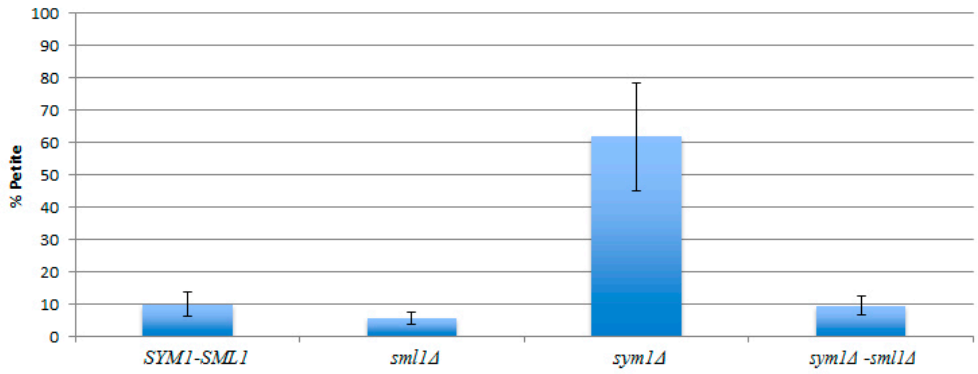

Figure 2.20. Analysis of mtDNA mutability performed on wild type strain (*SYM1-SML1*), null mutants (*sym1Δ* and *sml1Δ)* and double mutant (*sym1Δ* and *sml1Δ)* after 15 generations of growth at 37°C. Blue bars represent the percentage of *petite*. More than 4000 colonies per strain were scored. All values are means of three independent experiments. The error bar represents the standard deviation.

To better understand if this positive effect is specifically attributable to pyrimidine and/or purine metabolism we supplemented single intermediate of dNTPs biosynthetic pathway to the *sym1* mutant strain (*sym1*^{R51W}) in order to evaluate their capability to reduce the *petite* mutants frequency. We supplemented guanosine, adenosine, uridine, orotic acid and cytidine at different concentrations. Supplementation of guanosine and orotic acid at the highest concentration tested (250 µg/ml) had the most positive effects. Supplementation of adenosine showed a slight effect and no effect was observed

for uridine and cytidine (figure 2.21). So, supplementation of both pyrimidine and purine are able to ameliorate the mtDNA stability. However, these experiments should be repeated to reconfirm the results obtained.

A)

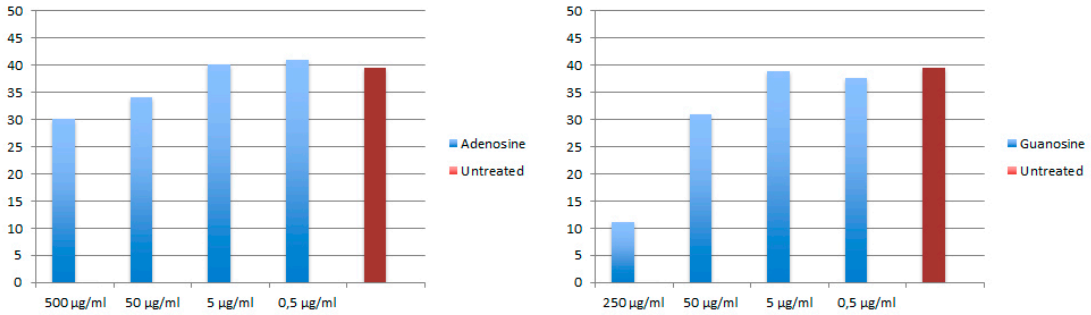

B)

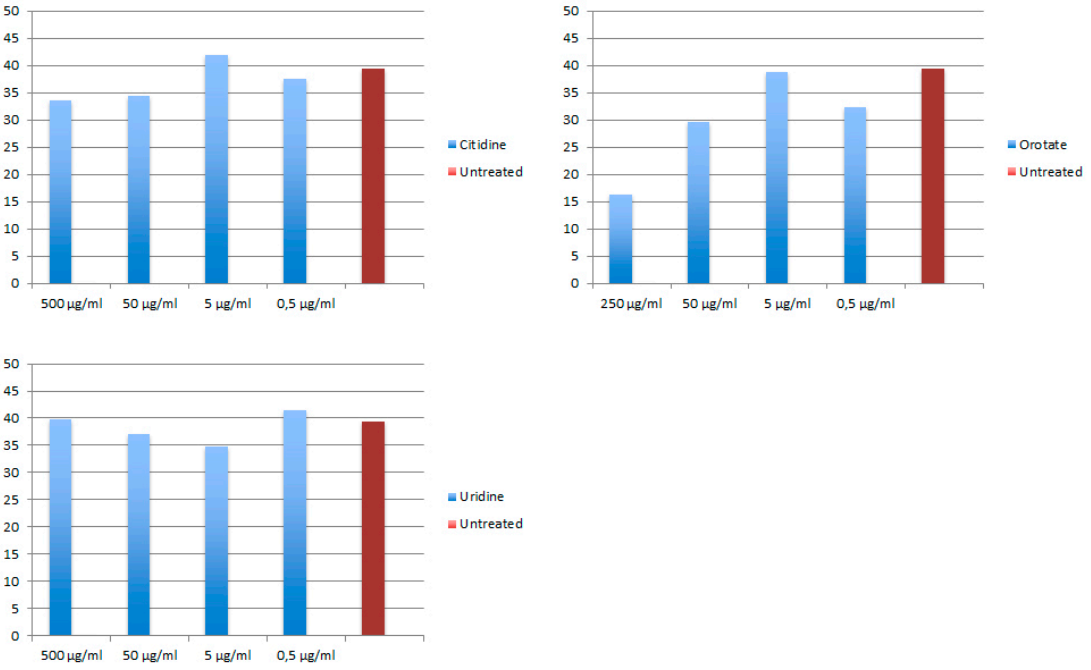

Figure 2.21. Analysis of mtDNA mutability performed on *sym1*^{R51W} mutant strain after 15 generations of growth at 37°C. The blue bars represent the percentage of *petite* after A) supplementation with intermediates of purine metabolism. B) Supplementation with intermediates of pyrimidine metabolism. Red bar represents the percentage of *petite* in absence of molecules.

Overall, the results obtained through the three strategies performed showed that the increased dNTPs pool ameliorate the mtDNA stability and also suggested that in yeast the dNTPs pool is defective in

sym1 mutant strains.

In the future a direct measurement of dNTPs into the mitochondria will may confirm this effect in the yeast cells. To measure the quantity of mitochondrial dNTPs I am setting up an enzymatic assay based on elongation of 5'-end-labeled oligonucleotide primers annealed to complementary oligonucleotyde templates (Roy *et al*., 1999).

Part of the results here presented have been included in the following publication:

Mitochondrial DNA depletion syndromes: yeast as a model for the study of the molecular mechanisms underlying the pathology caused by mutations in the human gene *MPV17*. Gilberti M., Baruffini E., Donnini C., Dallabona C. (2017, submitted).

3. Results and discussion – Section II

3.1. Study of missense variants in residues of Yars2/Msy1

Here I evaluated the alleged pathological role of six missense variants in *YARS2*, recently identified in 4 patients affected by MLASA by the Wellcome Trust Centre for Mitochondrial Research of the Newcastle University, taking advantage of the presence in yeast of the orthologous gene *MSY1*. The identified variants affect both conserved and not conserved residues between human and yeast proteins, as indicated by the protein alignment (figure 3.1). In particular the Yars2 amino acidic residues P122, L208, Y221 and L392 are conserved in the yeast protein Msy1 and correspond to the amino acidic residues P134, L226, Y239 and L411, respectively. The human residues G191 and C369 are not conserved in Msy1 and correspond to the amino acid R209 and L391, respectively.

```
Yars2   -----MAAPILRSFSWGRWSGTLNLSVLLPLGLRKAHSGAQGLLAAQKARGLFKDFFPET 55
Msy1    MLELRSCSNLVNSSRRLVPLVTYSGLSAITLPKSRFYSQPSALEVQGTSDSRSDNILDEL 60
              .: ::.*        * .    :.*   : :* ...* .  .: .  .::: *

Yars2   G-----TKIELPELFDRG--TASFPQTIYCGFDPTADSLHVGHLLALLGLFHLQRAGHNV 108
Msy1    KQRGLVSQVSQPESFLRTKLNGNDKIKLYCGVDPTAQSLHLGNLVPLMVLLHFYVKGHDI 120
              :::. ** * *   ...   .:***.****:***:*:*:.*: *:*:   **::

Yars2   IALVGGATARLGDPSGRTKEREALETERVRANARALRLGLEALAAN------HQQLFTDG 162
Msy1    VTVIGGATGKVGDPSGRKTERDVMENDIRQSNVASISQQLQRFFKNGLEYYRNRCALTED 180
        ::::****.::******..**:.:*.:  ::*. ::   *: :  *      ::  :*:.

Yars2   RSWGSFTVLDNSAWYQKQHLVDFLAAVGGHFRMGTLLSRQSVQLRLKSPEGMSLAEFFYQ 222
Msy1    VPSGKYTPRNNFNWWKDIKMLDFLADFGRHIRVQSMLARDSISSRLQTKNGLGFNEFTYQ 240
         . *.:*  :*  *::. :::**** .* *:*: ::*:*:*:. **:: :*:.: ** **

Yars2   VLQAYDFYYLFQRYGCRVQLGGSDQLGNIMSGYEFINKLTGED----VFGITVPLITSTT 278
Msy1    VLQAYDFYHLYKEENVTIQVGGNDQWGNITAGIDLINRIQPIKNKGLPFGITVPLLTTAT 300
        ********:*::. .  :*:**.** *** :* ::**::   .     *******:*::*

Yars2   GAKLGKSAGNAVWLNRDKTSPFELYQFFVRQPDDSVERYLKLFTFLPLPEIDHIMQLHVK 338
Msy1    GEKFGKSAGNAVFIDPSINTAYDVYQFFYNTLDADVPKFLKIFTFLNSSEIKKIVETHIK 360
        * *:********::: . .:.:::**** .  * .* ::**:****  .**.:*:: *:*

Yars2   EPERRGPQKRLAAEVTKLVHGREGLDSAKRCTQALYHSSIDALEVMSDQELKELFKEAPF 398
Msy1    SPSLRYGQTLLAKEVTDMLYGVGSGSDSEAISNIIFG---RYDGTLSAAKLVDLCKKARI 417
        .*. *  *. ** ***.:::*  . ..::  :: ::        .:*  :* :* *:* :

Yars2   SEFFLDPGTSVLDTCRKANAIPDGPRGYRMITEGGVSINHQQVTNPESVLIVGQHILKNG 458
Msy1    LQYADREIDLIKLICKLVNCSVSEAR--RKLSQGSVYLHHSKSKVNENISNLAPFLIDDR 475
         ::       :   *: .*.  . .*  * :::*.* ::*.: .  *.:  :. .::.:

Yars2   LSLLKIGKRNFYIIKWLQL 477
Msy1    VLILRIGKQKCFIIEMR-- 492
        : :*:***:: :**:
```

Figure 3.1. CLUSTAL Omega alignments of the Yars2 and Msy1 proteins. The missense variants conserved between the two proteins are shown in green. The missense variants not conserved between the two proteins are shown in red.

3.1.1. Construction of mutant strains

For the not conserved residues I mutagenized the yeast sequence in order to replace: a) the amino acid of the wild type Msy1 with the amino acid present in the wild type human Yars2, creating the so-called humanised version and b) the amino acid of the wild-type Msy1 with the mutated amino acid. If the humanized wild type variant is able to complement the oxidative growth defect of the *msy1*Δ strain it is possible to evaluate the effects of the novel missense variant identified in patients. For the conserved residues the corresponding yeast mutant allele was created and the impact of the mutations was evaluated comparing mutant and wild type strains phenotypes.

The construction of mutant strain requires special precaution. In fact, deletion or mutations in the *MSY1* gene lead to a complete loss of mitochondrial DNA (Edwards and Schimmel, 1987), an irreversible condition defined in yeast rho^0, making impossible to investigate the effects of pathological mutations on mitochondrial phenotypes. In order to avoid loss of mitochondrial DNA, the *MSY1* gene was disrupted in presence of the pFL38 plasmid carrying the wild-type allele *MSY1*. In this condition, mitochondrial DNA is maintained. *MSY1* was mutagenized by PCR overlap technique with appropriate primers to obtain the allelic variants $msy1^{hL391C}$, $msy1^{L391Y}$, $msy1^{L411S}$, $msy1^{hR209G}$, $msy1^{R209V}$, $msy1^{Y239H}$, $msy1^{P134R}$ and $msy1^{L226R}$ and subsequently cloned into the pFL39 vector. The strain W303-1B*msy1Δ*/pFL38-*MSY1* was then transformed with pFL39-*MSY1,* pFL39 harbouring the mutant allele created, or with the empty vector pFL39. To obtain strains containing only the pFL39 recombinant plasmid, I counter-selected the pFL38*MSY1* through plasmid shuffling on 5-FOA. The construction of the strain was described in detail in Materials and Methods.

In table 8 the human protein changes, the corresponding yeast humanized and mutant alleles are reported. In the patient 1 the mutation Cys369Tyr resulted in compound with a duplication in the second allele. The patient 2 resulted homozygous for the Leu392Ser. In the patient 3 Gly191Val resulted in compound with Tyr221Hys and the patient 4 was heterozygous for the mutations Pro122Arg and Leu208Arg.

Patient	c.DNA	Human protein change	Yeast humanized allele	Yeast mutant allele
1	c.1106G>A c.1147_1164dup	Cys369Tyr Val383_Glu388dup	hLeu391Cys	Leu391Tyr
2	c.1175T>C	Leu392Ser		Leu411Ser
3	c.572G>T c.661T>C	Gly191Val Tyr221His	hArg209Gly	Arg209Val Tyr239His
4	c.365C>G c.623T>G	Pro122Arg Leu208Arg		Pro134Arg Leu226Arg

Table 8. Overview of the patients carrying the missense mutations studied and the correspondent localization in yeast.

3.1.2 Phenotypic analysis

To study the potential pathological role of the missense variants, the strains obtained were characterized for their ability to grow in presence of ethanol 2% as oxidative carbon sources by spot assay. The analysis was conducted at two temperatures, both at the optimal one 28°C, and at the highest allowed temperature for the wild type strain 36°, to exacerbate mutant phenotype. The results are reported in figure 3.2. Similar results were obtained in presence of other oxidative carbon sources, acetate, glycerol or lactate (data non shown). With regard to the non conserved variants, as showed in figure 3.2, oxidative growth of the strains expressing the humanised versions *msy1*^{hL391C} and *msy1*^{hR209G} was similar to those of the wild type strain both at 28°C and 36°C. Growth of the strain expressing the variants corresponding to those identified in patients was quite different. The growth of the *msy1*^{L391Y} was reduced, particularly at 36°C, whereas the strain expressing *msy1*^{R209V} did not show a defective growth neither at 28°C nor at 36°C. As concern the conserved variants, the yeast strains expressing the allelic variants *msy1*^{Y239H} and *msy1*^{P134R} showed a severe oxidative growth defect already at 28°C. The strain harbouring the L226R variant showed a slight growth defect both at 28°C and at 36°C whereas *msy1*^{L411S} did not showed a defective growth neither at 28°C nor at 36°C. The obtained results did not show significant differences between the two growth temperatures.

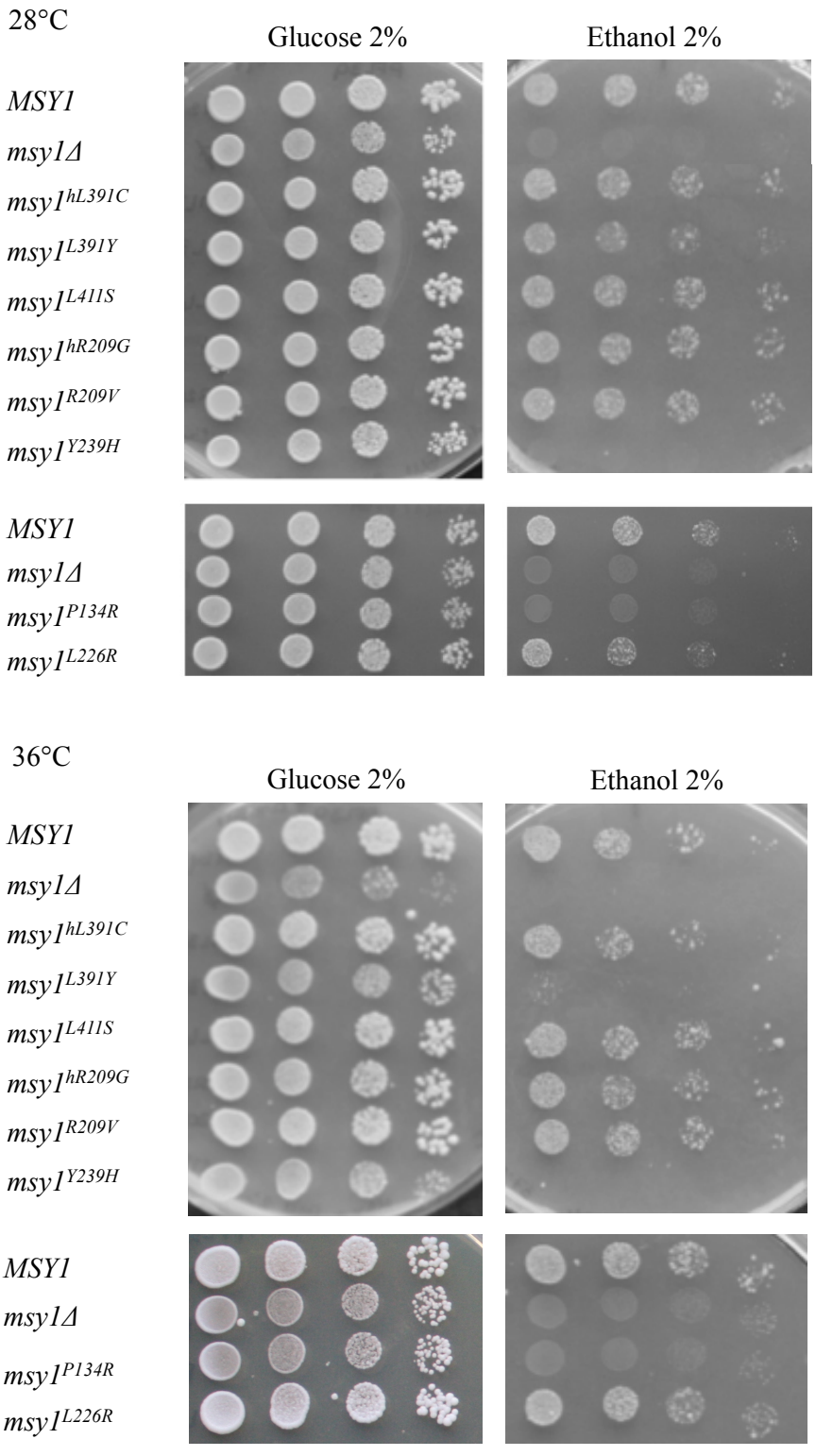

Figure 3.2. Oxidative growth phenotype at 28°C and 36°C of W303-1B*msy1Δ* transformed with pFL39*MSY1*, pFL39 empty vector or with mutant alleles. Equal amounts of serial dilutions of cells from exponentially grown cultures were spotted ($5x10^4$, $5x10^3$, $5x10^2$, $5x10^1$ cells/spot) onto YP plates supplemented with the indicated carbon sources. Growth was scored after 3 days of incubation.

The functionality of the mitochondrial respiratory complexes was evaluated by measuring the oxygen consumption of cells grown at 28°C. Cells were cultured and respiratory rate measured as described in Materials and Methods. The mutations Y239H and P134R determined a strong reduction in oxygen consumption, comparable to that of *msy1Δ*. Mutant $msy1^{L391Y}$ and $msy1^{R209V}$ showed a 27% and 11% reduction of the respiratory rate compared to their humanised version msy^{hL391C} and msy^{hR209G}, respectively. Mutant strains $msy1^{L411S}$ and $msy1^{L226R}$ showed a 21% and 40% reduction compared to wild type strain (figure 3.3).

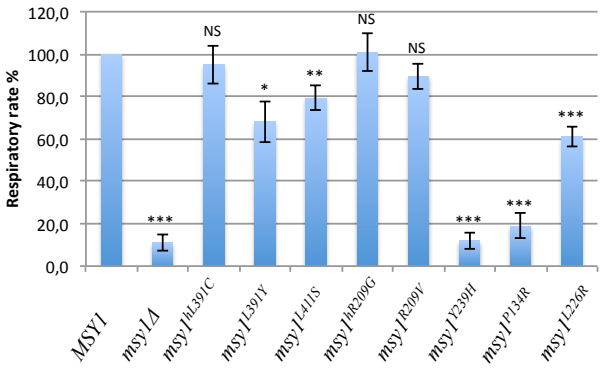

Figure 3.3. Oxygen consumption of W303-1B*msy1Δ* transformed with pFL39*MSY1,* pFL39 empty vector or with mutant alleles at 28°C grown in SC-Trp medium supplemented with 0.6% glucose. Cells were grown until glucose was exhausted to promote the expression of respiratory chain components. NS: not significat, *p<0.5, **p<0.01, ***p<0.001.

Taken together the phenotypic analyses confirmed an OXPHOS defect for all the mutations studied. In particular mutations Y239H and P134R induced severe defects, whereas the other mutations led to a less serious phenotype. The severity of the phenotypes observed in the mutant $msy1^{Y239H}$ is consistent with the role of this residue, conserved in all TyrRSs, in tyrosine recognition (Bonnefond *et al*., 2007 b). Interestingly the modelled missense changes L391Y and L411S reflected the human clinical phenotypes of the patients carrying the correspondent mutations (Sommerville *et al*., 2017), confirming yeast as a suitable model to evaluate the pathogenicity of YARS2 mutations. The validation of the mutation R209V, that did not showed a growth defect neither at 28°C nor at 36°C, but only a not significant slight reduction (11%) in oxygen consumption, is not completely obvious. The fact that the human corresponding mutation G191V (yR209V) is in the patient (table 8) in compound with the mutation Y221H (yY239H) characterized by a severe OXPHOS defect, could explain the pathology. This possibility can be evaluated in yeast through the creation and analysis of the hetero-allelic strain harbouring the two mutations in compound.

3.1.3 Construction of mutant heteroallelic strains and phenotypic analyses

To create the hetero-allelic yeast strain harbouring the mutations R209V and Y239H in compound, I performed the subcloning of the *MSY1* and *msy1*^{Y239H} alleles from pFL39 plasmid to pFL38 plasmid as described in Materials and Methods. Recombinant plasmids obtained pFL38*MSY1* and pFL38*msy1*^{Y239H} were introduced in *W303-1BΔmsy1*/pFL39*MSY1* or *W303-1BΔmsy1*/pFL39 *msy1*^{R209V} through the Li-Ac method (Gietz and Woods, 2002), to obtain the following strains:

W3031BΔmsy1/pFL39MSY1-pFL38MSY1 (wt-wt)

W3031BΔmsy1/pFL39msy^{R209V}*-pFL38 msy*^{Y239H} (R209V-Y239H)

The oxidative growth and the respiratory rate of the two strains are shown in figure 3.4. The hetero-allelic mutant strain (*msy1*^{Y239H} *msy1*^{R209V}) showed a defective oxidative growth. Oxygen consumption was reduced by approximately 30% compared to the wild type strain. These observations suggest that the combination of the two mutations is the cause of the pathology.

A)

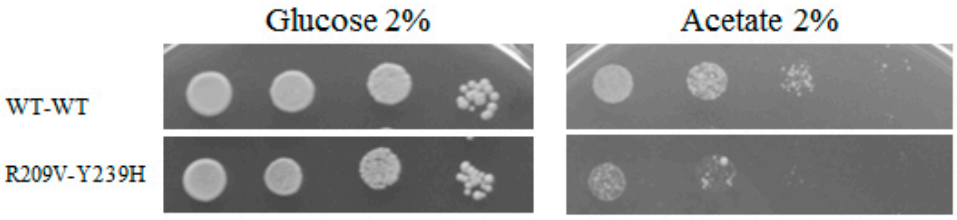

B)

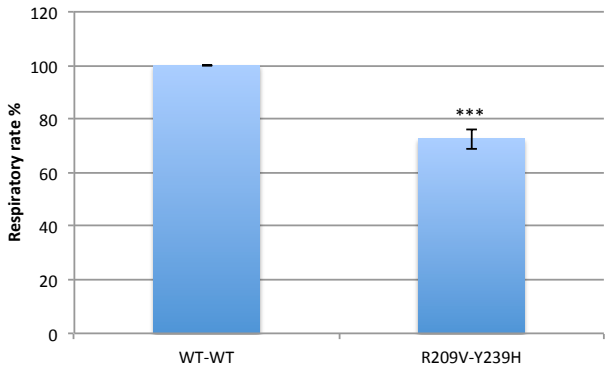

Figure 3.4. A) Oxidative growth phenotype at 28°C of W303-1B*msy1Δ* transformed with pFL39 and pFL38 plasmids carrying the indicated allelic variants. Equal amounts of serial dilutions of cells from exponentially grown cultures were spotted ($5x10^4$, $5x10^3$, $5x10^2$, $5x10^1$ cells/spot) onto YP plates supplemented with the indicated carbon sources. Growth was scored after 3 days of incubation. ***p<0.001. B) Oxygen consumption at 28°C of the indicated strains grown in SC-Trp-Ura medium supplemented with 0.6% glucose. Cells were grown until glucose was exhausted to promote the expression of respiratory chain components. **<0,001.

3.1.4 Effect of the tyrosine supplementation

It has been demonstrated that the negative effect of mutations in genes coding for the aminoacyl-tRNA synthetases can be ameliorated or rescued by the supplementation of the amino acid substrate specific for the aminoacylation reaction (Diodato *et al*., 2014 b).

I evaluated whether the tyrosine supplementation is able to rescue the impaired functionality of respiratory complexes in the mutant strains studied. Tyrosine is the natural substrate in the aminoacylation reaction catalysed by tyr-tRNA synthetase. So I measured oxygen consumption of the mutant strains cultured in a medium supplemented with tyrosine (40 µg/ml). Interestingly, in the mutant strains, except for those harbouring mutations that led to strong phenotype (P134R, Y239H), the supplementation of tyrosine leads to a recovery of respiration comparable to that observed in the wild type strain (figure 3.5).

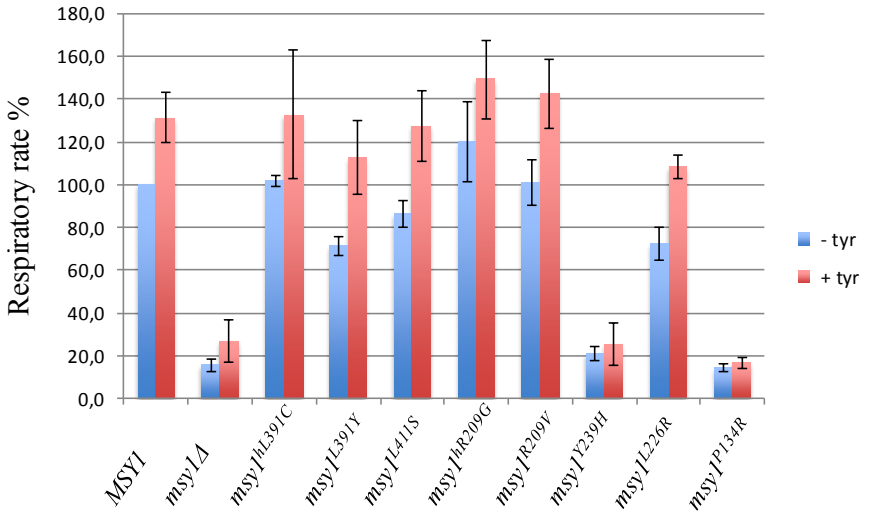

Figure 3.5 Oxygen consumption of W303-1B*msy1Δ* transformed with pFL39*MSY1*, pFL39 empty vector or with mutant alleles at 28°C grown in medium supplemented with 0.6% glucose. Cells were grown until glucose was exhausted to promote the expression of respiratory chain components. Blue bars represents the strain grown in SC-Trp-Tyr medium, whereas red bars represent the strains grown in SC-Trp medium supplemented with tyrosine (40 µg/ml).

These results suggest that when the enzyme activity is strongly affected the supplementation of specific substrate of the reaction is not effective, as in the case of the mutant variants *msy1*^{Y239H} and *msy1*^{P134R}. Conversely, when the enzyme is partially functional the tyrosine supplementation has a beneficial effect on mitochondrial protein synthesis, increasing the respiratory rate. Interestingly, tyrosine supplementation resulted in increased oxygen consumption also in the wild type strain. The observed

increase could be due to the fact that tyrosine is a limiting substrate for aminoacylation reaction, or to an indirect effect favouring the cellular metabolism supplying the Krebs' cycle (figure 3.6).

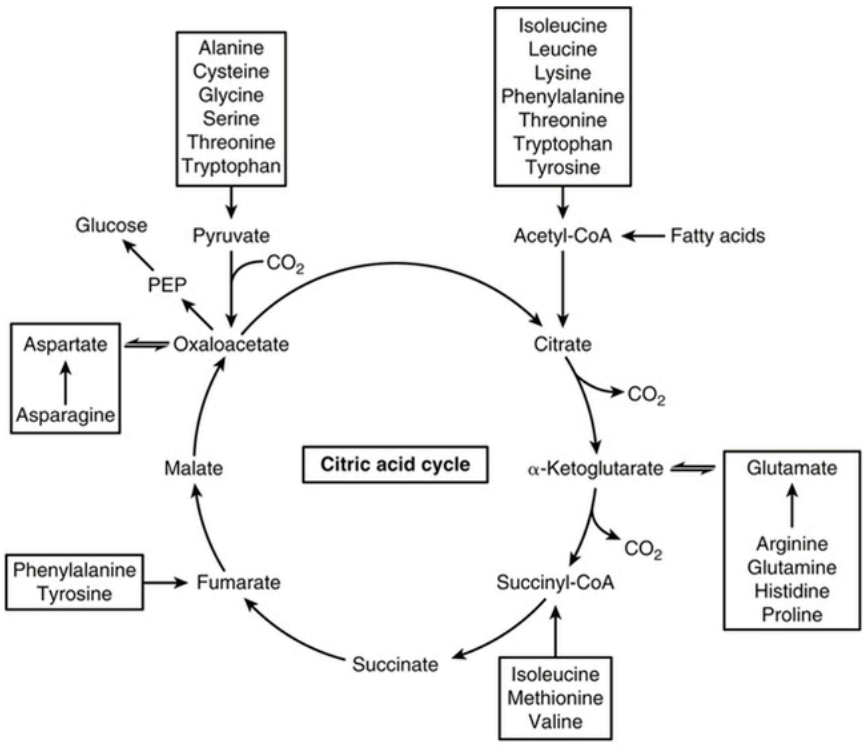

Figure 3.6. Schematic representation of Krebs cycle.

To understand by which mechanism tyrosine is able to ameliorate the oxygen consumption in wild type strain i) directly, as the substrate of the aminoacylation reaction, or ii) indirectly, improving the cellular metabolism via Krebs cycle, I compared the oxygen consumption in the wild type strain cultured in a medium supplemented with tyrosine or with phenylalanine, that enters in Krebs cycle in the same step of tyrosine and are present in similar concentrations in the yeast cell (Messenguy *et al*., 1980). As showed in figure 3.7 only tyrosine supplementation is able to induce a significant rescue in respiratory rate, suggesting that tyrosine is in yeast a limiting substrate for the aminoacylation reaction.

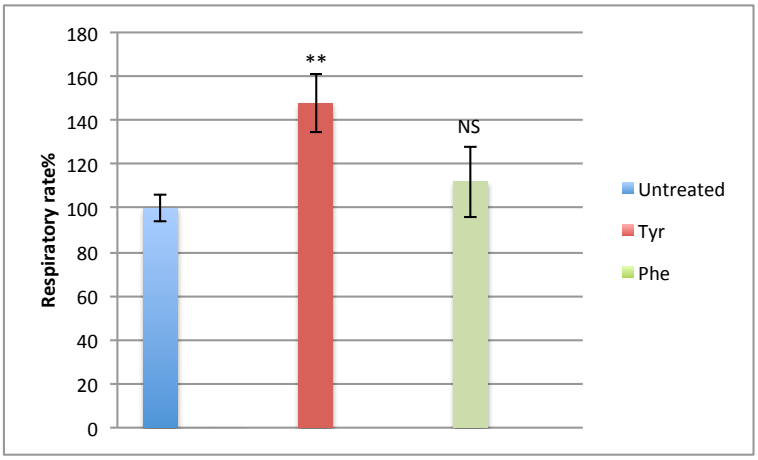

Figure. 3.7. Oxygen consumption of W303-1B*msy1Δ*/pFL39*MSY1* at 28°C grown in medium supplemented with 0.6% glucose. Cells were grown until glucose was exhausted to promote the expression of respiratory chain components. Blue Bar represents the strain grown in a SC-Trp-Tyr-Phe medium, red bar represents the strains grown in SC-Trp medium supplemented with tyrosine (40 µg/ml) and green bar represents the strains grown in SC-Trp medium supplemented with phenylalanine (40 µg/ml). **<0,01. NS: not significant.

Part of the findings discussed in this section are contained in the following publication:

Clinical Features, Molecular Heterogeneity, and Prognostic Implications in YARS2-Related Mitochondrial Myopathy. Sommerville E.W., Ng Y.S., Alston C.L., Dallabona C., Gilberti M., He L., Knowles C., Chin S.L., Schaefer A.M., Falkous G., Murdoch D., Longman C., de Visser M., Bindoff L.A., Rawles J.M., Dean J.C.S., Petty R.K., Farrugia M.E., Haack T.B., Prokisch H., McFarland R., Turnbull D.M., Donnini C., Taylor R.W., Gorman G.S. JAMA neurology, 2017 Jun 1;74(6):686-694.

3.2 Study of missense variants in residues of *QRSL1* and *GATB* coding for subunits of GatCAB complex

As described in Introduction, mutations in the GatCAB complex subunit A (*QRSL1*) have been identified as cause of a lethal infantile mitochondrial disorder (Kohda *et al*., 2016). Recently, the MRC Mitochondrial Biology Unit of Cambridge (UK) identified patients with variants in the *QRSL1* gene and in the *GATB* gene, coding for the subunit B of the GatCAB complex. These patients showed a severe clinical phenotype with prominent cardiomyopathy and lethal infantile lactic acidosis, with variable deficiencies of the respiratory chain enzymes, which is typical for defects in mitochondrial tRNA aminoacylation.

To validate the pathogenicity of the *QRSL1* and *GATB* variants identified in the patients we used the yeast as a model system taking advantage of the presence of the orthologous genes, *HER2* and *PET112*,

respectively. The human variants identified in three patients, the corresponding yeast humanized and mutant alleles are reported in table 9. In patient 1 the variant Gly133Val resulted in compound with a variant that induce an early stop in the second allele. In patient 2 three missense variants, Thr196Asn Arg197Lys Pro199His, were located in the same paternal allele, in compound with the variant Ala427Leu in maternal allele. In patient 3 Phe136Leu resulted in compound with a variant inducing frameshift and premature stop codon.

Patient	**Gene**	**Human protein change**	**Yeast humanized allele**	**Yeast mutant allele**
1	hQRSL1 *yHER2*	Gly133Val Tyr185*	hSer109Gly	Ser109Val
2	hQRSL1 *yHER2*	Thr196Asn; Arg197Lys; Pro199His Ala427Leu	hVal155Thr hPro397Ala	Val155Asn; Arg156Lys; Pro158His Pro397Leu
3	hGATB *yPET112*	Phe136Leu Ser194Trpfs*15		Phe103Leu

Table 9. Overview of the patients carrying the missense variants studied and the correspondent in yeast.

As shown by Qrsl1/Her2 protein alignment (figure 3.8 A) the human residues Arg197 and Pro199 are invariant from human to yeast, Arg156 and Pro158, respectively. On the contrary the human amino acid residues Gly133, Thr196 and Ala427 are not conserved in yeast, corresponding to Ser109, Val155 and Pro397, respectively. As previously described for the *YARS2*/*MSY1* mutations, for the analysis of pathogenicity of these three not conserved residues, it was necessary to create both the humanized version and the potentially pathological allele to compare their effect on mitochondrial function. As concern the non conserved variant Gly133Val (identified in patient 1) I constructed the yeast humanized and mutant alleles hSer109Gly and Ser109Val, respectively. As concern the non conserved variant Ala427Leu (identified in patient 2) I constructed the yeast humanized and mutant alleles hPro397Ala and Pro397Leu, respectively. The paternal allele of patient 2 showed three variants. Two of these variants, Arg167Lys and Pro199His, were in conserved residues in yeast, Arg156 and Pro158, respectively, whereas the third variant Thr196Asn was present in a not conserved residue. To validate the paternal allele variants I constructed the humanized allele hVal155Thr and the mutant allele Val155Asn,Arg156Lys,Pro158Hys.

Regarding the mutation in the *GATB* gene (identified in patient 3), as shown by protein alignment, the human residue Phe136 is invariant in yeast, Phe103 (figure 3.8 B). To validate the pathogenicity of the new variant p.Phe136Leu I introduced the change equivalent to the human variant into the yeast *PET112* wild-type gene.

A)

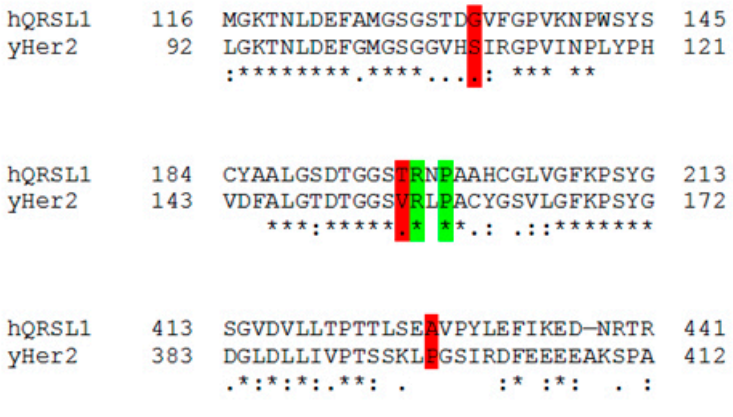

B)

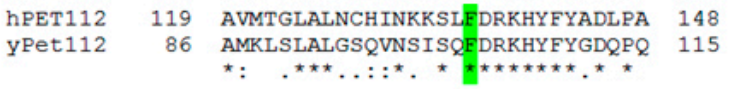

Figure 3.8. A) Portion of CLUSTAL Omega alignments of the Qrsl1 and Her2 proteins. B) Portion of CLUSTAL Omega alignments of the GatB and Pet112 proteins. The missense variants conserved between the proteins are shown in green. The missense variants not conserved between the proteins are shown in red.

3.2.1 Construction of mutant strains

The construction of the mutant strains was performed using the same approach previously described for the *MSY1* mutant strain, as also in this case the deletion of the genes lead to mitochondrial DNA loss (Merz and Westermann 2009, Mulero *et al*., 1994). Briefly, *HER2* and *PET112* were cloned under their natural promoters by PCR-amplification and inserted into the pFL38 vector. The pFL38-*HER2* or pFL38-*PET112* plasmid was introduced into the W303-1B strain through the Li-Ac method (Gietz and Woods, 2002) and disruption of the genomic *HER2* or *PET112* gene was performed in this strain. The

disruption was performed through one-step gene disruption by PCR-amplification of *KanMX4* cassette (Wach *et al*, 1994) from the BY4742 deleted strain using appropriate primers and transformation of the former strain; thus obtaining W303-1B*her2Δ*/pFL38-*HER2* and W303-1B*pet112Δ*/pFL38-*PET112*. *HER2* and *PET112* fragments were subcloned from pFL38 to pFL39. *HER2* and *PET112* were mutagenized by PCR overlap technique (Ho *et al*., 1989) with appropriate primers to obtain the humanized and mutant alleles, and subsequently they were cloned into the pFL39 vector. W303-1B*her2Δ*/pFL38-*HER2* was transformed with the pFL39 vector carrying the wild type (*HER2*) or the humanized ($her2^{hS109G}$ or $her2^{hV155T}$ or $her2^{hP397A}$) or the mutant ($her2^{S109V}$ or $her2^{V155N\text{-}R156K\text{-}P158H}$ or $her2^{P397L}$) alleles or with the empty vector as control, and then pFL38- *HER2* was lost through plasmid-shuffling. W303-1B*pet112Δ*/pFL38-*PET112* was transformed with the pFL39 vector carrying the wild type (*PET112*) or the mutant ($pet112^{F103L}$) allele or with the empty vector as control, and then pFL38-*PET112* was lost through plasmid-shuffling.

3.2.2 Phenotypic analyses

In order to reveal a possible respiratory growth defect of *HER2* mutant variants, serial dilutions of the strains were spotted on medium containing 2% ethanol as carbon source at 28°C. As shown in figure 3.9 A, the oxidative growth of the strains expressing the humanized versions $her2^{hS109G}$ and $her2^{hV155T}$ was similar to that of the wild type, whereas the strains expressing the mutant alleles $her2^{S109V}$, and $her2^{V155N\text{-}R156K\text{-}P158H}$ showed an oxidative growth severely reduced or totally absent. The strain with the humanized allele $her2^{hP397A}$ showed a slight reduction of growth respect to strain with the wild-type version, anyway the strain with mutant version $her2^{P397L}$ showed a more severe oxidative defective phenotype. To better define the oxidative growth deficiency I measured O_2 consumption. The analysis of the respiratory rate showed a reduction for all the mutants, although to a different extent (figure 3.9 B). In particular, parallelizing the growth defect, the mutant $her2^{V155N\text{-}R156K\text{-}P158H}$ behaved as the null mutant whereas the mutants $her2^{S109V}$ and the $her2^{P397L}$ showed a reduction of the respiratory rate respect to their humanized version of about 70% and 35% respectively. Overall the data obtained suggest a pathological role for all the analysed variants of *QRSL1* gene.

A)

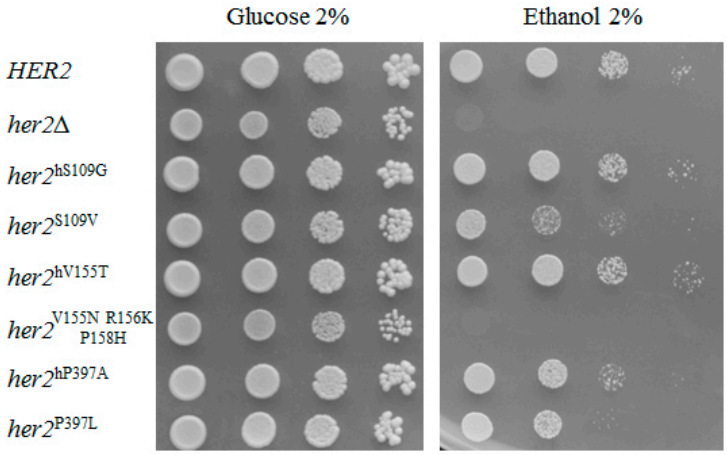

B)

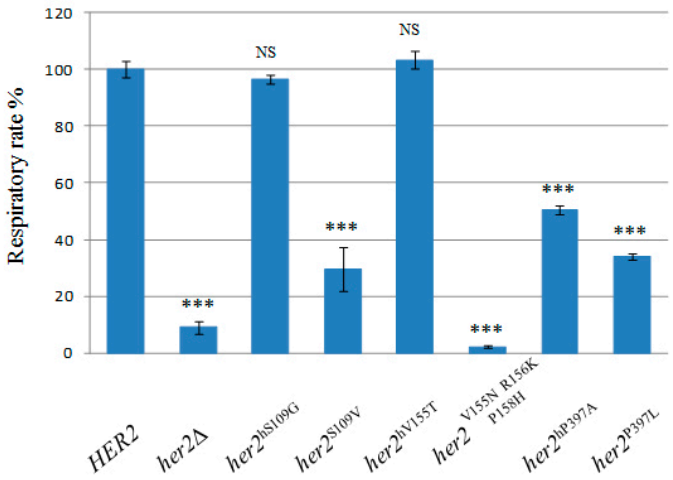

Figure 3.9. A) Oxidative growth phenotype at 28°C of W303-1B*her2Δ* transformed with pFL39 plasmid carrying the indicated allelic variants. Equal amounts of serial dilutions of cells from exponentially grown cultures were spotted ($5x10^4$, $5x10^3$, $5x10^2$, $5x10^1$ cells/spot) onto SC-Trp plates supplemented with the indicated carbon sources. Growth was scored after 3 days of incubation. B) Oxygen consumption at 28°C of the indicated strains grown in SC-Trp medium supplemented with 0.6% glucose. Cells were grown until glucose was exhausted to promote the expression of respiratory chain components. ***p<0.001. NS: not significant.

Regarding the *PET112* mutation, oxidative growth and O_2 consumption of the mutant strain *pet112*^{F103L}, measured in the same experimental condition described for the *her2* mutants, at 28°C, did not reveal any defect (data not shown). I then compared wild type and mutant strain in more stressing environmental conditions, high temperature (37°C) and absence of the amide donor glutamin. The use of more stressing condition is particularly helpful to emphasise the phenotype of mutants characterized

by a leaky phenotype. In particular based on the nature of GatFAB amidotransferase reaction that uses glutamine as a substrate, the absence of amide donor is a suitable condition for exacerbate the mt-tRNA aminoacylation phenotype. In these stressing conditions the mutant showed defective OXPHOS phenotype (figure 3.10 A) and a severe reduction of O_2 consumption (70%) (figure 3.10 B). These data support the pathogenic role of its human corresponding mutation.

A)

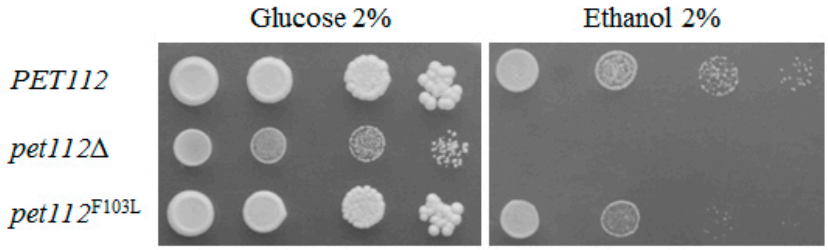

B)

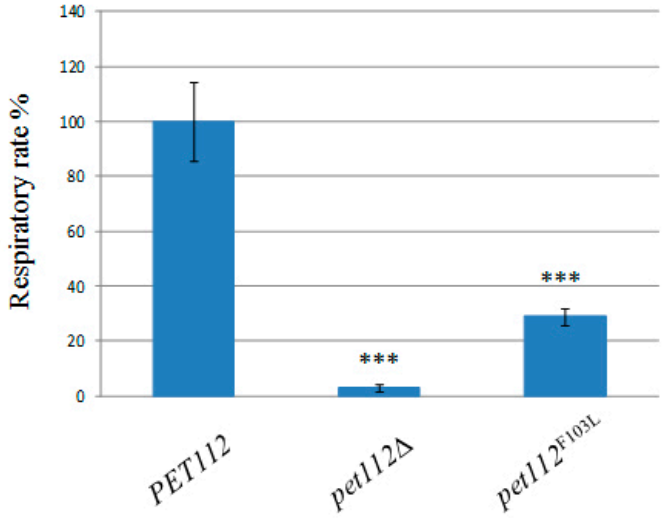

Figure 3.10. A) Oxidative growth phenotype at 37°C of W303-1B*pet112Δ* transformed with pFL39 plasmid carrying the indicated allelic variants. Equal amounts of serial dilutions of cells from exponentially grown cultures were spotted ($5x10^4$, $5x10^3$, $5x10^2$, $5x10^1$ cells/spot) onto SC-Trp-Gln medium supplemented with the indicated carbon sources. Growth was scored after 3 days of incubation.
B) Oxygen consumption at 37°C of the indicated strains grown in SC-Trp-Gln medium supplemented with 0.6% glucose. Cells were grown until glucose was exhausted to promote the expression of respiratory chain components. ***p<0.001. NS: not significant.

4. Materials and Methods

4.1 Strains used

S. cerevisiae strains used in this work are listed below:

Strain	Genotype	Reference
BY4741	*Mata; his3Δ1 leu2Δ0 met15Δ0 ura3Δ0*	Brachmann *et al*., 1998
BY4741 ρ^0	*Mata; his3Δ1 leu2Δ0 met15Δ0 ura3Δ0* ρ^0	This work
BY4741 *sym1Δ*	*Mata; his3Δ1 leu2Δ0 met15Δ0 ura3Δ0 sym1::kanMX4*	Euroscarf collection; Brachmann *et al*., 1998
BY4741 *sml1Δ*	*Mata; his3Δ1 leu2Δ0 met15Δ0 ura3Δ0 sml1::kanMX4*	Euroscarf collection; Brachmann *et al*., 1998
BY4741 *sym1Δ sml1Δ*	*Mata; his3Δ1 leu2Δ0 met15Δ0 ura3Δ0 sml1::kanMX4 sym1::Hig*^{R}	This work
W303-1B *msy1Δ*	*Matα ade2-1 leu2-3, 112 ura3-1 trp1-1 his3-11, 15 can1-100 msy1::kanMX4*	This work
W303-1B *her2Δ*	*Matα ade2-1 leu2-3, 112 ura3-1 trp1-1 his3-11, 15 can1-100 her2::kanMX4*	This work
W303-1B *pet112Δ*	*Matα ade2-1 leu2-3, 112 ura3-1 trp1-1 his3-11, 15 can1-100 pet112::kanMX4*	This work

The bacteria strain used in this work is listed below:

Strain	Genotype
DH10B	*F-mcrA Δ(mrr-hsdRMS-mcrBC) φ80d DlacZ ΔM15 ΔlacX74 deoR recA1 endA1 araD139 Δ(ara, leu)7697 galU galKλ-rpsL hupG*

4.2 Media and growth conditions

For yeast strains the following media were used:

- YP (1% peptone, 0.5% yeast extract)
- YPA (2% peptone, 1% yeast extract, 75mg/ml adenine)
- YNB (YNB ForMedium^{TM} w/o aminoacids w/o 1,9 g/l NH4SO4, 5 g/l NH4SO4).
- SC: YNB media enriched with drop-out powder (Kaiser *et al*. 1994).
- 5-FOA YNB: YNB ForMedium^{TM} with 1 g/l 5-Fluoroorotic Acid (Melford), 50 mg/l uracile with aminoacids necessary to complement the auxotrophies (Boeke *et al*., 1984).

If necessary singles amino acids could be excluded from complete drop-out to maintain selective pressure. As solidifying agent agar ForMedium^{TM} 2% was added. Carbon sources were added at final concentration of 2% if not specified differently. The following sources were used: Glucose (D),

Ethanol (E), Glycerol (G), Galactose (Gal), Lactate (L). *S. cerevisiae* was cultured at 28°C, in constant shaking 120 rpm if liquid media was used. To induce heat stress, cultures were incubated at 37°C in thermostat or water bath.

For *E. coli* LB media was used (1% bacto tryptone Difco™, 0.5% yeast extract Difco™, 0.5% NaCl, pH 7.2-7.5). Agar 2% and ampicillin (Sigma-Aldrich®) 100mg/ml were added if needed. For α-complementation selection 80µl of 5-bromo-4-chloro-3-indolyl-b-D-galactopyranoside (Xgal) 2% (dissolved in dimethilformamide) and 40µl isopropyl-beta-D-thiogalactopyranoside (IPTG) 23.8 mg/ml were added. Cultures were incubated at 37 °C in constant shaking if necessary.

4.3 Plasmids

Plasmid	Marker in *S.cerevisiae*	Type	Reference	Figure
pFL38	URA3	Centromeric	Bonneaud *et al*., 1991	4.1
pFL39	TRP1	Centromeric	Bonneaud *et al*., 1991	4.2
YEplac195	URA3	Multicopy	Gietz and Sugino, 1988	4.3

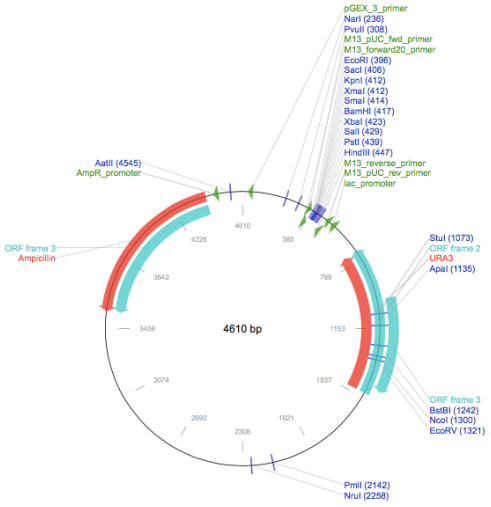

Figure 4.1. pFL38 plasmid

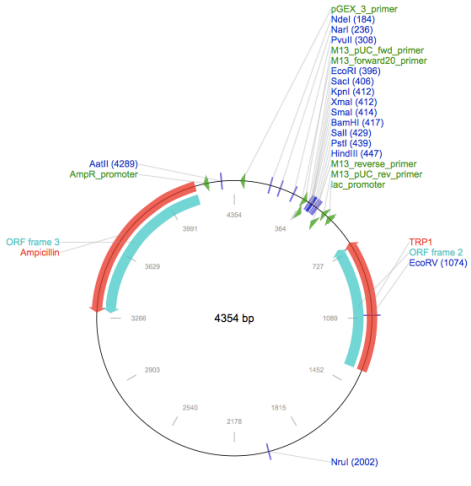

Figure 4.2. pFL39 plasmid

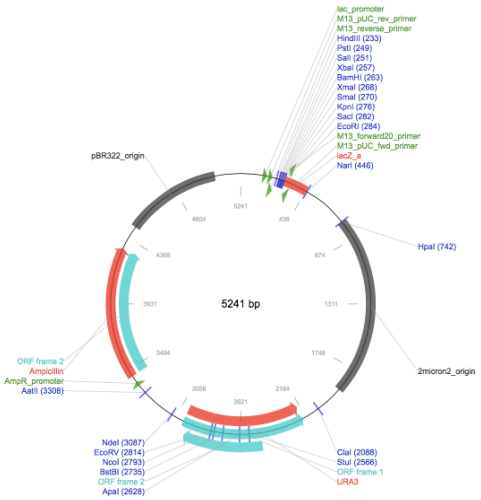

Figure 4.3. YEplac195 plasmid

4.4 Polymerase Chain Reactions

All the reactions were performed following manufacturer indications. Preparative reactions for gene cloning and site-specific mutagenesis were performed using KOD Hot Start high fidelity (HF) polymerase (Novagen®). All the reactions were performed using "Applied Biosystem 2720 Thermal Cycler". The primers utilize were indicated in the following table.

4.4.1 Real Time-qPCR

For Real Time-qPCR, cells, pregrown at 28°C in SC supplemented with 2% ethanol, were exponentially grown in SC supplemeted with 2% glucose at 28°C and transferred to SC medium supplemented with 0.6% glucose plus 2% ethanol at 37°C for 14 h.

Total RNA was extracted with hot acidic phenol (Ausubel *et al*., 1994), treated with DNase I (New England Biolabs), retrotranscribed with M-MuLV Reverse Transcriptase (NewEngland Biolabs) with oligo (dT) 20 primer (Euroclone) and murine RNase inhibitor (NewEngland Biolabs).

Quantitative PCRs were performed in 15 µl volume using Power Sybr Green mix with ROX (Life Technologies) in a 96-well plate. Triplicates were included for each reaction. The primers used for qPCR (qSYM1Fw and qSYM1Rv), at the final concentration of 120 nM, are listed in Table 10. All reactions were performed in the AB 7300 instrument (Life Technologies) at default settings:

- 2' at 50°C
- 10' at 95°C

- 15'' at 95°C - 1'at 60°C – 41 cycle

- 15'' at 60°C

For each analyzed gene, the level of expression was calculated using the comparative quantification algorithms -ΔΔCt. In this method the threshold cycles number Cts for the gene of interest in both the test sample (mutant strain) and calibrator sample (wild type strain) are adjusted in relation to a normalizer gene Ct from the same two samples. Normalizer gene *ACT1* was used. To determine the fold difference in expression we used the following expression:

Fold difference = $2^{-\Delta\Delta Ct}$

$\Delta Ct_{\text{sample}} - \Delta Ct_{\text{calibrator}} = \Delta\Delta Ct$

$Ct_{\text{target gene}} - Ct_{\text{norm. gene}} = \Delta Ct_{\text{sample}}$

$Ct_{\text{target gene}} - Ct_{\text{norm. gene}} = \Delta Ct_{\text{calibrator}}$

Statistical analysis was performed through an unpaired two-tailed t-test. Only p values of less than 0.05 were considered significant: *$p<0.05$, **<0.01, ***$p<0.001$.

	Primer
MSY1cFw	CCCCAAGCTTAATTTGTCCCAATTCGAAGG
MSY1cRv	CCCCGGTACCGTGTGACAGTGAAATGTTCG
MSY1DFw	TAATATTGGACTTGAAGCTG
MSY1DRv	AATATCACCTCACGCATGCC
MSY1P134RFw	GGGAAAGTTGGGGACAGAAGTGGTAGGAAAACAGAAAGAGACG
MSY1P134RRv	CGTCTCTTTCTGTTTTCCTACCACTTCTGTCCCCAACTTTCCC
MSY1hR209GFw	CTTAGCTGATTTTGGTGGCCACATTCGGGTACAATCTATGTTGGCG
MSY1R209VRv	CGCCAACATAGATTGTACCCGAATGTGCACACCAAAATCAGCTAAG
MSY1L226RFw	GGATTCAATTTCTTCGAGGCGTCAAACCAAAAATGGTCTGG
MSY1L226RRv	CCAGACCATTTTTGGTTTGACGCCTCGAAGAAATTGAATCC
MSY1Y239HFw	GGTCTGGGATTTAACGAATTTACTCACCAAGTTTTACAAGCGTACG
MSY1Y239HRv	CGTACGCTTGTAAAACTTGGTGAGTAAATTCGTTAAATCCCAGACC
MSY1hL391CFw	CCGGATCGGATTCAGAAGCCTGTTCGAATATTATTTTTGGACG
MSY1L391YRv	CGTCCAAAAATAATATTAGAATACGCTTCTGAATCCGATCCGG
MSY1L411SFw	CTGCTGCGAAGTTAGTTGATTCATGTAAAAAAGCCAGAATTTTGCAG
MSY1L411SRv	CTGCAAAATTCTGGCTTTTTTACATGAATCAACTAACTTCGCAGCAG
PET112DFW	CCCCGGTACCCTCATTGGAAACAATCCTCG
PET112DRV	GCACGGTTCCTATTTACACG
PET112cFW	CCCCGGTACCCTCATTGGAAACAATCCTCG
PET112cRV	CCCCCTGCAGCGTATCTTCATCCTCTCAACC
PET112F103LFW	GAATAGCATATCTCAGTTGGATAGGAAGCATTATTTTTATGG
PET112F103LRV	CCATAAAAATAATGCTTCCTATCCAACTGAGATATGCTATTC
HER2DFw	CTTAGCCTCATGACTTATCTGC
HER2DRv	CATGATTAACGTTGTCCTCAC
HER2cFW	CCCCGGTACCCTTCCTGCTCTTCTTGTTGTCC
HER2cRV	CCCCCTGCAGCCATACTTTCTCACCCAGC
HER2hS109GFw	GGTTCTGGGGGAGTACATGGAATAAGAGGGCCCGTAATTAACC
HER2hS109GRv	GGTTAATTACGGGCCCTCTTATTCCATGTACTCCCCCAGAACC
HER2S109VFw	GGTTCTGGGGGAGTACATGTAATAAGAGGGCCCGTAATTAACC
HER2S109VRv	GGTTAATTACGGGCCCTCTTATTACATGTACTCCCCCAGAAC
HER2hV155TFw	GGAACAGATACTGGTGGCTCCACTAGGCTCCCCGCATGCTATGGATCTG
HER2hV155TRv	CAGATCCATAGCATGCGGGGAGCCTAGTGGAGCCACCAGTATCTGTTCC
HER2V155NR156KP158HF	GGAACAGATACTGGTGGCTCCAATAAGCTCCACGCATGCTATGGATCTG
HER2V155NR156KP158H	CAGATCCATAGCATGCGTGGAGCTTATTGGAGCCACCAGTATCTGTTCC
HER2hP397AFw	CCACATCGTCCAAGCTTGCTGGATCCATAAGGGACTTCG
HER2hP397ARv	CGAAGTCCCTTATGGATCCAGCAAGCTTGGACGATGTGG
HER2P397LFw	CCACATCGTCCAAGCTTCTTGGATCCATAAGGGACTTCG
HER2P397LRv	CGAAGTCCCTTATGGATCCAAGAAGCTTGGACGATGTGG
qSYM1Fw	CGCCGCTAGGTTTGCCATTT
qSYM1RV	AGTGTAGGCCACCATTGCTCT

Table 10. Primers

4.5 Construction of *msy1* mutant strains

MSY1 and its upstream and downstream regions were cloned by PCR-amplification using KOD Hot Start HF DNA polymerase (Novagen®), MSY1cFw and MSY1cRv as primers (see Table 10) and genomic DNA from W303-1B strain. *MSY1* was then cloned in a pFL38 vector after digestion with *Hind*III-*Kpn*I restriction enzimes. The pFL38-*MSY1* plasmid was introduced into the W303-1B strain through the Li-Ac method (Gietz and Woods, 2002), obtaing the strain W303-1B/pFL38-*MSY1,* and disruption of the genomic *MSY1* gene was performed in this strain. *MSY1* disruption was performed through one-step gene disruption by PCR-amplification of *KanMX4* cassette (Wach *et al.*, 1994) from the genomic DNA of BY4742*msy1Δ* strain using KOD HF DNA polymerase (Novagen®) and MSY1DFw and MSY1DRv as primers (see Table 10). Transformation of the former strain (W303-1B/pFL38-*MSY1)* with *KanMX4* cassette was performed through high efficiency yeast transformation protocol (Gietz and Woods, 2002), thus obtaining W303-1B*msy1Δ*/pFL38-*MSY1* strain. The *msy1::KanMX4* cassette could recombine either at the *MSY1* gene harboured on pFL38, or at the wild-type gene in the genome, or less frequently, at another chromosomal locus by non homologous recombination. To distinguish between these cases we performed plasmid shuffling on 5-FOA and then checked the phenotype of the *msy1Δ* strains on geneticin and on non-fermentable carbon sources. Cells in which the genomic *MSY1* locus was disrupted were not able to grow on oxidative carbon sources, due to the loss of mtDNA after pFL38*MSY1* counter selection in 5-FOA plates, but able to grow in presence of geneticin. Cells in which the *msy1::KanMX4* cassette recombined at the *MSY1* plasmid copy maintained mtDNA and were able to grow on non-fermentable carbon sources but not able to grow in presence of geneticin, and cells in which the *msy1::KanMX4* cassette recombined at another chromosomal locus are able to rescue in presence of geneticin and on non-fermentable carbon sources. In the following table an overview of the possible recombination events of the *msy1::KanMX4* cassette in the W3031B-pFL38*MSY1* strain was reported. The homologous recombination at genomic *MSY1* wild type locus is the wanted event.

Recombination event	**Phenotype in presence of pFL38*MSY1***	**Phenotype in absence of pFL38*MSY1***
Homologous recombination at genomic *MSY1* locus	Geneticine +; ethanol +	Geneticine +; ethanol -
Homologous recombination at plasmidic *MSY1* locus	Geneticine +; ethanol +	Geneticine -; ethanol +
Non homologous recombination	Geneticine +; ethanol +	Geneticine +; ethanol +

MSY1 fragment was sub cloned from pFL38 to pFL39. The mutations studied were introduced in *MSY1* by PCR overlap technique (Ho *et al*., 1989) with appropriate primers (table 10) and with pFL38*MSY1* as template, to obtain the mutant alleles $msy1^{hL391C}$, $msy1^{L391Y}$, $msy1^{L411S}$, $msy1^{hR209G}$, $msy1^{R209V}$, $msy1^{Y239H}$, $msy1^{P134R}$ and $msy1^{L226R}$ and subsequently cloned into the pFL39 vector. W303-1B*msy1Δ*/pFL38-*MSY1* was transformed with pFL39-*MSY1,* pFL39 harbouring the mutant alleles created or the empty vector pFL39, and then pFL38-*MSY1* was lost through plasmid-shuffling on 5-FOA.

4.5.1 Plasmid shuffling

Strains which contained pFL38*MSY1* plasmid and pFL39 plasmid carrying a mutant allele, and in which the chromosomal copy of the *MSY1* gene has been disrupted, underwent plasmid shuffling on 5-FOA medium to counter-select pFL38*MSY1* plasmid. Cells were grown in SC-Trp solid medium for 24h in order to counter-select pFL38*MSY1* plasmid. Then the plate was replicated twice on 5-FOA medium, on which only the cells that had lost the plasmid could grow, since 5-FOA is toxic in the presence of the genic product of *URA3* gene. Finally, the plate was replicated on SC-Trp and on SC-Ura, to check the loss of plasmid.

4.6 Construction of *MSY1* heteroallelic strains

The subcloning of alleles *MSY1 and* $msy1^{Y239H}$ from pFL39 plasmid, to pFL38 plasmid was performed through digestion of pFL38 plasmid and *pFL39MSY1* and *pFL39* $msy1^{Y239H}$ recombinant plasmid with the restriction enzymes *Hind*III-HF and *Kpn*I-HF. The digested alleles were inserted in the pFL38 plasmid. Recombinant plasmids obtained pFL38*MSY1 and* pFL38$msy1^{Y239H}$ were introduced in *W303-1BΔmsy1*/pFL39*MSY1* or *W303-1BΔmsy1*/pFL39 $msy1^{R209V}$ through the Li-Ac method (Gietz and Woods, 2002), to obtain the strains *W3031BΔmsy1/pFL39MSY1-pFL38MSY1* and *W3031BΔmsy1/pFL39*msy^{R209V}*-pFL38* msy^{Y239H}.

4.7 Construction of *pet112 and her2* mutant strains

The yeast strains harbouring the mutations studied in *HER2* and *PET112* genes were created using the same approach describe for *msy1* mutant strain using appropriate primer listed in the table 10.

4.8 Nucleic Acid Manipulation

All the manipulations were carried out with standard techniques (Maniatis *et al*., 1982). Genomic DNA from S. cerevisiae was extracted as previously described (Hoffman and Winston, 1987; Lõoke *et al*. 2011). Plasmid DNA was extracted from E. coli with Wizard® Plus SV Minipreps DNA purification system commercial kit, or following standard procedures (Sambrook and Russel, 2001). DNA recovery from agarose gel and purification of PCR products were carried out with GenElute™ PCR-Clean Up kit (Sigma-Aldrich®) commercial kit. Enzymatic manipulations (restriction, dephosporilation and ligation,) were carried out following manufacturer indications (New England Biolabs® Inc. NEB, Invitrogen™). Sequencing of all genes was performed with external service (GATC BIOTECH).

4.9 Transformation procedures

4.9.1 *S. cerevisiae* transformation

Yeast transformation was carried out with Lithium Acetate (LiAc) as described by Gietz and Woods, 2002.

4.9.2 E. coli transformation

$CaCl_2$ competent cells were prepared and transformed with standard techniques (Maniatis *et al.,* 1982).

4.10 Protein analyses

4.10.1 Isolation of mitochondria and protein extraction

Cells, pregrown at 28°C in SC supplemented with 2% ethanol, were exponentially grown in SC supplemeted with 2% glucose at 28°C and transferred to SC medium supplemented with 0.6% glucose plus 2% ethanol at 37°C for 14 h.

To determine the cellular localization (mitochondrial vs cytosolic) of the Sym1 wt or mutant protein we have extracted mitochondrial and cytosolic protein fraction as previously reported (Glick and Pon, 1995) with minor modifications: cell wall was removed using digestion buffer containing 1.2M sorbitol, 60mM K-phosphate pH 7.5, 1mM EDTA, 1% β-mercaptoethanol, 1mg/ml Zymolyase®-20T (Nacalai tesque) to obtain spheroplasts. Spheroplast were homogenized by glass/Teflon potter using 30

gentle strokes on ice. The supernatant containing the cytosolic fraction was separated from mitochondrial pellet by centrifugation.

To determine Sym1 protein stability we have performed total protein extraction with the trichloroacetic acid (TCA) method by chilling the cells supplemented with 120 mM NaOH, 0.5% β-mercaptoethanol, 650 μM PMSF and 25% TCA on ice, then re-suspending the proteins in laemmli sample buffer at pH 6.8.

Mitochondrial proteins for BN-PAGE analyses were obtained by suspending the cells in extraction buffer containing 0.6 M sorbitol, 10 mM imidazole, 0.5 mM EDTA, 0.1% BSA and 1mM PMSF. Cells were broken by vortexing on ice using glass beads and mitochondrial proteins were obtained by centrifugation and re-suspended in the extraction buffer.

Quantification of protein concentration was performed by Bradford's method (Bradford, 1976) using Bio-Rad protein assay following the manufacturer's instructions.

4.10.2 Gel electrophoresis and western blot analysis

Total protein extract or mitochondrial protein extract was load on 12% SDS–polyacrylamide gel and Western Blot (WB) was performed.

For two-dimensional BNGE, 150 mg of protein from isolated mitochondria was treated as previously described (Nijtmans *et al.,* 2002); then the samples were loaded and run into a 3–11% gradient non denaturating 1D-BNGE. The denaturing 2D-BNGE electrophoresis was performed as previously described (Dallabona *et al.,* 2010).

Gels were electroblotted onto nitrocellulose filters and sequentially immunostained with specific antibodies against HA (Roche Applied Science), Por1 and Pgk1 (Abcam Mitoscience). After incubation with the appropriate secondary antibodies, ECL Western blotting Substrate (Clarity^{TM}, BioRad) was used for final detection. Signals were quantified through Quantity One Software (Bio-Rad).

4.11 Phenotypic analysis

4.11.1 Spot assay

Cells were pregrown o/n on YP or SC medium supplemented with 2% glucose at 28°C. When the cells were in exponential phase, they were diluted to obtain the concentrations 10^7, 10^6, 10^5, 10^4 cells/ml.

From these suspensions 5µl were spotted in ordered rows on agar plates and then incubated for several days at 28°C, 36°C or 37°C.

4.11.2 Mitochondrial DNA mutation frequency

Strains were pregrown at 28°C in SC medium supplemented with 2% ethanol in order to counterselect the *petite* cells that could be present in the population and then inoculated in SC supplemented with 2% glucose and incubated for 4 h at 28°C. Then 2% ethanol was added and the cultures were shifted at 37°C. After 15 generations of growth at 37°C, cells were plated on SC agar plates supplemented with 2% ethanol and 0.25% glucose at a dilution giving approximately 250 cells/plate. *Petite* frequencies were defined as the percentage of colonies showing the *petite* phenotype after a 5-day incubation at 28°C. If necessary molecules to test were added in the medium before the shift at 37°C. The molecules of the Selleck chemical library and Prestwick chemical library were dissolved in DMSO, so as control the cell were treated also with this solvent.

4.11.3 MIC determination

Strains were pregrown at 28°C in SC liquid medium supplemented with 2% ethanol and then inoculated in SC supplemented with 2% glucose at the final concentration of $5x10^5$cell/ml and incubated for 4 h at 28°C. Then 2% ethanol and the molecule were added and the cultures were shifted at 37°C. after 24 h the absorbance at 600 nm was determined. The molecules were tested starting from the concentration of 512 µM and sequentially halved. As control the cell were treated also with DMSO.

4.11.4 Competition test ρ^+/ρ^0

BY4741 ρ^+ and BY4741 ρ^0 strains were pregrown in SC liquid medium supplemented with 2% glucose and then were inoculated in SC medium supplemented with 2% glucose at the final concentration of 10^6 cell/ml (50% ρ^+ and 50% ρ^0) and incubated for 4 h at 28°C. Then 2% ethanol was added and the cultures were supplemented with i) 3,2 µl of the molecule to test ii) DMSO as control, and were shifted at 37°C for 24 h. Cells were plated on SC agar plates supplemented with 2% ethanol and 0.25% glucose at a dilution giving approximately 250 cells/plate. *Petite* frequencies were defined as the percentage of colonies showing the *petite* phenotype after a 5-day incubation at 28°C.

4.11.5 Mitochondrial respiration

Oxygen consumption rate was measured at 30°C from yeast cell suspensions cultured for 18 hrs at 28˚C in SC medium supplemented with 0.6% glucose until exhaustion using a Clark-type oxygen electrode (Oxygraph System Hansatech Instruments England) with 1 ml of air-saturated respiration buffer (0.1 M phthalate–KOH, pH 5.0), 0.5% glucose. Values were normalized to the *wild type* strain and represented as the mean of at least three values ± SD. Statistical analysis was performed on the values before the normalization by paired, two-tail Student's t test. Only p values of less than 0.05 were considered significant: *p<0.05, **<0.01, ***p<0.001.

4.12 High throughput screening: Drug drop test

12x12 plates were filled with 90 ml of YP solid medium supplemented with i) 4% ethanol and 0.5X streptomycin-ampicillin. Cells were inoculated in YP medium + 2% ethanol and incubated at 28°C in constant shaking. After 3 days of growth, cells were inoculated in YP medium + 2% glucose 6h at 28°C and then 1,5x10^5 (*sym1*^{R51W}) or 2x10^5 (*sym1Δ*) cells are seeded onto the plates. After the seed, sterile filters of 6 mm of diameter were put on the agar surface and spotted with 2,5 µl of the compound to test, varying the quantity both of the filters and the molecule depending on primary or secondary screening. All the compounds of the chemical library are solubilized in DMSO, so as negative control one filter was spotted with DMSO and as positive control of growth 5µl of wild type strain was spotted on the medium (a number of cells equal as the mutant strain seeded in the same area). Plates were incubated at 37°C for 7 days and the growth of the mutant strain was monitored (Couplan *et al*., 2011)

References

Al-Hussaini A, Faqeih E, El-Hattab AW, Alfadhel M, Asery A, Alsaleem B, Bakhsh E, Ali A, Alasmari A, Lone K, Nahari A, Eyaid W, Al Balwi M, Craig K, Butterworth A, He L, Taylor RW. **Clinical and molecular characteristics of mitochondrial DNA depletion syndrome associated with neonatal cholestasis and liver failure.** J Pediatr. 2014; 164(3):553-9.

AlSaman A, Tomoum H, Invernizzi F, Zeviani M. **Hepatocerebral form of mitochondrial DNA depletion syndrome due to mutation in MPV17 gene.** Saudi J Gastroenterol. 2012; 18(4):285-9.

Antonellis A, Green E. **The role of aminoacyl-tRNA synthetases in genetic diseases.** Ann Rev Genomics Hum Genet 2008, 9:87–107.

Antonenkov VD, Isomursu A, Mennerich D, Vapola MH, Weiher H, Kietzmann T, Hiltunen JK. **The Human Mitochondrial DNA Depletion Syndrome Gene MPV17 Encodes a Non-selective Channel That Modulates Membrane Potential**. J Biol Chem. 2015; 29;290(22):13840-61.

Ardissone A, Lamantea E, Quartararo J, Dallabona C, Carrara F, Moroni I, Donnini C, Garavaglia B, Zeviani M, Uziel G. **A Novel Homozygous YARS2 Mutation in Two Italian Siblings and a Review of Literature.** JIMD Rep. 2015 ;20:95-101.

Armstrong JW. **A review of high-throughput screening approaches for drug discovery**. Thousand Oaks, CA: HTS Consulting Ltd. 1999; 19-33.

Ashburn TT, Thor KB. **Drug repositioning: identifying and developing new uses for existing drugs**. Nat. Rev. Drug Discov. 2004; 3:673–683.

Aubé J. **Drug repurposing and the medicinal chemist**. ACS Med. Chem. Lett. 2012; 3:442–444.

Ausubel, F.M., Brent, R., Kingston, R.E., Moore, D.D., Seidman, J.G., Smith, J.A., Struhl, K. **Current Protocols in Molecular Biology.** 1994. Wiley, New York.

Barberis A, Gunde T, Berset C, Audetat S, Luthi U. **Yeast as a screening tool.** Drug Discovery Today: Technologies. 2005; 2, 2187-92.

Barros MH, Rak M, Paulela JA, Tzagoloff A. **Characterization of Gtf1p, the connector subunit of yeast mitochondrial tRNA-dependent amidotransferase.** J Biol Chem. 2011; 23;286(38):32937-47.

Bassett DE Jr, Boguski MS, Hieter P. **Yeast genes and human disease.** Nature. 1996; 379 589- 90.

Bedouelle H, and Winter G. **A model of synthetase/transfer RNA interaction as deduced by protein engineering.** Nature 1986; 320, 371–373.

Bedouelle, H. **Tyrosyl-tRNA synthetases.** In Aminoacyl-tRNA Synthetases, M. Ibba, C. Francklyn, and S. Cusack, eds. (Georgetown, TX: Landes Biosciences). 2005; pp. 111–124.

Beebe K, Mock M, Merriman E, Schimmel P. **Distinct domains of tRNA synthetase recognize the same base pair.** Nature. 2008, 3;451(7174):90-3.

Bijarnia-Mahay S, Mohan N, Goyal D, Verma IC. **Mitochondrial DNA depletion syndrome causing liver failure.** Indian Pediatr. 2014; 51(8):666-8.

Blakely EL, Butterworth A, Hadden RD, Bodi I, He L, McFarland R, Taylor RW. **MPV17 mutation causes neuropathy and leukoencephalopathy with multiple mtDNA deletions in muscle.** Neuromuscul Disord. 2012; 22(7):587-91.

Boeke JD, LaCroute F, Fink GR, **A positive selection for mutants lacking orotidine-5'-phosphate decarboxylase activity in yeast: 5-fluoro-orotic acid resistance**. Mol. Gen. Genet. 1984; 197, 345-6.

Boireau A, Marechal PM, Meunier M, Dubedat P, Moussaoui S. **The anti-oxidant ebselen antagonizes the release of the apoptogenic factor cytochrome c induced by Fe2+/citrate in rat liver mitochondria**. Neurosci Lett 2000; 289(2):95–98

Bolotin M, Coen MD, Deutsch J, Dujon B, Netter P, Petrochilo E, Slonimski PP**. La recombinaison des mitochondries chez Saccharomyces cerevisiae**. Bull. Inst. Pasteur, 1971 69, 215-39.

Bonneaud N, Ozier-Kalogeropoulos O, Li GY, Labouesse M, Minvielle-Sebastia L, Lacroute F. **A family of low and high copy replicative, integrative and single-stranded S. cerevisiae/E. coli shuttle vectors**. Yeast. 1991; 7(6):609-615.

Bonnefond L, Fender A, Rudinger-Thirion J, Giegé R, Florentz C, Sissler M. (a) **Toward the full set of human mitochondrial aminoacyl-tRNA synthetases: characterization of AspRS and TyrRS.** Biochemistry. 2005; 29; 44(12):4805-16.

Bonnefond L, Frugier M, Touzé E, Lorber B, Florentz C, Giegé R, Sauter C, Rudinger-Thirion J. (b) **Crystal structure of human mitochondrial tyrosyl-tRNA synthetase reveals common and idiosyncratic features**. Structure. 2007; 15(11):1505-16.

Bonnefond L, Giege´R, and Rudinger-Thirion, J. **Evolution of the $tRNA^{Tyr}$/TyrRS aminoacylation systems.** Biochimie 2005; 87, 873–883.

Bottani E, Giordano C, Civiletto G, Di Meo I, Auricchio A, Ciusani E, Marchet S, Lamperti C, d'Amati G, Viscomi C, Zeviani M. **AAV-mediated liver-specific MPV17 expression restores mtDNA levels and prevents diet-induced liver failure**. Mol Ther. 2014; 22(1):10-7.

Brachmann CB, Davies A, Cost GJ, Caputo E, Li J, Hieter P, Boeke JD. **Designer Deletion Strains derived from Saccharomyces cerevisiae S288C: a Useful set of Strains and Plasmids for PCR-mediated Gene Disruption and Other Applications.** Yeast, 1998; 14, 115-132.

Bradford MM. **A rapid and sensitive method for the quantitation of microgram quantities of proteins utilizing the principle of protein dye binding.** Anal. Biochem. 1976;72, 248 – 254.

Burrage LC, Tang S, Wang J, Donti TR, Walkiewicz M, Luchak JM, Chen LC, Schmitt ES, Niu Z, Erana R, Hunter JV, Graham BH, Wong LJ, Scaglia F. **Mitochondrial myopathy, lactic acidosis, and sideroblastic anemia (MLASA) plus associated with a novel de novo mutation (m.8969G>A) in the mitochondrial encoded ATP6 gene.** Mol Genet Metab. 2014; 113(3):207-12.

Bykhovskaya Y, Casas K, Mengesha E, Inbal A, Fischel-Ghodsian N. **Missense mutation in pseudouridine synthase 1 (PUS1) causes mitochondrial myopathy and sideroblastic anemia (MLASA).** Am J Hum Genet. 2004; 74(6):1303-1308.

Cámara Y, González-Vioque E, Scarpelli M, Torres-Torronteras J, Caballero A, Hirano M, Martí R. **Administration of deoxyribonucleosides or inhibition of their catabolism as a pharmacological approach for mitochondrial DNA depletion syndrome.** Hum Mol Genet. 2014 May 1;23(9):2459-67.

Carnero A. **High Throughput Screening in drug discovery.** Clinical and Translational Oncology. 2006; 8, 482-90.

Chabes, A, Domkin V, Thelander L. **Yeast Sml1, a Protein Inhibitor of Ribonucleotide Reductase**. J Biol Chem. 1999; 274(51), pp. 36679-83.

Chihara T, Luginbuhl D, Luo L. **Cytoplasmic and mitochondrial protein translation in axonal and dendritic terminal arborization**. Nat Neurosci 2007; 10(7):828-837.

Chinnery PF, Hudson G. **Mitochondrial genetics.** Br Med Bull 2013; 106:135–59.

Chinnery PF. **Mitochondrial Disorders Overview.** In: Adam MP, Ardinger HH, Pagon RA, Wallace SE, Bean LJH, Mefford HC, Stephens K, Amemiya A, Ledbetter N, editors. GeneReviews® [Internet]. Seattle (WA): University of Washington, Seattle; 1993-2017. 2000 Jun 8 [updated 2014 Aug 14].

Choi YR, Hong YB, Jung SC, Lee JH, Kim YJ, Park HJ, Lee J, Koo H, Lee JS, Jwa DH, Jung N, Woo SY, Kim SB, Chung KW, Choi BO. **A novel homozygous MPV17 mutation in two families with axonal sensorimotor polyneuropathy**. BMC Neurol. 2015; 5;15:179.

Chun-Yuan Chan, Catherine Prudom, Summer M. Raines, Sahba Charkhzarrin, Sandra D. Melman, Leyma P. De Haro, Chris Allen, Samuel A. Lee, Larry A. Sklar, Karlett J. Parra. **Inhibitors of V-ATPase Proton Transport Reveal Uncoupling Functions of Tether Linking Cytosolic and Membrane Domains of V0 Subunit a (Vph1p)**. J Biol Chem. 2012; 23; 287(13): 10236–10250.

Coll O, Colell A, Garcia-Ruiz C, Kaplowitz N, Fernandez-Checa JC. **Sensitivity of the 2-oxoglutarate carrier to alcohol intake contributes to mitochondrial glutathione depletion.** Hepatology 38 2003; 692–702.

Copeland WC. **Defects in mitochondrial DNA replication and human disease.** Crit Rev Biochem Mol Biol. 2012; 47(1):64-74.

Couplan E, Aiyar RS, Kucharczyk R, Kabala A, Ezkurdia N, Gagneur J, St Onge RP, Salin B, Soubigou F, Le Cann M, Steinmetz LM, di Rago JP, Blondel M. **A yeast-based assay identifies drugs active against human mitochondrial disorders.** Proc Natl Acad Sci U S A. 2011; 19;108(29):11989-94.

Curnow AW, Hong Kw, Yuan R, Kim Si, Martins O, Winkler W, Henkin T.M, Söll D. **Glu-tRNAGln amidotransferase: a novel heterotrimeric enzyme required for correct decoding of glutamine codons during translation.** Proc Natl Acad Sci U S A. 1997; 28;94(22):11819-26.

Dalla Rosa I, Cámara Y, Durigon R, Moss CF, Vidoni S, Akman G, Hunt L, Johnson MA, Grocott S, Wang L, Thorburn DR, Hirano M, Poulton J, Taylor RW, Elgar G, Martí R, Voshol P, Holt IJ, Spinazzola A. **MPV17 Loss Causes Deoxynucleotide Insufficiency and Slow DNA Replication in Mitochondria.** PLoS Genet. 2016; 13;12(1):e1005779.

Dallabona C, Marsano RM, Arzuffi P, Ghezzi D, Mancini P, Zeviani M, Ferrero I, Donnini C. **Sym1, the yeast ortholog of the MPV17 human disease protein, is a stress-induced bioenergetic and morphogenetic mitochondrial modulator.** Hum Mol Genet. 2010; 15;19(6):1098-107.

Dallabona C. Ph.D. thesis. **SYM1, l'ortologo di lievito del gene umano MPV17, codifica per una proteina indotta da stress che modula lo stato bioenergetico e morfogenetico del mitocondrio.**

Daum G, Lees ND, Bard M, Dickson R. **Biochemistry, cell biology and molecular biology of lipids of**

Saccharomyces cerevisiae. Yeast. 1998; 14(16):1471-510.

Debeljak N, Horvat S, Vouk K, Lee M, Rozman D. **Characterization of the mouse lanosterol 14alpha-demethylase (CYP51), a new member of the evolutionarily most conserved cytochrome P450 family.** Arch Biochem Biophys 2000. 379:37–45.

Desai R, Frazier AE, Durigon R, Patel H, Jones AW, Dalla Rosa I, Lake NJ, Compton AG, Mountford HS, Tucker EJ, Mitchell ALR, Jackson D, Sesay A, Di Re M, van den Heuvel LP, Burke D, Francis D, Lunke S, McGillivray G, Mandelstam S, Mochel F, Keren B, Jardel C, Turner AM, Ian Andrews P, Smeitink J, Spelbrink JN, Heales SJ, Kohda M, Ohtake A, Murayama K, Okazaki Y, Lombès A, Holt IJ, Thorburn DR, Spinazzola A. **ATAD3 gene cluster deletions cause cerebellar dysfunction associated with altered mitochondrial DNA and cholesterol metabolism.** Brain. 2017; 1;140(6):1595-1610.

Diodato D, Melchionda L, Haack TB, Dallabona C, Baruffini E, Donnini C, Granata T, Ragona F, Balestri P, Margollicci M, Lamantea E, Nasca A, Powell CA, Minczuk M, Strom TM, Meitinger T, Prokisch H, Lamperti C, Zeviani M, Ghezzi D. (b). **VARS2 and TARS2 mutations in patients with mitochondrial encephalomyopathies.** Hum Mutat. 2014; 35(8):983-9.

Diodato D., Ghezzi D., Tiranti V. (a). **The Mitochondrial Aminoacyl tRNA Synthetases: Genes and Syndromes** Int J Cell Biol. 2014.

Dujon B. **Mitochondrial genetics and functions. Molecular biology of the yeast Saccharomyces: life cycle and inheritance.** Cold Spring Harbor Laboratory Press, Cold Spring Harbor, NY. 1981.

Echevarria L, Clemente P, Hernández-Sierra R, Gallardo M E< Fernández-Morena M A, Garesse R. **Glutamyl-tRNA amidotransferase is essential for mammalian mitochondrial translation in vivo.** Biochem J. 2014; 460(1):91-101.

Edwards H, Schimmel P. **An E. coli aminoacyl-tRNA synthetase can substitute for yeast mitochondrial enzyme function in vivo.** Cell. 1987; 51(4):643-649.

El-Hattab AW, Craigen WJ, Scaglia F. (a). **Mitochondrial DNA maintenance defects**. Biochim Biophys Acta. 2017; 1863(6):1539-1555.

El-Hattab AW, Scaglia F. **Mitochondrial Cardiomyopathies.** Front Cardiovasc Med. 2016; 25;3:25.

El-Hattab AW, Li FY, Schmitt E, Zhang S, Craigen WJ, Wong LJ. **MPV17-associated hepatocerebral mitochondrial DNA depletion syndrome: new patients and novel mutations.** Mol Genet Metab. 2010; 99:300–308.

El-Hattab AW, Scaglia F. **Mitochondrial DNA depletion syndromes: review and updates of genetic basis, manifestations, and therapeutic options**. Neurother. J. Am. Soc. Exp. Neurother. 2013; 10 (2) 186–198.

El-Hattab AW, Zarante AM, Almannai M, Scaglia F**.** (b). **Therapies for mitochondrial diseases and current clinical trials. Mol Genet Metab.** 2017; 18. pii: S1096-7192(17)30531-0.

Elustondo P, Martin LA, Karten B. Mitochondrial cholesterol import. Biochim Biophys Acta. 2017 Jan;1862(1):90-101.

Ephrussi B, Hottinguer H and Tavlitzki J. 1949. **Action de l'acriflavine sur les levures. II. Ittude gdnetique du mutant petite colonie.** Ann. Inst. Pasteur (Paris) 76, pp. 419-50.

Eriani G, Delarue M, Poch O, Gangloff J, Moras D. **Partition of tRNA synthetases into two classes based on mutually exclusive sets of sequence motifs.** Nature. 1990; 13;347(6289):203-6.

Feng L., Tumbula-Hansen, D., Min, B., Namgoong, S., Salazar, J., Orellana, O., and Söll, D. **Transfer RNA-dependent amidotransferases: Key enzymes for Asn-tRNA and Gln-tRNA synthesis in nature. In The aminoacyl-tRNA synthetases** (eds. M. Ibba *et al*.), pp. 314-319. Landes Biosciences, Georgetown, TX. 2004.

Feng L, Sheppard K, Tumbula-Hansen D, Söll D. **Gln-tRNAGln formation from Glu-tRNAGln requires cooperation of an asparaginase and a Glu-tRNAGln kinase.** J Biol Chem. 2005; 280(9):8150-5.

Frechin M, Senger B, Brayé M, Kern D, Martin RP, Becker HD. **Yeast mitochondrial Gln-tRNA(Gln) is generated by a GatFAB-mediated transamidation pathway involving Arc1p-controlled subcellular sorting of cytosolic GluRS.** Genes Dev. 2009; 1;23(9):1119-30.

Gakh, O, Cavadini P, Isaya G. **Mitochondrial Processing Peptidases.** Biochim Biophys Acta, 2002; 1592(1), pp. 63-77.

Garone C, Rubio JC, Calvo SE, Naini A, Tanji K, Dimauro S, Mootha VK, Hirano M**. MPV17 Mutations Causing Adult-Onset Multisystemic Disorder With Multiple Mitochondrial DNA Deletions.** Arch Neurol. 2012; 69(12):1648-51.

Gasser T, Dichgans M, Finsterer J, Hausmanowa-Petrusewicz I, Jurkat-Rott K, Klopstock T, Leguern E, Lehesjoki AE, Lehmann-Horn F, Lynch T, *et al.* **Efns Task Force on Molecular Diagnosis of Neurologic Disorders: Guidelines for the Molecular Diagnosis of Inherited Neurologic Diseases**. **Second of Two Parts.** Eur J eurol, 2001; 8(5), pp. 407-24.

Gietz RD, Sugino A. **New yeast-*Escherichia coli* shuttle vectors constructed with in vitro mutagenized yeast genes lacking six-base pair restriction sites.** *Gene.* 1988; 74, 527-534.

Gietz RD, Woods RA. **Transformation of Yeast by Lithium Acetate/Single-Stranded Carrier DNA/Polyethylene Glycol Method.** Methods Enzymol. 2002; 350, pp. 87-96.

Glick BS, Pon LA. **Isolation of highly purified mitochondria from Saccharomyces cerevisiae**. Methods Enzymol. 1995; 260:213-23.

Goffeau A, Barrell BG, Bussey H, Davis RW, Dujon B, Feldman H, Galiber F, Hoheise JD, Jacq C, Johnston M, Louis EJ, Mewes HW, Murakami Y, Philippsen P, Tetteli H, Oliver SG. **Life with 6000 genes.** Science, 1996; 546, 563-7.

Haggarty SJ, Mayer TU, Miyamoto DT, Fathi R, King RW, Mitchison TJ, Schreiber SL. **Dissecting cellular processes using small molecules: identification of colchicine- like, taxol-like and other small molecules that perturb mitosis.** Chem. Biol. 2000; 7, 275-86.

Hargrove TY, Friggeri L, Wawrzak Z, Sivakumaran S, Yazlovitskaya EM, Hiebert SW, Guengerich FP, Waterman MR, Lepesheva GI. **Human sterol 14α-demethylase as a target for anticancer chemotherapy: towards structure-aided drug design.** J Lipid Res. 2016;57(8):1552-63.

Haslam JM, Astin AM, Nichols WW. **The Effects of Altered Sterol Composition on the Mitochondrial Adenine NucleotideTransporter of Saccharomyces cerevisiae**. Biochem J. 1977; 166, 559-563

Hayashi T, Su TP. **Sigma-1 receptor chaperones at the ER-mitochondrioninterface regulate Ca(2þ) signaling and cell survival.** Cell. 2007;131:596e610.
Ho SN, Hunt HD, Horton RM, Pullen JK, Pease LR. **Site-directed mutagenesis by overlap extension using the polymerase chain reaction.** Gene. 1989; 77(1):51-59.

Hoffman CS and Winston F. **A ten-minute DNA preparation from yeast efficiently releases autonomous plasmids for transformation of Escherichia coli.** Gene, 1987; 57, 267-72.

Hughes TR. **Yeast and drug discovery Funct Integr Genomics.** 2002; 2:199–211

Huh WK, Falvo JV, Gerke LC, Carroll AS, Howson RW, Weissman JS, O'Shea EK. **Global analysis of protein localization in budding yeast.** Nature. 2003 ;16;425(6959):686-91.

Ibba M, Soll D. **Aminoacyl-tRNA synthesis.** Annu Rev Biochem. 2000; 69:617-50.

Ibba M ,Söll,D .2004. **Aminoacyl-tRNAs: Setting the limits of the genetic code**. Genes & Dev. 2004; 18: 731-738.

Kaiser C, Michaelis S, Mitchell A. **Methods in Yeast Genetics: a Laboratory Course Manual.** Cold Spring Harbor Laboratory Press, Cold Spring Harbor, NY. 1994.

Kaji S, Murayama K, Nagata I, Nagasaka H, Takayanagi M, Ohtake A, Iwasa H, Nishiyama M, Okazaki Y, Harashima H, Eitoku T, Yamamoto M, Matsushita H, Kitamoto K, Sakata S, Katayama T, Sugimoto S, Fujimoto Y, Murakami J, Kanzaki S, Shiraki K. **Fluctuating liver functions in siblings with MPV17 mutations and possible improvement associated with dietary and pharmaceutical treatments targeting respiratory chain complex II.** Mol Genet Metab. 2009;97(4):292-6.

Kane PM. The **where, when, and how of organelle acidification by the yeast vacu- olar H^+-ATPase, Microbiol.** Mol. Biol. 2006,Rev. 70 177–191.

Karadimas CL, Vu TH, Holve SA, Chronopoulou P, Quinzii C, Johnsen SD, Kurth J, Eggers E, Palenzuela L, Tanji K, Bonilla E, De Vivo DC, DiMauro S, Hirano M. **Navajo neurohepatopathy is caused by a mutation in the MPV17 gene. Am J Hum Genet.** 2006;79(3):544-8.

Karasawa M, Zwacka RM, Reuter A, Fink T, Hsieh CL, Lichter P, Francke U, Weiher H. **The human homolog of the glomerulosclerosis gene Mpv17: structure and genomic organization.** Hum Mol Genet. 1993;2(11):1829-34.

Kim J, Kang E, Kim Y, Kim JM, Lee BH, Murayama K, Kim GH, Choi IH, Kim KM, Yoo HW. **MPV17 mutations in patients with hepatocerebral mitochondrial DNA depletion syndrome.** Mol Genet Metab Rep. 2016 4;8:74-6.

Kohda M, Tokuzawa Y, Kishita Y, Nyuzuki H, Moriyama Y, Mizuno Y, Hirata T, Yatsuka Y, Yamashita Sugahara Y, Nakachi Y. *et al.* **A Comprehensive Genomic Analysis Reveals the Genetic Landscape of Mitochondrial Respiratory Chain Complex Deficiencies.** PLoS genetics 2016; 12, e1005679.

Koehler, C. M. **New Developments in Mitochondrial Assembly.** Annu Rev Cell Dev Biol. 2004; 20, pp. 309-35.

Kojima M, Morozumi T, Onishi A, Mitsuhashi T. **Structure of the pig sterol 14alpha-demethylase (CYP51) gene and its expression in the testis and other tissues**. J Biochem (Tokyo) 2000; 127:805–811.

Krauss J, Astrinidis P, Frohnhöfer HG, Walderich B, Nüsslein-Volhard C. **Transparent, a gene affecting stripe formation in Zebrafish, encodes the mitochondrial protein Mpv17 that is required for iridophore survival.** Biol Open. 2013 ;15; 2(9): 979.

Lapointe J, Duplain L, and Proulx M. **A single glutamyl-tRNA synthetase aminoacylates tRNAGlu and tRNAGln in Bacillus subtilis and efficiently misacylates Escherichia coli tRNAGln1 in vitro.** J. Bacteriol. 1986; 165: 88-93.

Lee CP, and RajBhandary UL. **Mutants of Escherichia coli initiator tRNA which suppress amber codons in Saccharomyces cerevisiae and are aminoacylated with tyrosine by yeast extracts**. Proc. Natl. Acad. Sci. USA 1991; 88, 11378–11382.

Lipsky MS, Sharp LK . **From idea to market: the drug approval process.** J Am Board Fam Pract 2001; 14:362–367

Long Y, Lin Z, Xia M, Zheng W, Li Z. **Mechanism of HERG potassium channel inhibition by tetra-n-octylammonium bromide and benzethonium chloride**. Toxicol Appl Pharmacol. 2013; 1;267(2):155-66.

Lõoke M, Kristjuhan K, Kristjuhan A. **Extraction of genomic DNA from yeasts for PCR- based applications**. Biotechniques. 2011; 50, 325-8.

Lum PY, Armour CD, Stepaniants SB, Cavet G, Wolf MK, *et al*. **Discovering modes of action for therapeutic compounds using a genome-wide screen of yeast heterozygotes.** Cell 116: 2004; 121–137.

Mandel H, Hartman C, Berkowitz D, Elpeleg O.N, Manov I, Iancu TC. **The hepatic mitochondrial DNA depletion syndrome: ultrastructural changes in liver biopsies.** Hepatology, 2001;34, 776–784.

Maniatis T, Fritsch E, Sambrook J. **Molecular cloning. A laboratory manual.** Cold Spring Harbor Laboratory Press, Cold Spring Harbor, NY. 1982;

Mayer TU, Kapoor TM, Haggarty SJ, King RW, Schreiber SL, Mitchison TJ. **Small molecule inhibitor of mitotic spindle bipolarity identified in a phenotype-based screen.** Science, 1999; 286, 971-4.

McShane MA, Hammans SR, Sweeney M, Holt IJ, Beattie TJ, Brett EM, Harding AE. **Pearson syndrome and mitochondrial encephalomyopathy in a patient with a deletion of mtDNA**. Am J Hum Genet.1991; 48(1):39-42.

Merz S, Westermann B. **Genome-wide deletion mutant analysis reveals genes required for respiratory growth, mitochondrial genome maintenance and mitochondrial protein synthesis in Saccharomyces cerevisiae.** Genome Biol. 2009;10:R95.

Messenguy F, Colin D, Ten Have JP. **Regulation of compartmentation of amino acid pools in Saccharomyces cerevisiae and ist effects on metabolic control.** Eur. J. Biochem. 1980; 108:439.

Meyer zum Gottesberge AM, Felix H. **Abnormal Basement Membrane in the Inner Ear and the Kidney of the Mpv17-/- Mouse Strain: Ultrastructural and Immunohistochemical Investigations.** Histochem Cell Biol. 2005; 124(6), pp. 507-16.

Moebius FF, Bermoser K, Reiter RJ, Hanner M, Glossmann H. **Yeast sterol C8-C7 isomerase: identification and characterization of a high-affinity binding site for enzyme inhibitors**. Biochemistry 1996 35: 16871–16878.

Mounolou JC, Jacob H, Slonimsky PP. **Mitochondrial DNA from yeast "petite" mutants: specific changes in buoyant density corresponding to different cytoplasmic mutations**. *Biochem. Biophys. Res. Commun*. 1966; 24**,** 218-224.

Moussaoui S, Obinu MC, Daniel N, Reibaud M, Blanchard V, Imperato A. **The antioxidant ebselen prevents neurotoxicity and clinical symptoms in a primate model of Parkinson's disease**. Exp Neurol 2000,166(2):235–245.

Mulero JJ, Rosenthal JK, Fox TD. **PET112, a Saccharomyces cerevisiae nuclear gene required to maintain rho+ mitochondrial DNA**. Curr Genet. 1994;25:299-304.

Mundy G, Garrett R, Harris S, Chan J, Chen D, Rossini G, Boyce B, Zhao M, Gutierrez G. **Stimulation of bone formation in vitro and in rodents by statins.** Science, 1999; 286, 1946- 49.

Munnich A, Rötig A, Rio M. **Defects of the respiratory chain.** In: JM, S., Van Den, B.G., JH, W. (Eds.), Inborn Metabolic Diseases Diagnosis and Treatment, 5th edn. Springer, Germany, Berlin-Heidelberg. 2012; pp. 223–238.

Nagao A, Suzuki T, Katoh T, Sakaguchi Y, Suzuki T. **Biogenesis of glutaminyl- mt tRNAGln in human mitochondria**. Proc Natl Acad Sci U S A. 2009; 22;106(38):16209-14.

Nakajima J, Eminoglu TF, Vatansever G, Nakashima M, Tsurusaki Y, Saitsu H, Kawashima H, Matsumoto N, Miyake N. **A novel homozygous YARS2 mutation causes severe myopathy, lactic acidosis, and sideroblastic anemia 2.** J Hum Genet. 2014;59(4):229-32.

Nakamura A, Yao M, Chimnaronk S, Sakai N, Tanaka I. **Ammonia channel couples glutaminase with transamidase reactions in GatCAB**. Science. 2006;30;312(5782):1954-8.

Narayanaswami V, Sies H . **Oxidative damage to mitochondria and protection by ebselen and other antioxidants.** Biochem Pharmacol 1990; 40(7):1623– 1629

Navarro-Sastre A, García-Silva MT, Martín-Hernández E, Lluch M, Briones P, Ribes A. **Functional splicing assay supporting that c.70 + 5G > A mutation in the MPV17 gene is disease causing.** J Inherit Metab Dis. 2010;33.

Navarro-Sastre A, Martín-Hernández E, Campos Y, Quintana E, Medina E, de Las Heras RS, Lluch M, Muñoz A, del Hoyo P, Martín R, Gort L, Briones P, Ribes A. **Lethal hepatopathy and leukodystrophy caused by a novel mutation in MPV17 gene: description of an alternative MPV17 spliced form.** Mol Genet Metab. 2008;94(2):234-9.

Navarro-Sastre A, Tort F, Garcia-Villoria J, Pons MR, Nascimento A, Colomer J, Campistol J, Yoldi ME, López-Gallardo E, Montoya J, Unceta M, Martinez MJ, Briones P, Ribes A. **Mitochondrial DNA depletion syndrome: new descriptions and the use of citrate synthase as a helpful tool to better characterise the patients.** Mol Genet Metab. 2012 ;107(3):409-15.

Nijtmans LG, Henderson NS, Holt, IJ. **Blue native electrophoresis to study mitochondrial and other protein complexes.** Methods, 2002; 26, 327–334.

Nitahara Y, Aoyama Y, Horiuchi T, Noshiro M, Yoshida Y. **Purification and characterization of rat sterol 14-demethy- lase P450 (CYP51) expressed in Escherichia coli.** J Biochem (Tokyo) 1999; 126:927–933.

Nogueira Célia , Ligia S Almeida, Claudia Nesti, Ilaria Pezzini, Arnaldo Videira,3 Laura Vilarinho, 1,5 and Filippo M Santorelli. **Syndromes associated with mitochondrial DNA depletion** Ital J Pediatr. 2014; 40: 34.

Nohturfft A, Zhang SC.**Coordination** of **lipid metabolism** in **membrane biogenesis**. Annu Rev Cell Dev Biol. 2009; 25:539-66.

Pagani MA, Casamayor A, Serrano R, Atrian S, Ariño J. **Disruption of iron homeo- stasis in Saccharomyces cerevisiae by high zinc levels: a genome-wide study, Mol**. Microbiol. 2007, 65 521–537.

Paradies G, Petrosillo G, Gadaleta MN, Ruggiero FM. **The effect of aging and acetyl-L-carnitine on the pyruvate transport and oxidation in rat heart mitochon- dria**. FEBS Lett. 454 ,1999; 207–209.

Paradies G, Ruggiero FM, Dinoi P. **Decreased activity of the phosphate carrier and modification of lipids in cardiac mitochondria from senescent rats, Int. J.** Biochem. 24 ,1992; 783–787.

Parlo RA, Coleman PS. **Enhanced rate of citrate export from cholesterol-rich hepatoma mitochondria. The truncated Krebs cycle and other metabolic ramifications of mitochondrial membrane cholesterol**. J. Biol. Chem. 259 ,1984; 9997–10003.

Patricia Santofimia-Castano, Gines M, Salido, and Antonio Gonzalez. **Ebselen Alters Mitochondrial Physiology and Reduces Viability of Rat Hippocampal Astrocytes**. DNA AND CELL BIOLOGY 2013,Volume 32, Number 4, Pp. 147–155

Pearson HA, Lobel JS, Kocoshis SA, Naiman JL, Windmiller J, Lammi AT, Hoffman R, Marsh JC. **A new syndrome of refractory sideroblastic anemia with vacuolization of marrow precursors and exocrine pancreatic dysfunction.** J Pediatr. 1979; 95(6):976-84.

Piekutowska-Abramczuk D, Pronicki M, Strawa K, Karkucińska-Więckowska A, Szymańska-Dębińska T, Fidziańska A, Więckowski MR, Jurkiewicz D, Ciara E, Jankowska I, Sykut-Cegielska J, Krajewska-Walasek M, Płoski R, Pronicka E. **Novel c.191C>G (p.Pro64Arg) MPV17 mutation identified in two pairs of unrelated Polish siblings with mitochondrial hepatoencephalopathy**. Clin Genet. 2014 ;85(6):573-7.

Pitayu L, Baruffini E, Rotig A, Lodi T, Delahodde A. **Yeast model for drug discovery: Identification of molecules acting as potential therapeutics for POLG-related diseases**. Human Molecular Genetics, 2015, Vol. 25, No. 4 715–727

Pyal A, Paramasivam A, Meena AK, Bhavana VB, Thangaraj K. **MPV17 hepatocerebral mitochondrial DNA depletion syndrome presenting as acute flaccid paralysis - A case report**. Mitochondrion. 2017; 30. pii: S1567-7249(16)30282-3.

Rainey MM, Korostyshevsky D, Lee S, Perlstein EO. **The antidepressant sertraline targets intracellular vesiculogenic membranes in yeast.** Genetics. 2010;185(4):1221-33.

Rehling P, Pfanner ,Meisinger. **Insertion of Hydrophobic Membrane Proteins into the Inner Mitochondrial Membrane--a Guided Tour**.J Mol Biol. 2003; 326(3), pp. 639-57.

Reinhold R, Krüger V, Meinecke M, Schulz C, Schmidt B, Grunau SD, Guiard B, Wiedemann N, van der Laan M, Wagner R, Rehling P, Dudek. **The channel-forming Sym1 protein is transported by the TIM23 complex in a presequence-independent manner.** Mol Cell Biol. 2012;32(24):5009-21.

Resnick M A, Cox BS. **Yeast as an Honorary Mammal.** Mutat Res, 2000 451(1-2), pp. 1-11.

Riley LG, Cooper S, Hickey P, Rudinger-Thirion J, McKenzie M, Compton A, Lim SC, Thorburn D, Ryan MT, Giegé R, Bahlo M, Christodoulou J**. Mutation of the mitochondrial tyrosyl-tRNA synthetase gene, YARS2, causes myopathy, lactic acidosis, and sideroblastic anemia--MLASA syndrome.** Am J Hum Genet. 2010; 9;87(1):52-9.

Riley LG, Menezes MJ, Rudinger-Thirion J, Duff R, de Lonlay P, Rotig A, Tchan MC, Davis M, Cooper ST, Christodoulou J. **Phenotypic variability and identification of novel YARS2 mutations in YARS2 mitochondrial myopathy, lactic acidosis and sideroblastic anaemia.** Orphanet J Rare Dis. 2013; 17;8:193.

Riley LG, Rudinger-Thirion J, Schmitz-Abe K, Thorburn DR, Davis RL, Teo J, Arbuckle S, Cooper ST, Campagna DR, Frugier M, Markianos K, Sue CM, Fleming MD, Christodoulou J. **LARS2 Variants Associated with Hydrops, Lactic Acidosis, Sideroblastic Anemia, and Multisystem Failure.** JIMD Rep. 2016; 28:49-57.

Rinehart J, Krett B, Rubio MA, Alfonzo JD, Söll D. **Saccharomyces cerevisiae imports the cytosolic pathway for Gln-tRNA synthesis into the mitochondrion**. Genes Dev. 2005;1;19(5):583-92.

Rokka A, Antonenkov VD, Soininen R, Immonen HL, Pirilä PL, Bergmann U, Sormunen RT, Weckström M, Benz R, Hiltunen JK. **Pxmp2 is a channel-forming protein in Mammalian peroxisomal membrane.** PLoS One. 2009; 4(4):e5090.

Rötig A. **Human diseases with impaired mitochondrial protein synthesis.** Biochim Biophys Acta. 2011; 1807(9):1198-205.

Rowberg RE. **Pharmaceutical research and development: a description and analysis of the process.** CRS report for Congress (Order Code RL30913) US Library of Congress, Wash- ington, D.C. 2001.

Roy Beatrice, Claire Beuneu, Pascal Roux, Henri Buc, Genevieve Lemaire, and Michel Lepoivre. **Simultaneous Determination of Pyrimidine or Purine Deoxyribonucleoside Triphosphates,Using a Polymerase Assay.** Analytical Biochemistry 1999;269, 403–409

Rychter J, Espín F, Gallego D, *et al* .**Colonic smooth muscle cells and colonic motility patterns as a target for irritable bowel syndrome therapy: mechanisms of action of otilonium bromide**. Ther Adv Gastroenterol. 2014; 7: 156–66.

Sambrook J and Russel DW. **Molecular Cloning: a Laboratory Manual**. Cold Spring Harbor Laboratory Press, Cold Spring Harbor, NY. 2001.

Sarkhy AA, Al-Sunaid A, Abdullah A, AlFadhel M, Eiyad W. **A novel MPV17 gene mutation in a Saudi infant causing fatal progressive liver failure**. Ann Saudi Med. 2014;34(2):175-8.

Sarzi E, Bourdon A, Chrétien D, Zarhrate M, Corcos J, Slama A, Cormier-Daire V, de Lonlay P, Munnich A, Rötig A. **Mitochondrial DNA depletion is a prevalent cause of multiple respiratory chain deficiency in childhood**. J Pediatr. 2007;150(5):531-4..

Sasarman F, Nishimura T, Thiffault I, Shoubridge EA. **A novel mutation in YARS2 causes myopathy with lactic acidosis and sideroblastic anemia.** Hum Mutat. 2012; 33(8):1201-1206.

Schenkel J, Zwacka R M, C. Rutenberg, A. Reuter, R. Waldherr and H. Weiher. **Functional Rescue of the Glomerulosclerosis Phenotype in Mpv17 Mice by Transgenesis with the Human Mpv17 Homologue**. Kidney Int, 48(1), 1995. pp. 80-4.

Schön A, Kannangara CG, Gough S, Söll D. **Protein biosynthesis in organelles requires misaminoacylation**

of tRNA. Nature 331, 1988;187-190.

Schon EA, DiMauro S, Hirano M. **Human mitochondrial DNA: roles of inherited and somatic mutations**. Nature reviews. Genetics. 2012;13:878–890.

Sekine S, Nureki O, Shimada A, Vassylyev DG, Yokoyama S. **Structural basis for anticodon recognition by discriminating glutamyl-tRNA synthetase.** Nat. Struct. Biol. 2001; 8: 203-206.

Serrano R, Bernal D, Simon E, Ariño J. **Copper and iron are the limiting factors for growth of the yeast Saccharomyces cerevisiae in an alkaline environment.** J. Biol. Chem. 2004, 279 19698–19704.

Shahni R, Wedatilake Y, Cleary MA, Lindley KJ, Sibson KR, Rahman S. **A distinct mitochondrial myopathy, lactic acidosis and sideroblastic anemia (MLASA) phenotype associates with YARS2 mutations.** Am J Med Genet A. 2013;161A(9):2334-8.

Smirnova EV, Lakunina VA, Tarassov I, Krasheninnikov IA, Kamenski PA **Noncanonical functions of aminoacyl-tRNA synthetases.** Biochemistry (Mosc). 2012; 77(1):15-25.

Smith AM, Ron Ammar R, Corey Nislow C, Giaever G. **A survey of yeast genomic assays for drug and target discovery**. Pharmacology & Therapeutics, 2010; 127, 156-64.

Sommerville E.W. Ng Y.S., Alston C.L., Dallabona C., Gilberti M., He L., Knowles C., Chin S.L., Schaefer A.M., Falkous G., Murdoch D., Longman C., de Visser M., Bindoff L.A., Rawles J.M., Dean J.C.S., Petty R.K., Farrugia M.E., Haack T.B., Prokisch H., McFarland R., Turnbull D.M., Donnini C., Taylor R.W., Gorman G.S. **Clinical Features, Molecular Heterogeneity, and Prognostic Implications in YARS2-Related Mitochondrial Myopathy**. JAMA neurology, 2017 ;74(6):686-694.

Spinazzola A, Santer R, Akman OH, Tsiakas K, Schaefer H, Ding X, Karadimas CL, Shanske S, Ganesh J, Di Mauro S, Zeviani M. **Hepatocerebral form of mitochondrial DNA depletion syndrome: novel MPV17 mutations.** Arch Neurol. 2008 ;65(8):1108-13.

Spinazzola A, Viscomi C, Fernandez-Vizarra E, Carrara F, D'Adamo P, Calvo S, *et al*. **MPV17 encodes an inner mitochondrial membrane protein and is mutated in infantile hepatic mitochondrial DNA depletion.** Nat Genet. 2006;38:570–575.

Spinazzola A. **Mitochondrial DNA mutations and depletion in pediatric medicine.** Semin. Fetal Neonatal Med. 16 (4) 2011 Aug 190–196.

Stromstedt M, Rozman D, Waterman MR. **The ubiquitously expressed human CYP51 encodes lanosterol 14 alpha- demethylase, a cytochrome P450 whose expression is reg- ulated by oxysterols.** Arch Biochem Biophys 1996. 329:73–81.

Suomalainen A, Isohanni P. **Mitochondria DNA depletion syndromes – many genes, common mechanisms.** Neuromusc Disorders. 2010; 20:429–437

Tang Hei-Man Vincent, Siu Kam-Leung, Wong Chi-Ming, Jin Dong-Yan. **Loss of Yeast Peroxiredoxin Tsa1p Induces Genome Instability through Activation of the DNA Damage Checkpoint and Elevation of dNTP Levels**. PLoS Genet. 2009 ; 5(10): e1000697.

Tardiff DF, Lindquist S. **Phenotypic screens for compounds that target the cellular pathologies underlying Parkinson's Disease.** Drug Discov Today Technol. 2013; 10(1): e121–e128.

Thomson M, McKiernan P , Buckel J, Mayer D, Kelly D. **Generalised Mitochondrial Cytopathy Is an Absolute Contraindication to Orthotopic Liver Transplant in Childhood**. J Pediatr Gastroenterol Nutr, 1998; 26(4), pp. 478-81.

Tiano L, Fedeli D, Santoni G, Davies I, Wakabayashi T, Falcioni G. **Ebselen prevents mitochondrial ageing due to oxidative stress: in vitro study of fish erythrocytes**. Mitochondrion 2003, 2(6):428–436.

Tolkunova E, Park H, Xia J, King M P, Davidson E. **The human lysyl-tRNA synthetase gene encodes both the cytoplasmic and mitochondrial enzymes by means of an unusual alternative splicing of the primary transcript**. J biol Chem 2000; 275(45):35063-35069.

Trott A, Morano KA. **SYM1 is the stress-induced Saccharomyces cerevisiae ortholog of the mammalian kidney disease gene Mpv17 and is required for ethanol metabolism and tolerance during heat shock**. Eukaryot Cell. 2004;3(3):620-31.

Tuller G, Daum G**. Import of sterols into mitochondria of the yeast Saccharomyces cerevisiae.** FEBS Lett. 1995; 18;372(1):29-32.

Tzagoloff A and Dieckmann CL. **Pet Genes of Saccharomyces Cerevisiae. Microbiol Rev**, 1990; 54(3), pp. 211-25.

Uesono Y, Araki T, Toh-E A. **Local anesthetics, antipsychotic phenothiazines, and cationic surfactants shut down intracellular reactions through membrane perturbation in yeast**. Biosci Biotechnol Biochem. 2008;72(11):2884-94.

Uusimaa J, Evans J, Smith C, Butterworth A, Craig K, Ashley N, Liao C, Carver J, Diot A, Macleod L, Hargreaves I, Al-Hussaini A, Faqeih E, Asery A, Al Balwi M, Eyaid W, Al-Sunaid A, Kelly D, van Mourik I, Ball S, Jarvis J, Mulay A, Hadzic N, Samyn M, Baker A, Rahman S, Stewart H, Morris AA, Seller A, Fratter C, Taylor RW, Poulton J. **Clinical, biochemical, cellular and molecular characterization of mitochondrial DNA depletion syndrome due to novel mutations in the MPV17 gene.** Eur J Hum Genet. 2014 ;22(2):184-91.

Venter JC, Adams MD, Myers EW, Li PW, Mural R.J, Sutton GG, *et al*. **The sequence of the human genome**. Science., 2001; 201, 1304-51.

Vilarinho S, Choi M, Jain D, Malhotra A, Kulkarni S, Pashankar D, Phatak U, Patel M, Bale A, Mane S, Lifton RP, Mistry PK. **Individual exome analysis in diagnosis and management of paediatric liver failure of indeterminate aetiology**. J Hepatol. 2014;61(5):1056-63.

Viscomi C, Zeviani M. **MtDNA-maintenance defects: syndromes and genes.** J Inherit Metab Dis. 2017; 40(4):587-599.

Viscomi C, Spinazzola A, Maggioni M, Fernandez-Vizarra E, Massa V, Pagano C, Vettor R, Mora M, Zeviani M. **Early-Onset Liver Mtdna Depletion and Late-Onset Proteinuric Nephropathy in Mpv17 Knockout Mice**. Hum Mol Genet, 18(1), 2009;pp. 12-26.

Wach A, Brachat A, Pohlmann R, Philippsen P. **New heterologous modules for classical or PCR-based gene disruptions in Saccharomyces cerevisiae.** Yeast. 1994; 10(13):1793-1808.

Weiher H, Uoda T, Gray DA, Sharpe AH, Jaenisch R. **Transgenic Mouse Model of Kidney Disease: Insertional Inactivation of Ubiquitously Expressed Gene Leads to Nephrotic Syndrome.** Cell, 1990; 62(3), pp.425-34.

Weiher,H. **Glomerular Sclerosis in Transgenic Mice: The Mpv-17 Gene and Its Human Homologue.** Adv

Nephrol Necker Hosp, 22, 1993; pp. 37-42.

Wiedemann U, Frazier A E , Pfanner U. **The Protein Import Machinery of Mitochondria**. J Biol Chem, 279(15), 2004; pp. 14473-6.

Wilcox M. **Gamma-glutamyl phosphate attached to glutamine-specific tRNA. A precursor of glutaminyl-tRNA in Bacillus subtilis**. Eur J Biochem. 1969;11(3):405-12.

Woese CR, Olsen GJ, Ibba M, Söll D. **Aminoacyl-tRNA synthetases, the genetic code, and the evolutionary process**. Microbiol. Mol. Biol. Rev. 2000; 64: 202-236.

Wong LJ, Brunetti-Pierri U, Zhang Q, Yazigi U, Bove KE, Dahms BB, Puchowicz MA, Gonzalez- Gomez I, Schmitt ES, Truong CK, *et al*. **Mutations in the Mpv17 Gene Are Responsible for Rapidly Progressive Liver Failure in Infancy.** Hepatology 2007; 46(4), pp. 1218-27.

Yang D, Oyaizu Y, Oyaizu H, Olsen G J, Woese CR. **Mitochondrial origins. Proc. Natl.** Acad. Sci. 1985; 82: 4443-4447.

Yaremchuk A, Kriklivyi I, Tukalo M, and Cusack S. **Class I tyrosyl-tRNA synthetase has a class II mode of cognate tRNA recogni-tion.** EMBO J. 2002; 21, 3829–3840.

Ylikallio E, Suomalainen A. **Mechanisms of mitochondrial diseases.** Ann Med. 2012 ;44(1):41-59.

Zarn JA, Brüschweiler BJ, Schlatter JR. **Azole fungicides affect mammalian steroidogenesis by inhibiting sterol 14 alpha-demethylase and aromatase.** Environ Health Perspect. 2003; 111(3):255-61.

Zeviani M, Amati P, Comi G, Fratta G, Mariotti C, Tiranti V. **Searching for genes affecting the structural integrity of the mitochondrial genome.** Biochim Biophys Acta. 1995; 24;1271(1):153-8.

Zeviani M, Antozzi C. **Mitochondrial disorders.** Mol Hum Reprod. 1997; 3(2):133-48.

Zhang Y.-Q., Gamarra S., Garcia-Effron G., Park S., DPerlin.S., Rao R. **Requirement for ergosterol in V-ATPase function underlies antifungal activity of azole drugs**. PLoS Pathog. 2010,6

Zhang Y, Rao R.**Beyond ergosterol: linking pH to antifungal mechanisms**. Virulence 2010,1 551–554.

Zinser E, Paltauf F, Daum G. **Sterol composition of yeast organelle membranes and subcellular distribution of enzymes involved in sterol metabolism.** J Bacteriol. 1993; 175(10):2853-8.